The contribution of DNA DSB repair pathways to the repair of chromosome breaks throughout the cell cycle

Inaugural-Dissertation

zur

Erlangung des Doktorgrades

Dr. rer. nat.

der Fakultät für Biologie

an der

Universität Duisburg-Essen

vorgelegt von

Tamara Theresa Yasmin Murmann-Konda

aus Bonn

Dezember, 2016

Die der vorliegenden Arbeit zugrunde liegenden Experimente wurden am Institut für Medizinische Strahlenbiologie an der Universität Duisburg-Essen, Standort Essen, durchgeführt.

1. Gutachter: Prof. Dr. Georg Iliakis

2. Gutachter: Prof. Dr. Dominik Boos

Vorsitzender des Prüfungsausschusses: Prof. Dr. Dirk Hermann

Tag der mündlichen Prüfung: 08.03.2017

“There is nothing like looking, if you want to find something.
You certainly usually find something, if you look;
But it is not always quite the something you were after”

J.R.R. Tolkien

Table of Contents

LIST OF ABBREVIATIONS

°C	Degree centigrade
µM	Micro Molar
53BP1	p53 binding protein 1
alt-EJ	alternative End joining
ATM	Ataxia telangiectasia mutated
ATR	Ataxia telangiectasia mutated Rad3 related
BER	Base excision repair
BLM	Bloom syndrome helicase
B-NHEJ	backup- non homologous end joining
BRCA1; BRCA2	Breast cancer gene 1, Breast cancer gene 2
BrdU, BrdUrd	Bromodeoxyuridine
BSA	Bovine serum albumin
CB	chromatid breaks
CDK	Cyclin dependent kinases
CDS	Clustered Damage sites
CE	Chromatid exchanges
Chk1, Chk2	Checkpoint kinases 1 and 2
CHO	Chinese hamster ovary
c-NHEJ	classical- Non homologous end joining
CR	Chromosomal rearrangements
CSR	Class switch recombination
CtIP	CtBP-interacting protein
DAPI	4',6-diamidino-2-phenylindole
DDR	DNA damage response
DMSO	Dimethyl sulfoxide
DNA	Deoxyribonucleic acid
Dna2	DNA replication helicase/nuclease 2
DNA-PK	DNA protein kinase
DNA-PKcs	DNA protein kinase catalytic subunit
DSBR	double strand break repair
DSBs	Double strand breaks
e.g.	exempli gratia

EdU	5-ethynyl-2’-deoxyuridine
Exo1	Exonuclease 1
FACS	Fluorescence activated cell sorting
FBS	Fetal Bovine Serum
g	Gramm
Gy	Gray
h	hour
HRR	Homologous recombination repair
h-tert	Human telomerase reverse transciptase
i.e.	id est
IR	Ionizing Radiation
LET	Linear Energy Transfer
Lig1, Lig3, Lig4	Ligase 1, Ligase3, Ligase 4
m	Mutant
M	Molar
mA	Milli Ampere
Mdc1	Mediator of DNA damage checkpoint 1
MEM	Minimal Essential Medium
min	minutes
ml	millilitre
mM	Milli Molar
mm	Millimeters
MMEJ	microhomology mediate end joining
MMR	mismatch repair
MRN	Complex of Mre11, Rad51 and Nbs1
NBS1	Nijmegen breakage syndrome 1 protein
NEAA	Non essential amino acids
neg.	negative
NER	Nucleotide excision repair
ng	Nano gramm
nM	Nanometer
nM	Nano Molar
PAXX	Paralog of XRCC4 and XLF

PBS	Phosphate buffered saline
PCC	Premature Chromosome Condensation
PFA	Paraformaldehyde
PI	Propidium Iodide
PIK	Phosphatidylinositole-3 kinase
PLK	Polo like kinase
pos.	positive
RAG1/RAG2	Recombination activating gene 1 and 2
RIF1	replication timing regulator factor 1
RPA	Replication protein A
rpm	Round per minute
RT	Room temperature
RT	Room temperature
SD	Standard Deviation
SDSA	Synthesis dependent strand annealing
SI unit	Système international d'unités
SSBs	Single Strand breaks
WRN	Werner syndrome protein
wt	wildtype
XLF	XRCC4 like Factor
XRCC	X-ray cross complementing proteins
XRCC3, XRCC2, XRCC4	X-ray repair cross complementing protein 2, 3, 4

LIST OF FIGURES

LIST OF TABLES

ABSTRACT

Ionizing radiation (IR) induced DNA double strand breaks (DSBs) pose a major threat to cellular homeostasis, as unrepaired or misrepaired DSBs can lead to chromosomal aberrations that threaten genomic stability and cell survival. Higher eukaryotes have evolved highly sophisticated DSB repair pathways to mitigate the consequences associated with DSBs. Higher eukaryotes repair DSBs predominantly by classical DNA-PK dependent non homologous end joining (c-NHEJ), or by homologous recombination repair (HRR). While c-NHEJ can be engaged in all cell cycle phases, HRR is restricted to the later S- and G_2- phase of the cell cycle due to its requirement for a sister chromatid. Recently, an alternative (alt-EJ), error prone DSB repair pathway operating as a backup for failures in c-NHEJ and HRR was shown to function throughout the whole cell cycle with peak activity in the G_2-phase of the cell cycle.

Previous experiments in our laboratory suggest a dose dependent choice for the engagement of repair pathways in the repair of IR induced DSBs.

We here investigated the contribution of HRR, c-NHEJ and alt-EJ to the repair of IR induced chromatid breaks, as measured by premature chromosome condensation, by exposing different wildtype, HRR mutant or c-NHEJ mutant cell lines to a broad spectrum of IR doses. Particular focus is placed on the G_2-phase of the cell cycle, where all three DSB repair pathways can engage. Our results suggest a dose dependent repair pathway switch from slow HRR to fast c-NHEJ. Data obtained show that HRR is mainly engaged in the processing of CBs after exposure of low doses (<2 Gy). C-NHEJ on the other hand gains ground in the repair of IR induced chromatid breaks in a dose dependent manner. Moreover, we investigated the formation of chromosomal exchanges. We found a clear contribution of c-NHEJ and alt-EJ to CE formation at high IR doses (5 Gy), while the contribution of DSB repair pathways to CE formation after low doses of IR still need to be clarified.

Finally yet importantly, we developed a protocol for the premature chromosome condensation technique using EdU staining to discriminate between S-phase and G_2-phase PCCs. This technique allows for the first time cell cycle dependent analysis of IR induced cytogenetic damage and paves the way to further mechanistic investigation.

1. INTRODUCTION

Ionizing Radiation (IR) induced DNA double strand breaks (DSBs) pose a major threat to cellular homeostasis, as unrepaired or misrepaired DSBs can lead to chromosomal aberrations that threaten genomic stability and can contribute to carcinogenesis (**Figure 1**).

To ensure genomic integrity higher eukaryotes engage an orchestrated DNA damage response (DDR) that is followed by the activation of cell cycle checkpoints and most importantly of DNA DSB repair processes (**Figure 1**). The two main repair mechanisms that take care of DSBs in higher eukaryotes include homologous recombination repair (HRR) and classical non homologous end joining (c-NHEJ). HRR is a slow process with half times over 1 h. Yet, it is the only known pathway capable to restore both, the sequence and integrity at the DNA by rejoining the correct ends using a homologous sister chromatid, and is therefore, considered to be error free. However, the need for sequence homology limits HRR to the late S-phase and G_2-phase of the cell cycle, where a sister chromatid becomes available. Core factors involved in HRR include proteins of the Rad52 epistasis group, with central players Rad51 and its paralogues, which aid in homology search and strand invasion (Krejci, et al. 2012; Symington and Gautier 2011).

C-NHEJ contrasts the complexity of HRR and relies on a different set of repair proteins. It utilizes the Ku70/80 heterodimer, as well as the catalytic subunit of DNA-PK, which leads to the recruitment of other crucial molecules that are involved in DNA end processing and ligation including DNA Ligase 4 and its cofactor XRCC4. Furthermore, as c-NHEJ does not require sequences homology it is not restricted to a particular cell cycle phase operating thus throughout the cell cycle. One of its main features is speed. C-NHEJ, which is impressively active in higher eukaryotes, acts fast and removes DSBs from the genome with half times of 10-30 minutes. Although, c-NHEJ restores chromosome continuity, it does not have a proofreading mechanism to ensure joining of the correct DSBs. This property renders c-NHEJ an in principle error-prone pathway (Davis and Chen 2013; Mahaney, et al. 2009).

In the last decades, a third pathway often referred to as backup- non homologous end joining (B-NHEJ), microhomology mediated end joining (MEEJ), or alternative end joining (alt-EJ) came to the front. Alt-EJ drew the attention of scientist in the field,

due to its highly error prone nature and frequent implications in the formation of recurrent translocations that are diagnostic of many hematological malignancies and which are also found in solid tumors. Alt-EJ has three characteristic: First, alt-EJ appears to be mainly active when conservative DSB repair pathways fail to engage, serving thus as a backup pathway to HRR and c-NHEJ. Second, alt-EJ introduces excessive deletions at the break junctions. And third, alt-EJ is less faithful in the restoration of the DNA sequence at the junction and is associated with increased formation of chromosomal rearrangements. alt-EJ is not restricted to a particular cell cycle phase; yet it shows peak activity during the G_2-phase of the cell cycle. Up to date proteins such as Parp-1, Ligase 3 and Ligase 1, as well as the MRN complex and XRCC1, CtIP and polymerase θ have been implicated in the molecular set up of alt-EJ (Bunting and Nussenzweig 2013; Chan, et al. 2010; Frit, et al. 2014; Mladenov and Iliakis 2011; Paul, et al. 2013; Simsek and Jasin 2010).

Even though rapid developments in our understanding of DSB repair pathway regulation has been achieved, key questions remain unanswered. For example, it is still unknown which cellular mechanism and processes determine repair pathway choice. This is of particular importance as the above-mentioned DSB repair pathways show different fidelities and efficiencies, and their choice will determine genomic stability and ultimately the cell's fate to the inducing insult.

The present thesis aims to elucidate regulatory mechanisms determining the contributions of the different DSB repair pathways to the processing of IR induced chromatid breaks.

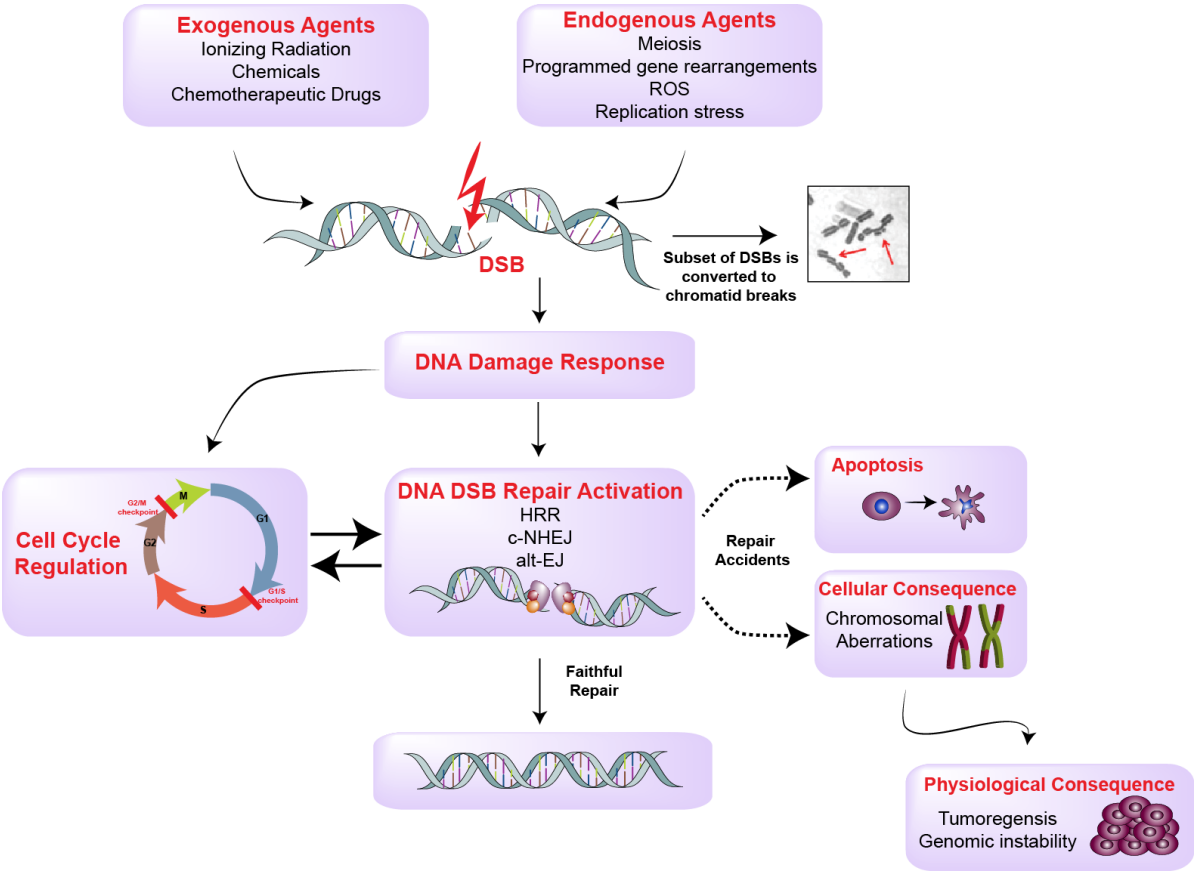

Figure 1: DNA damage induction and its consequences. Exogenous as well as endogenous agents are capable of DSB induction. A subset of DSBs is converted to Chromatid breaks. DNA damage triggers the DNA Damage Response (DDR), which regulates the cell cycle, as well as the activation of DSB repair pathways. If repair pathways fail to engage successfully, repair accidents may occur which can lead to cell death. Other cellular consequences of such accidents include the formation of chromosomal aberrations that contribute to genomic instability and tumorigenesis.

1.1 Ionizing radiation and DNA damage induction

IR finds application in the clinic for diagnostic therapeutic purposes. IR has also gained ground in scientific research due to its property to induce random DSBs. This is particularly attractive as it provides a perfect stage to investigate DNA damage response mechanisms.

1.1.1 An excursion to the physics of Ionizing Radiation

From a physical point of view, IR is defined as energy, deposited to matter that is high enough to eject one or more orbital electrons from an atom, leaving an electrically charged atom behind.

Generally, IR can be differentiated into electromagnetic radiation like gamma-rays and X-rays and into particulate radiation comprising heavy ions, protons, neutrons or α-particles. The focus of the next section is on X-rays, as they are used for the experiments in the present thesis.

X-rays are produced by electrical devices that accelerate electrons to high energy levels, which are abruptly stopped in the anode to generate photons. They can be considered as waves that fall into the higher segment of the electromagnetic spectrum, showing a decreased wavelength, increased frequencies and an increased photon energy (Hall and Giaccia 2006).

The absorption properties of X-rays as they traverse matter depend on the energy of photons, as well as composition of targeted matter. For X-rays with high energies the Compton process dominates, while for X-rays with low energy levels the so called photoelectric process predominates.

In Compton process, X-rays interact with loosely bound electrons in the outermost shell. In this way, part of the photon energy is passed to the electron as kinetic energy and the photon continues with reduced speed at a different direction i.e. it becomes scattered. The electron proceeds as a fast electron, which is able to ionize other atoms, which can generate the breakage of chemical bonds leaving ionized atoms behind.

In contrast, during the photoelectric process, the photon interacts with a strongly bound inner shell electron of the absorbing material. The photon gives up all its energy to the electron and releases it from the atom, with the remaining energy stored as kinetics energy. The gap left behind in the outer shell must be filled by another electron falling in from an outer shell of either the same atom, or by conduction of an electron from outside the atom (Hall and Giaccia 2006).

Ionization events are not randomly distributed in space but rather tend to localize along particle tracks. Hence, different types of radiation deposit their energy to the material through which they pass, at different rates. The quantity describing the density of deposited energy, to material, is called linear energy transfer (LET) (Mladenov and Iliakis 2011; Schipler and Iliakis 2013).

High LET radiation, like some kinds of particulate radiation, is densely ionizing, producing more ionization events on tracks. Furthermore, high LET radiation is often directly ionizing, meaning that it directly disrupt the atomic structure of the absorbing material leading immediately to chemical and biological changes (Lomax 2013).

In contrast to particulate high LET radiation, low LET radiation like X-rays and gamma-rays are indirectly ionizing. They do not cause chemical or biological damage themselves but rather give up their energy to produce fast moving secondary electrons, which then generate the chemical and biological effects. In both processes, damage can be generated directly by targeting molecules (e.g. DNA), or through reaction with water molecules, producing thus free radicals. Those free radicals are able to diffuse far enough to reach and damage critical targets. The latter effect is also known as indirect effect to discriminate from direct effects.

Since cells consist to 70% of water, it is most likely that radiation interacts with water molecules. Upon the interaction of radiation with a water molecule, an electron is ejected from the water molecules leaving behind an electrically charged ion radical. This radical in turn interacts with another molecule to form highly reactive hydroxyl radical.

$$H_2O \rightarrow H_2O^+ + e^-$$

$$H_2O^+ + H_2O \rightarrow H_3O^+ + OH\bullet$$

It is estimated that hydroxyl radicals‘ account for two thirds of radiation induced DNA damage in mammalian cells (Hall and Giaccia 2006).
As a measure of the absorbed dose the International Standard unit (SI unit) Gray (Gy) is used throughout this thesis. The unit Grey describes the radiation energy absorbed per unit mass. Consequently, 1 Gy equals 1 Joule per kilogram.

1.1.2 IR-induced DNA lesions

Ionizing radiation induces a plethora of DNA damages. Per Gy a cell suffers around 1300 purine and pyrimidine lesions, 1000 single strand breaks (SSBs) and 20-40 DSBs (Goodhead 1994; Lomax 2013).

Most of the IR induced lesions are confined to one DNA strand (base lesions, single strand breaks) and can be rapidly excised to restore the DNA strand. Repair processes taking care of such lesions include base excision repair (BER), nucleotide excision repair (NER) or mismatch repair (MMR) (Iliakis, et al. 2015a).

More challenging however is the induction of the highly toxic DNA DSB.
The yield of DSBs increases linearly with IR dose (Barnard, et al. 2013). Furthermore, DSBs can be induced either directly by disrupting the sugar phosphate backbone at both DNA strands or they can be induced through the generation of two SSBs that are in close proximity to each other in the opposite strand. DSBs are particularly challenging to cells as they do not leave an intact template in the second strand and consequently have special needs for their repair.

Induction of DSBs by IR is commonly associated with the generation of clustered DNA lesions. Such clustered lesions may not only comprise the DSB but also sugar and base damages in the vicinity (Goodhead 1994; O'Neill and Wardman 2009).

Moreover, it is also important to mention, that a small subset of DSBs (10 – 20%) is transformed to chromatid breaks (CBs) which can be visualized via classical cytogenetic approaches (Iliakis, et al. 2007).

Figure 2 summarizes the above outlined effects of ionizing radiation and the resulting DNA lesions.

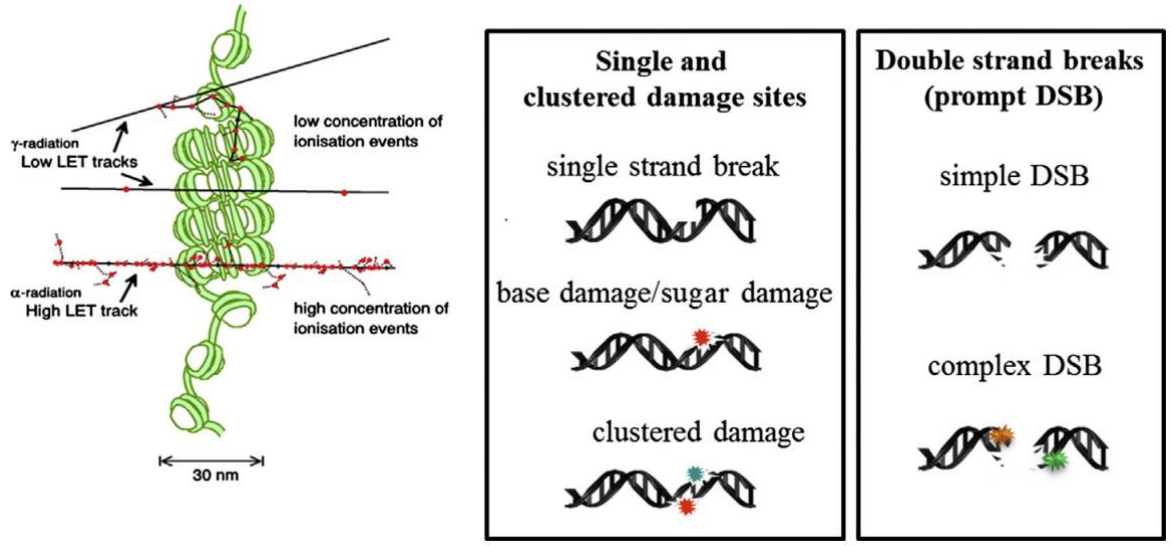

Figure 2: An overview of the lesions induced by ionizing radiation. Ionizing radiation produces a plethora of different lesions including for example single strand breaks, base- or sugar damages and the highly toxic DSB (Figure adapted from (Lomax 2013)).

1.1.3 DNA DSBs and their role in physiological processes

Despite the fact that DSBs are considered as the most severe DNA lesions that a cell can encounter, they do also serve as necessary intermediates in physiological processes like V(D)J-recombination and class switch recombination (CSR). Both mechanisms are important for the generation and development of T- and B- cells.

V(D)J-recombination generates a diverse repertoire of antibodies, T-cell receptors and immunoglobulins by rearranging pre-existing segments that comprise the variable (V) regions, the diversity (D) segment and the joining segment (J). Rearrangement occurs through DSB induction by the endonuclease RAG1 and RAG2 (Recombination activating gene 1 and 2) and rejoining gives rise to immunoglobulins, antibodies and T-cell receptors (Lieber, et al. 2004; Schatz and Swanson 2011).

CSR on the other hand, occurs in antigen-stimulated mature B cells and allows the switch from IgM to IgA, IgG or IgE. Also in CSR, DSBs are induced in ways designed to alter the heavy chain on immunoglobulins (Stavnezer, et al. 2008).

However, not the immune system alone benefits from the programmed induction of DSBs. Also during meiosis DSBs are produced as essential intermediates. Particularly, during the first meiotic division DSBs are needed to promote the pairing

interaction between homologous chromosomes and the exchange of genetic material between them. These interactions aid in the genetic variation of organisms (Murakami and Keeney 2008).

1.2 DNA damage sensing and cell cycle checkpoint activation in higher eukaryotes

The critical importance of the DNA damage response (DDR) becomes obvious when we consider consequences associated with defects in DDR, which can directly contribute to ageing, neurodegenerative diseases, developmental defects and cancer.

Activation of DDR starts within seconds after DNA damage induction. As depicted in **Figure 3**, DDR comprises a network of sensors that sense the presence of a DSB and transmit the signal to downstream effectors through a transduction cascade. Effectors in turn activate mechanisms, which will aid in the coordination of: (1) cell cycle checkpoints to avoid replication or segregation of damaged DNA; (2) DNA damage repair; (3) apoptotic processes in case the DNA damage cannot be repaired. (4) A variety of additional cellular responses (Khanna and Jackson 2001; Sulli, et al. 2012; Zhou and Elledge 2000).

Central to the DDR signaling cascade is the activation of the signal transducer Ataxia Telangiectasia Mutated (ATM) and Ataxia Telangiectasia and Rad3-Related Protein (ATR), both of which belong to the class of phosphoinositide kinase (PIK) - related proteins. Direct targets of ATM and ATR are the checkpoint kinases 1 (Chk1) and checkpoint kinase 2 (Chk2), which are engaged in spreading the signal throughout the nucleus, resulting in the activation of cell cycle checkpoints (Shibata and Jeggo 2014; Vignard, et al. 2013).

Downstream of Chk1 and Chk2 are effector molecules such as Breast Cancer 1 (BRCA1), p53, Nibrin (NBS1) or the E3 ubiquitin-protein kinase (Mdm2) that execute functions in DNA repair, transcription regulation and cell cycle control (Vignard, et al. 2013).

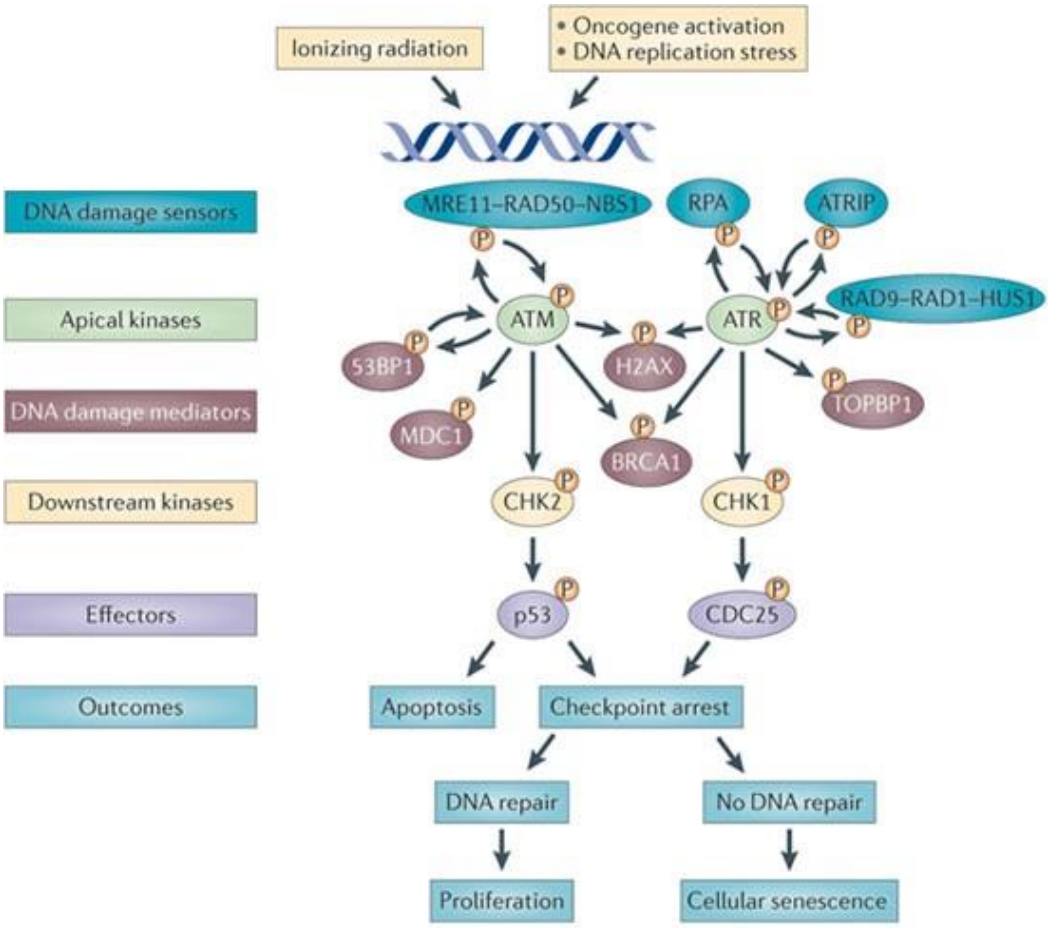

Figure 3: An overview of the DNA Damage Response (DDR) as a consequence to DNA double strand break induction. Cells activate an orchestrated cascade of DNA damage sensors, mediator and effectors. Central to this cascade are ATM and ATR, which regulate molecules involved in the activation of cell cycle checkpoints, apoptosis, as well as DNA repair (Figure adapted from (Sulli, et al. 2012)).

1.2.1 DNA damage sensing

It is not yet fully elucidated which molecules are involved in sensing of DNA damage and directs the activation of the signal transducer ATM and ATR. However, molecules that are able to bind to DNA ends have been implicated in DSB sensing.

Among others, the MRN complex (Mre11/Rad50/Nbs1) represents one major DSB sensor. The binding of the MRN complex to the DSB induces the recruitment of ATM to the DSB site via the interaction with the C-terminus of Nbs1. This interaction triggers the autophosphorylation of ATM and its conversion into an active monomer. The binding of the DSB ends by MRN is further accompanied by several changes in chromatin structure. Most prominent in this respect is the phosphorylation of the H2A histone variant H2AX on Ser-139 generating γH2AX (Pilch, et al. 2003; Podhorecka, et al. 2010). The phosphorylation of H2AX is prerequisite for the recruitment of MDC1

(mediator of DNA damage checkpoint protein 1). On the one hand MDC1 interacts with Mre11 to tether the MRN complex and ATM to the DSB site, allowing ATM to amplify the DDR signal by extending the region of phosphorylated H2AX. On the other hand, MDC1 initiates the recruitment of the E3 ubiquitin ligases RNF8 and RNF168. RNF8 in turn ubiquitinylates damaged chromatin allowing thereupon the recruitment of the p53 binding protein (53BP1), as well as of BRCA1. Both molecules assist in the activation of DSB repair pathways (Kinner, et al. 2008; Shibata and Jeggo 2014).

After DSB sensing ATM and ATR trigger further processes like the activation of the cell cycle checkpoint discussed in the next section.

1.2.2 Cell cycle checkpoint activation

As a consequence to DNA damage, DDR also regulates the activation of cell cycle checkpoints, which will prevent the replication of damaged DNA (G_1/S-checkpoint), halt the firing of origins of replication (intra-S-phase checkpoint), avoid its segregation and provide cells with time for repair (G_2/M- checkpoint).

Generally, the cell cycle is controlled by the interplay between cyclins, whose concentrations vary throughout the cell cycle and the cyclin dependent protein kinases.

If DNA damage occurs in the G_1 phase, cells activate the G_1/S – checkpoint. The G_1/S – checkpoint is regulated by blocking the Cdk2-Cyclin E kinase in an inactive state, while at the same time stabilizing the tumor suppressor p53. Specifically, ATM activates the serine-threonine kinase Chk2, which phosphorylates Cdc25A at Serine-123 leading to ubiquitination of Cdc25A, followed by proteasomal mediated degradation. This reduces the abundance of Cdc25A locking CDK1-Clyclin E in an inactive state and stopping the progression of cells to the S-phase (Iliakis, et al. 2003).

In addition, a second path leading to an arrest of cells in the G_1 phase is achieved by the stabilization of p53, triggered by an ATM dependent phosphorylation. Stabilization of p53 activates the transcription of the CDK inhibitor p21, which binds

to the CDK2 – Cyclin E kinase complex, thus halting cells back in G_1-phase (Iliakis, et al. 2003; Shaltiel, et al. 2015).

A further level of cell cycle regulation, upon DSB induction, is accomplished by the intra S – phase checkpoint, which causes a transient stop in the firing of replicons that wait to be replicated. The induced delay in S-phase is short and only targets parts of the genome.

Similar to the G_1 arrest, Chk2 targets the degradation of Cdc25A leading to the deprivation of cyclin E and cyclin A in association with CDK2. This deprivation prevents the loading of Cdc45 initiation factor onto chromatin and in this way prevents the firing of the remaining pool of competent replication origins (Iliakis, et al. 2003).

Additionally, cells can halt the cell cycle at the G_2/M border. Throughout the literature it has been suggested that the G_2/M – checkpoint not only averts the segregation of damaged material, but rather is an active response to IR with a central role in G_2 – repair (Zhou and Elledge 2000).

The paramount target in the G_2/M – checkpoint is the CDK1 – Cyclin B complex, which is essential for the progression towards mitosis.

The G_2/M – checkpoint response is orchestrated through ATM and its phosphorylation of the downstream targets Chk1 and Chk2. Furthermore, findings in our laboratory suggest absolute requirements of ATR for G_2 – checkpoint induction, if DSBs are induced in the G_2 – phase of the cell cycle (Fan 2009). Redundant pathways have been suggested to engage in the G_2 – checkpoint activation.

One of these pathways compromises the inhibitory phosphorylation of CDK1, mediated by Chk2, which phosphorylates the phosphatase Cdc25C. Phosphorylation of Cdc25C causes its inactivation and binding to the protein 14-3-3, as well as its translocation into the cytoplasm. This renders Cdc25C incapable of removing the inhibitory phosphate groups on CDK1 and thus stops the transition of the cell to M-phase (Khanna and Jackson 2001).

Further, G_2 – checkpoint control is attained through regulation of CDK1 activity by Wee1, Myt1, as well as the polo-like kinase (PLK) (Khanna and Jackson 2001). Also,

p53-dependent transcriptional repression of CDK1 and Cyclin B promoter has been implicated in maintaining the G_2/M – checkpoint in mammalian cells.

At last, the activation of cell cycle checkpoints, upon DSB induction, provides the cell with time for repair and adds to cellular homeostasis.

1.3 Repair of IR induced DNA DSBs in higher eukaryotes

1.3.1 Challenges faced by DSB repair pathways

To rectify the adverse consequences of DSBs, higher eukaryotes have evolved highly sophisticated repair mechanisms. Nevertheless, those repair mechanisms have to accomplish two distinct feats. First, it must be ensured that the right DNA ends are put back together, and that the ends are not joined with the ends from other broken DNA molecules, which can be found in close proximity. As will be outlined later, wrongly rejoined DNA ends form translocations.

The second accomplishment, which must be met by the DNA DSB repair machinery, is to restore the sequence around the broken site to prevent mutations.

In principle, higher eukaryotic cells have developed two distinct DSB repair pathways, namely homologous recombination repair and classical-non homologous end joining. Their properties differ first: in their molecular set up, in their efficiency to process DSBs, in the time required and, last but not least, in their activity throughout the cell cycle.

Next to HRR and c-NHEJ, a third alternative end joining (alt-EJ) pathway must be taken into consideration, as it has been described to backup for failures in c-NHEJ, as well as HRR at the cost of increased translocation formation.

Having outlined the challenges DNA DSB repair machineries have to deal with, a more detailed look on the mechanism behind each DSB repair pathway follows.

1.3.2 Homologous Recombination Repair (HRR)

HRR is an evolutionary old and relatively slow process. It is thought that HRR accounts for the repair of 25% of all DSBs in higher eukaryotes. Nonetheless, the value of HRR lies in its capability to restore both, the DNA sequence as well as the

integrity of the DNA due to its templated nature. Yet, its templated nature limits HRR to the late S-phase and G_2-phase of the cells cycle, where a sister chromatid becomes available (Takata, et al. 1998).

Steps involved in HRR include the recognition of the DSBs, followed by DNA end resection to yield 3' single stranded overhangs, homology search and strand invasion, leading finally to the resolution of the DSB.

In more detail, DSBs are sensed by the MRN complex, constituting the Mre11 nuclease, the ATP-binding polypeptide Rad50, and NBS1, a polypeptide bearing several protein-protein interaction domains. Together with the resection-promoting factor CtIP, MRN re-localizes to the breaks initiating short range resection of DSB ends. Long-range resection on the other hand is carried out with the aid of Exo1, Dna2 and BLM, generating 3' ssDNA overhangs. 3' ssDNA overhangs are rapidly coated with the replication protein A (RPA) heterodimer to prevent further nucleolytic cleavage, as well as to stabilize the 3' single stranded overhangs and to avoid secondary structures (**Figure 4**) (Paull and Deshpande 2014; Trujillo, et al. 1998).

Next, the Rad51 recombinase interacts with the RPA coated ssDNA 3' overhangs to form a nucleoprotein filament, the presynaptic complex. Thereby, Rad51 filament assembly is catalyzed by BRCA2 (**Figure 4**). Additional molecules aiding in the formation of the presynaptic complex include Rad52 and the paralogs of Rad51 comprising, Rad51B, Rad51C, Rad51D, XRCC2 and XRCC3 (Suwaki, et al. 2011). Once the presynaptic complex is assembled, a duplex DNA molecule is captured and homology search is carried out by the Rad51 nucleoprotein filament, leading to the formation of the displacement loop (D-loop). In the following steps DNA synthesis and branch-migration is carried out by the chromatin remodeling functions of Rad54, while Rad51 is subsequently removed from the DNA (Heyer, et al. 2010; Mazin, et al. 2010).

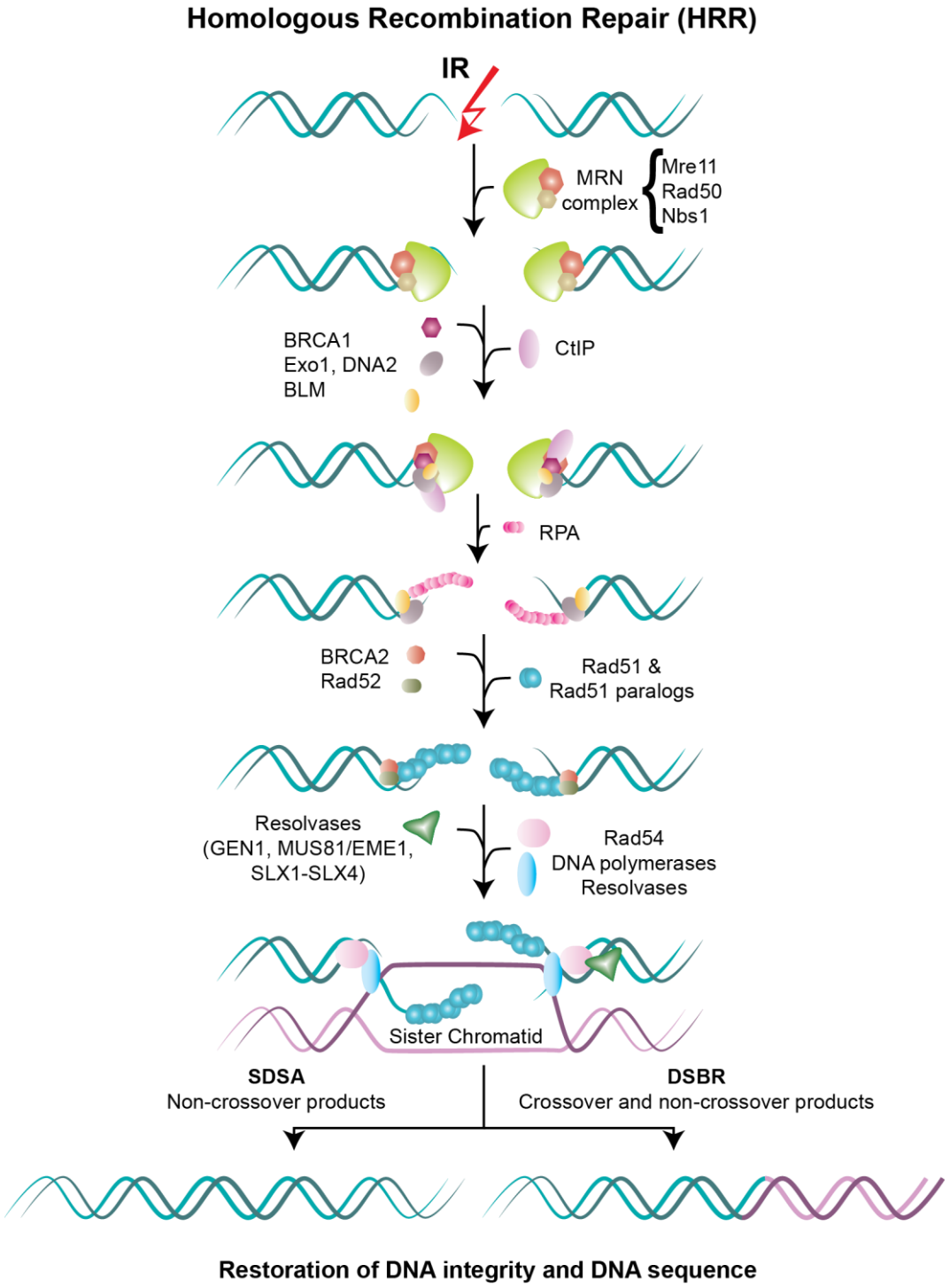

Figure 4: Processing of DSB ends by HRR. Central steps involved in HRR include the recognition of the DSB by the MRN complex followed by DSB end resection conducted by molecules such as CtIP, Exo1, BLM, BRCA1 and Dna2, to yield 3' single stranded overhangs, which are rapidly coated with RPA. In the following steps Rad51 engages in homology search and strand invasion with the aid of its paralogs. Resolution of the DSB is then either carried out by single strand annealing (SDSA) or double strand break repair (DSBR) with the help of resolvases and Rad54 to restore the original sequence of DNA molecules (Graphic modified from (Iliakis, et al. 2015a)).

To finish off HRR, two different processes can be engaged: either synthesis dependent strand annealing (SDSA) or double strand break repair (DSBR).

In SDSA the D-loop is unwound and one 3’ ssDNA overhang participates in the formation of a single Holliday junction with the process being terminated by gap-filling DNA synthesis carried out by DNA polymerases. SDSA produces non-crossover products. In the second process (DSBR), both 3’ overhangs are engaged to form an intermediate harboring two Holliday junctions followed by gap filling DNA synthesis and ligation, yielding either crossover or non-crossover products (San Filippo, et al. 2008).
The final steps of HRR, like Holliday junction resolution, gap filling and DNA synthesis as well as the ligation are carried out by resolvases like GEN1, MUS81/EME1, SLX1-SLX4 (**Figure 4**) (Dueva and Iliakis 2013; Matos and West 2014; Sarbajna and West 2014). Finally, HRR brings together the right DNA DSB ends and the sequence around the break site is restored to its original state (**Figure 4**).

1.3.3 Classical non homologous end joining (c-NHEJ)

Although, HRR is an error free pathway, it is mainly utilized by prokaryotes as well as lower eukaryotes. For the eliminations of DSBs in higher eukaryotes, the evolutionary younger c-NHEJ repair pathway is employed. As mentioned above, c-NHEJ relies on an entirely different set of proteins, and its beauty as compared to HRR lies in its simplicity and speed.

In contrast to HRR, c-NHEJ does not need sequence homology and is therefore not restricted to a specific cell cycle phase. One of its main characteristics is speed, as c-NHEJ repairs DSBs with half times of 15-30 minutes as it simply rejoins DSB ends to restore the integrity in the DNA (DiBiase, et al. 2000; Mladenov and Iliakis 2011).

As presented in **Figure 5** c-NHEJ starts with the binding of the Ku70/80 heterodimer, which encircles the DNA and firmly binds to the DSB ends probably to also protect them from nucleolytic processing. Lately, it has been shown that also a paralog of XRCC4 and XLF called PAXX interacts with the Ku heterodimer for stabilization purposes (Ochi, et al. 2015). Once bound to the DSB, the Ku heterodimer changes its conformation, stimulating the recruitment of the catalytic subunit DNA-PK, DNA-PKcs, whose activity increases drastically upon interaction with Ku. The catalytic subunit of DNA-PK is especially important for the phosphorylation of substrates that

promote DSB end-processing to provide ligatable DSB ends. Specifically, IR-induced DSBs are “dirty” in the sense that they often do not have 5’ phosphate and 3’ hydroxyl DNA termini that can be directly ligated (Burma, et al. 2006; Deriano and Roth 2013; Mahaney, et al. 2009).

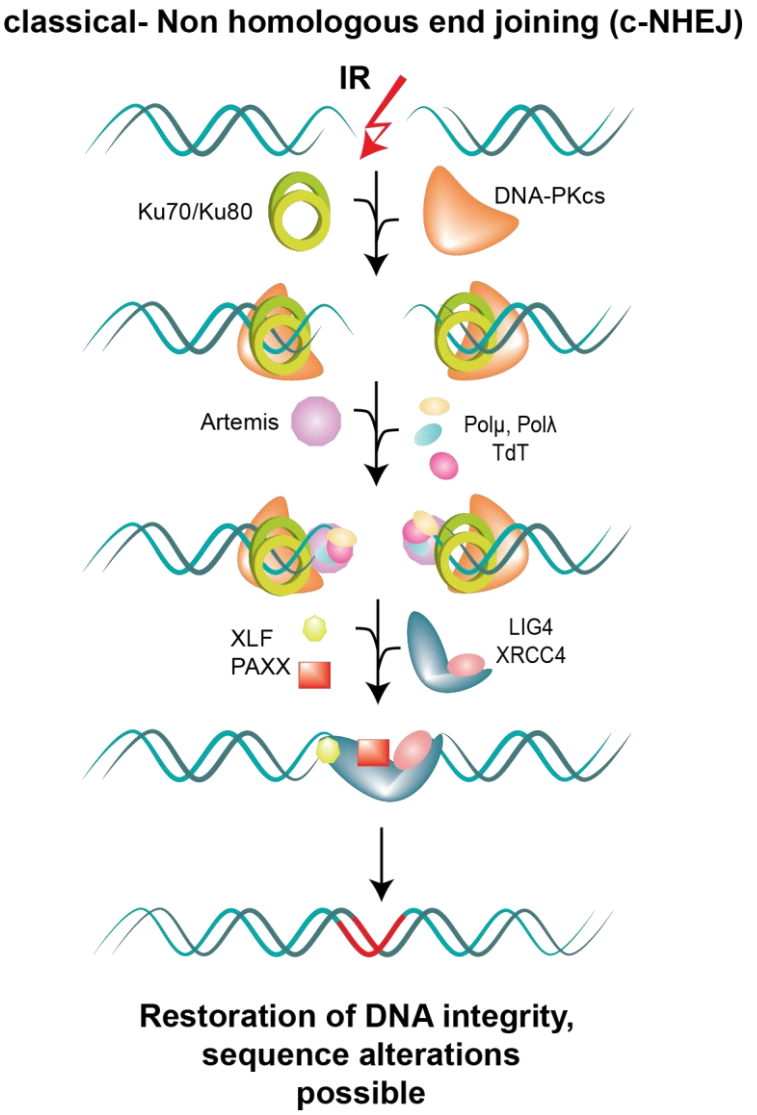

Figure 5: DSB processing by classical non-homologous end joining. C-NHEJ comprises a relatively small repertoire of molecules. Main steps involved in c-NHEJ include the binding of the Ku70/80 heterodimer to the DSB ends, which leads to the recruitment of DNA-PK. End processing enzymes help in cleaning up DSB ends to make them ligatable. Ligation is carried out by the Lig4/XRCC4/XLF complex. C-NHEJ is potentially error prone (see text) and may therefore, result in small scale alterations (Graphic modified from (Iliakis, et al. 2015b)).

One of the end-processing substrates phosphorylated by DNA-PK is the endonuclease Artemis. Artemis has been shown to carry out hairpin opening in order to remove ssDNA overhangs containing damaged nucleotides (Lieber 2010a). After DSB end “cleaning” the final step of c-NHEJ is the ligation of DSB ends, carried out by the coordinated action of the DNA XRCC4 – Lig4 and XLF complex (**Figure 5**).

Although, c-NHEJ restores chromosome continuity, it does not ensure that the correct DSB ends are rejoined and that the sequence around the break side is reestablished. This renders c-NHEJ a potentially error prone pathway, that can contribute to translocation formation.

1.3.4 Alternative end joining (alt-EJ)

Alt-EJ has drawn a lot of attention in the scientific field due to its highly error prone nature and its frequent implications in recurrent translocations found in many hematological diseases. Alt-EJ is considered to be suppressed when HRR and c-NHEJ are available and thus serves as a last resort when any of the other pathways is not able to engage and is therefore, often termed backup- end joining to emphasize such putative backup functions (Cho and Greenberg 2015; Mateos-Gomez, et al. 2015; Soni, et al. 2014). Throughout the literature, alt-EJ is described by three main characteristic. First, alt-EJ is less faithful in the restoration of the DNA, and is accompanied by high levels of translocations. Second, in comparison to c-NHEJ, alt-EJ comes with slower kinetics, ranging from 30 minutes to 20 h. Third, alt-EJ is not limited to a particular cell cycle phase, but a peak activity in the G_2-phase could be experimentally shown (Wu, et al. 2008).
Another feature often referred to alt-EJ is the use of microhomologies. Some reports suggest that alt-EJ benefits from short patches of microhomology ranging from 5 – 25 nucleotides distant from the DSB ends. Other reports however speculate that alt-EJ does not necessarily require microhomology, but may benefit from it when present. Even the presence of two distinct alt-EJ pathways has been suggested. One relaying on microhomology and the other acting independently of microhomology (Aparicio, et al. 2014; Decottignies 2013; Mansour, et al. 2010; Nussenzweig and Nussenzweig 2007).

So far, molecules suggested to participate in alt-EJ include Mre11 and CtIP both participating in end resection (Zhang and Jasin 2011). Also Ligase 3 has been demonstrated to carry out functions in alt-EJ (Wang, et al. 2005). When Ligase 3 is compromised, it was experimentally demonstrated that Ligase 1 can take over Ligase 3 functions (Soni, et al. 2014). Another important molecule is Parp-1 (Audebert, et al. 2004). Studies indicated that Parp-1 competes with the Ku70/80 heterodimer for DSB ends and in this way sets the stage for repair pathway choice. Recent reports also

suggest an involvement of the human polymerase θ, which was indicated to facilitate end – joining of DNA ends that contain microhomologies (Chan, et al. 2010; Kent, et al. 2015). Moreover, studies applying RNAi screening of known DNA damage response molecules identified further genes associated with alt-EJ. Those identified genes involve, FAAP24, NTHL1, RAD53B, POLA1, SOD1, RUVBL2, GEN1, TIP60, DNA2, SH6, FANCA and PRP19/PS04 (Howard, et al. 2015).

Figure 6 provides and summarizes a graphical presentation of the steps and molecules engaged in alt-EJ.

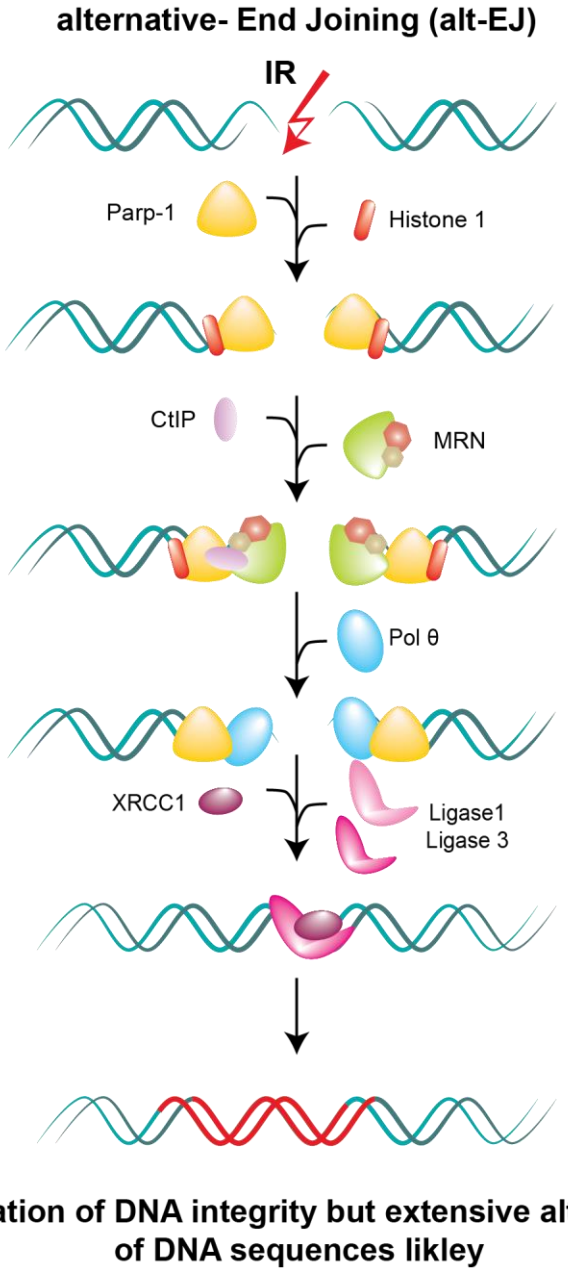

Figure 6: Repair of DSB breaks by alternative end joining. Alt-EJ engages in the repair of DSBs when c-NHEJ or HRR are somehow compromised, but at the price of a large increase in translocation

formation due to its highly error prone nature. Molecules identified to engage in alt-EJ include Parp-1, which is thought to bind to DSB ends. Alt-EJ seems also to benefit from resection. Hence, Mre11 and CtIP have also been shown to play a role. Ligation is carried out by Ligase 3 or Ligase 1 (Graphic modified from (Iliakis, et al. 2015b)).

1.4 Contribution of DSB repair pathways to processing errors and chromosomal aberration formation

If cells fail to repair DSBs or repair occurs by rejoining incorrect ends chromosomal rearrangements (CRs) occur, which will inevitably contribute to cell killing, genomic instability and cancer.

The ability to faithfully repair DSBs also depends on the inherent propensities for errors in the processing of DSBs by the different repair pathways.

The next section will unravel connections between DSB and CR formation and will discuss how DSB repair pathways contribute to CR formation.

1.4.1 DSBs and the formation of Chromosomal rearrangements (CRs)

CRs are defined as major changes in the structure of the native chromosome.

Looking back into ionizing radiation history, it actually was the study of microscopically visible chromosome aberrations in eukaryotes that was used to investigate the biological consequences of ionizing radiation (Durante, et al. 2013).

In fact, first correlations between IR and CR formation were reported by Karl Sax back in 1938. At that time Karl Sax postulated the so called “breakage and reunion” theory, describing the mechanisms of IR induced CRs; in this way he laid the foundations for correlations between IR and CR formation (Sax 1940). Yet, Sax’ theory was followed by an alternative theory proposed by Revell in the late 1950s which he called the “Exchange – theory” (Hlatky, et al. 2002; Revell 1974).

The “breakage and reunion” theory assumes that through energy loss by IR, breaks in the broken chromosome are induced, which Sax named “primary breaks”. This pair of broken chromosome ends is thought to freely-move around and is able to participate in random rejoining events. Basically, such primary breaks can, according to Sax, face three different fates: First, the majority (90%) of such breaks will get rejoined, second breaks may remain open and directly lead to terminal deletions,

which will become visible as chromatid breaks and third, the broken ends may rejoin with ends from other chromosome, forming translocations (**Figure 7**) (Natarajan 2002).

The alternative “Exchange theory” put forward by Revell, assumes that the initial damage is an unstable-lesion. Revell hypothesized that such unstable lesions decay to a normal state. If however, more unstable-lesions are brought together in pairs, they may take part in an exchange process and hence give rise to aberrations that can be visualized in metaphase. In this theory, breaks are only secondary and may arise when the exchange process fails (**Figure 7**) (Natarajan 2002).

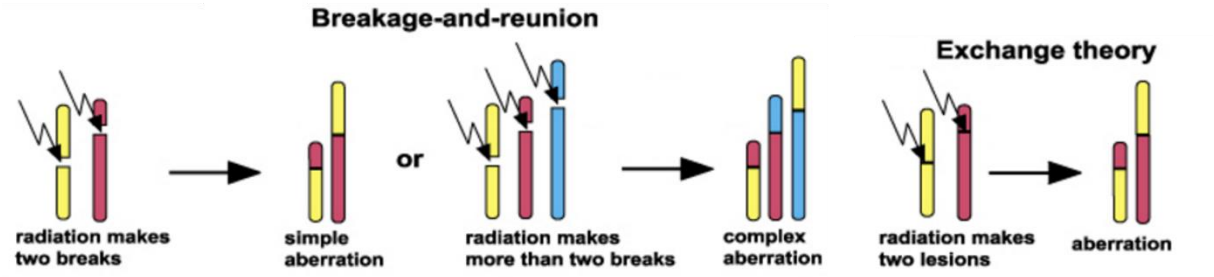

Figure 7: Models of Sax’ “Breakage and reunion” theory and Revell’s “exchange theory”. In the breakage and reunion theory the primary lesion is a break which engages in the formation of CRs. In the exchange theory radiation induces two labile lesions, which when they interact lead to aberrations (Graphic adapted from (Hlatky, et al. 2002)).

A lot of effort has been invested by cytogeneticists to elucidate the molecular mechanisms of CR formation. Today, most scientists favor the “breakage and reunion theory” and it is widely accepted, that DSBs are the primary lesion underlying CRs.

Taking into consideration that each chromatid comprises one continuous DNA molecule, unrepaired DSBs will present as chromatid breaks while misrepaired DSBs will manifest at times as CRs. Both types of aberrations can be visualized microscopically and have been intensively used as validated biomarkers for the assessment of cancer risk in humans and after radiation exposure.

1.4.2 Inherent propensities of DSB repair pathways to the formation of chromosomal rearrangements

Several steps are involved in the formation of CRs, the first being the induction of multiple DSBs in the same or different chromosomes. Second, repair mechanisms, which become activated upon DSB induction, must fail to correctly eliminate DSBs.

Finally, DSB ends must encounter wrong DSB ends for their ligation to give rise to the formation of CRs. (Cornforth 2001; Roukos, et al. 2013).

How do the different DSB processing pathways contribute now to the formation of CRs?

Let's first have a closer look at HRR and its capacity for CR formation. Even though HRR is considered to be error free due to its templated nature, its potential to form CRs lies in its requirement for sequence homology. Thus, inappropriate template choice can lead to CRs. Since there is a high abundance of repetitive sequences in the human genome (e.g. pseudogenes, repeats) invasions of homologous sequences on an ectopic chromosome can result in CR formation. CRs formed under such conditions are most likely of the exchange-type including for example inversions, reciprocal translocations, dicentrics, deletions or insertions (Kasparek and Humphrey 2011).

Moreover, inappropriate template choice can also occur in a sister chromatid and thus can give rise to unequal sister chromatid exchanges including duplications or deletions. However, several studies claim that HRR is unlikely to produce large amounts of CRs and that HRR is very efficient in their suppression. Particularly, studies in cell lines bearing mutations in HRR factors like BRCA1, CtIP or Rad51 and its paralogues show high levels of CRs (Soni, et al. 2014). Additional evidence that HRR is unlikely to induce CRs is given by the fact that translocation junctions often fail to show sequence homologies.

As mentioned previously, c-NHEJ by nature is error prone on two counts. First, it does not ensure DNA sequence restoration, and second it does not have a build in mechanism to ensure that the correct DSB ends are joined. Consequently, a single DSB is enough for c-NHEJ to form intrachromosomal rearrangements like for example inversions. Furthermore, c-NHEJ is also capable of forming CRs of the exchange type. Formation of such CRs require two DSBs that occur either on the same chromosome, or on different chromosomes giving rise to deletions, insertions, dicentric chromosomes, acentric fragments or translocations (Ghezraoui, et al. 2014; Kasparek and Humphrey 2011).

Although, c-NHEJ is error prone by nature many studies also point towards a suppressive role of c-NHEJ in CR formation. As described before, one of the most important features of c-NHEJ is its speed. Thus, the chance that right DSB ends will be rejoined is quite high. In addition, it has been outlined that the Ku70/80 heterodimer together with DNA-PK holds the DSB ends close together making misjoining events unlikely. Moreover, several reports demonstrated that spontaneous CRs are more frequent in $Ku70^{-/-}$, $Ku80^{-/-}$, $Lig4^{-/-}$, or $XRCC4^{-/-}$ cells. Also the inhibition of DNA-PKcs results in a strong increase in the formation of chromosomal translocations hinting towards a suppressive role of c-NHEJ in CR formation (Iliakis, et al. 2004; Lieber 2010b).

As a last resort for failed DSB repair by HRR or c-NHEJ, alt-EJ comes into play.

Since alt-EJ is a relatively slow process increasing the half-times of DSB ends, DSB ends may have more time to encounter each other thereby getting rejoined in a wrong way and form CRs of the exchange type. Besides, the prolonged half time of DSB ends, they do also bear a high risk for nuclease – mediated degradation and recombination, which can end up in deletions and fragments. Moreover, proteins implicated in alt-EJ show only weak interactions with the DSB ends leading to inefficient synapsis and rendering rejoining less efficient and slow. A translocation, frequently implicated to be due to the rejoining by alt-EJ, occurs between breaks in the igH locus and breaks in genes such as c-my in another chromosome (Saribasak, et al. 2011). This type of translocation is recurrent and often causes leukemia.

Figure 8 gives a schematic overview about the probabilities of the DSB repair pathways to contribute to the formation of chromosomal aberrations.

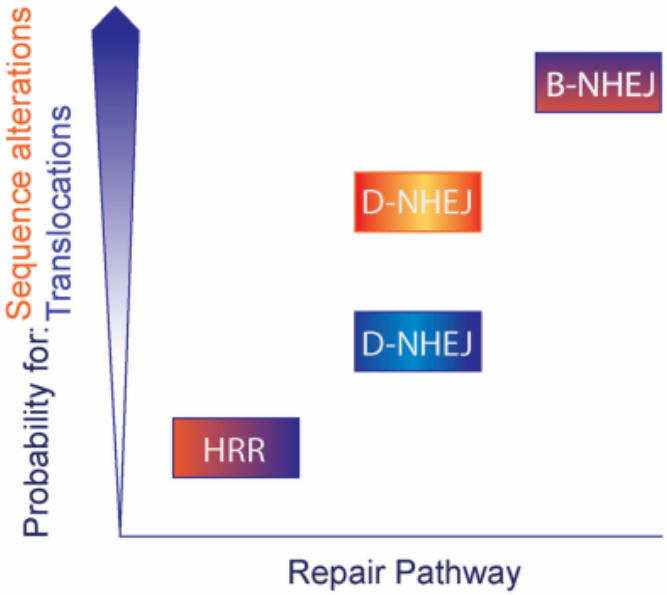

Figure 8: Probability of DSB repair pathways to induce chromosomal rearrangements. HRR is less likely to contribute to the formation of CRs due to its templated nature. C-NHEJ can theoretically cooperate in the formation of translocations as it lacks proofing mechanisms. Its speed however also suggests that often the right ends are rejoined. alt-EJ is highly error prone and often leads to the formation of translocations (Figure taken from (Schipler and Iliakis 2013)).

1.5 DSB repair pathway choice

Probably one of the most controversially discussed topics in the field of DNA repair concerns the DSB repair pathway choice. Why should we put efforts in understanding such a contested field? First, because the DSB repair pathway choice is not among equals and will therefore critically determine a cell's fate, and second because mechanistic insights into DSB repair pathway choice may be translated to the clinic to find potentially new therapeutic targets and exploit better strategies for chemo- or radiation therapy.

Components suggested to play a role in the DSB repair pathway selection include the cell cycle stage, DSB end resection, radiation dose, the chemical nature and complexity of the DSB and the chromatin structure.

The different requirements of repair by HRR for example restrict HRR to the late S- and G_2-phase. In contrast, c-NHEJ can be activated throughout the whole cell cycle but has been implicated to be more prevalent in G_1-phase, as HRR cannot function. alt-EJ could also be engaged throughout the whole cell cycle, but has been experimentally shown to have a peak activity in G_2-phase (Wu, et al. 2008).

Moreover, cell cycle dependent regulation of DSB repair pathway choice arises from the CDKs. CDK dependent phosphorylation of some components of the HRR machinery have been found to be activated at the beginning of the S – phase. Such molecules include for example Rad51, BRCA1, BLM and CtIP. Those proteins, or the transcripts used for the expression of these proteins, are only present at low levels in the G_1-phase giving thus way to c-NHEJ. Experiments have indicated that CDKs at the onset of S – phase also phosphorylate molecules that are involved in resection (CtIP, Exo1, Dna2) and may therefore shunt DSB repair to HRR. On the other hand, DSB end resection in G_1-phase is influenced by the low activity of the Cdc28/CDK, favoring repair by c-NHEJ (Aylon, et al. 2004; Symington and Gautier 2011).

In fact, DSB end resection seems to play a key role in DSB repair pathway choice. Especially, the antagonizing interactions between 53BP1 and BRCA1 have been described extensively. While 53BP1 suppresses resection in G_1 – phase, thereby promoting c-NHEJ, BRCA1 antagonizes this action by removing 53BP1 from the DSB site and allowing the stimulation of HRR. The ability of 53BP1 to inhibit resection is also due to the replication timing regulator factor 1 (RIF1) by blocking the recruitment of BRCA1 in the G_1 – phase. In S- and G_2 – phase however, BRCA1 and CtIP have been shown to antagonize the recruitment of RIF1 to the DSB (Aparicio, et al. 2014; Zimmermann, et al. 2013).

Despite regulatory functions of the cell cycle in the repair pathway choice, also the nature of the DSB ends has been suspected in DSB repair pathway decision. DSB ends with a 3’ hydroxyl and a 5’ phosphate group could be directly ligated by c-NHEJ. IR however often induces ‘dirty’ ends, which need processing to render them ligatable. Such processing can be carried out by the polynucleotide kinase 3’ phosphatase (PNKP), Aprataxin, Ku, or Artemis, which most likely shunt repair to c-NHEJ. Additionally, DSB ends may be processed by the MRN/CtIP complex and the exonuclease WRN. The resulting single stranded DNA overhangs are often too long, making c-NHEJ incapable to engage at the ends and depending on the cell cycle stage, repair by alt-EJ or HRR may be favored (Aparicio, et al. 2014).

Additional reports also suggest a role of chromatin in DSB repair pathway choice. Legube and Clouaire (Clouaire and Legube 2015) described that DSBs that are induced in active genes are channeled to HRR repair. Other scientists state that

repair of DSB in heterochromatin and euchromatin respectively, may be repaired by different DSB repair pathways. Similarly, chromatin modifications caused upon DSB induction may stabilize certain molecules, whereas other molecules may be inhibited from assessing the DSB, contributing thus to DSB repair pathway choice.

1.5.1 Previous work on the relative contributions of DSB repair pathways on the processing of IR induced DSBs and chromatid breaks

Previous experiments in our lab shed light on the contribution of the three DSB repair pathways in different cell cycle phases after exposure of different CHO mutants to high doses of IR.

Specifically, wildtype (V79) and cells mutated in components of c-NHEJ like Ku80 (xrs5) and DNA-PK (XR-C-1-3), as well as cells mutated in the Rad51 paralogues XRCC3 (irs1-SF) and XRCC2 (irs1) were exposed to 20 Gy IR. DSB rejoining was measured by means of pulsed field gel electrophoresis (PFGE) at different times after IR in either asynchronous cells or in cells sorted in the G_1- or the G_2-phase of the cell cycle, to make estimations of the contributions of the different DSB repair pathways, in different cell cycle phases.

V79 (wt) cells, repaired nearly 80% of IR induced DSBs within the first 1 h after irradiation when measured in asynchronous cells. Furthermore, similar results were obtained for V79 cells sorted in G_1- or G_2-phase of the cell cycle. Thus, the repair capacity of wildtype cells seems similar in these phases of the cell cycle (**Figure 9**).

Next, DSB repair capacity was measured in c-NHEJ mutants comprising defects in Ku80 (xrs5) or DNA-PK (XR-C-1-3). Asynchronous cells revealed repair deficiencies, resulting from mutations in c-NHEJ components. More interesting, however was the observation that both c-NHEJ mutant cell lines (xrs5 and XR-C-1-3) showed different capabilities of DSB repair when sorted in the G_1 – or G_2 – phase of the cell cycle. While G_1 – sorted cells were less efficient in repairing IR induced DSBs, as compared to the repair in asynchronous cells, G_2 – sorted cells showed better DSB repair at all times post IR (**Figure 9**).

To investigate whether this observation could be attributed to an enhanced function of HRR, which could be expected in the G_2-phse of the cell cycle, IR induced DSB

repair was measured in cells with mutations in the Rad51 paralogues XRCC2 (irs1) and XRCC3 (irs1-SF). Both HRR mutant cell lines demonstrated a rapid repair of DSBs regardless of whether rejoining was measured in asynchronous, or in G_1 or G_2 sorted cells (**Figure 9**). These results suggest that HRR has only a minor contribution to the repair of IR induced DSBs at high IR doses when measured with PFGE. For the c-NHEJ mutants however, results suggest an enhanced function of alt-EJ particularly for cells sorted in G_2-phase. Furthermore, the results obtained also suggest a predominant role of c-NHEJ in the repair of DSBs after exposure of cells to high IR doses.

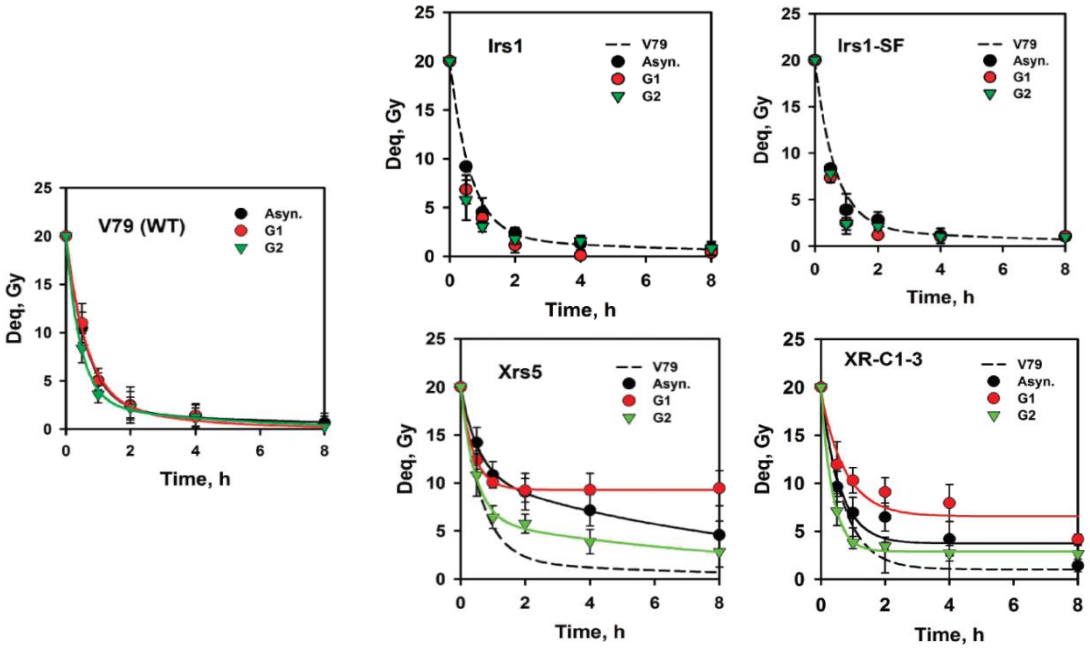

Figure 9: Rejoining of IR induced DSBs in wildtype, c-NHEJ or HRR deficient Chinese hamster cell lines measured by pulsed – field gel electrophoresis. Figure adapted from (Wu, et al. 2008).

Another hint towards a dose dependent repair pathway regulation comes from immunofluorescence-based work carried out in our laboratory. Rad51 foci formation was measured in the late S- and G_2-phase as an estimation of DSBs that are repaired by HRR. Observed data revealed that Rad51 foci reach a plateau with increasing radiation dose suggesting a saturation of HRR with increasing radiation dose (**Figure 10**). Thus, a dose dependent regulation of repair pathway utilization was suggested.

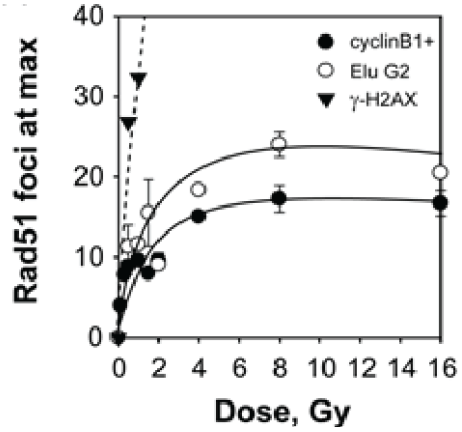

Figure 10: Decreasing contribution of HRR with increasing IR dose. Measuring Rad51 foci as a parameter for the activity of HRR in G_2-phase cells reveals saturation of Rad51 foci with increasing IR dose suggesting a saturation of HRR activity (Graphic adapted from (Demond 2016)).

1.5.1.1 Contributions of DSB repair pathways to the processing of IR induced chromatid breaks

Upon DSB induction, a small subset of DSBs is converted to chromatid breaks (CBs), which can be visualized via classical cytogenetic techniques in the following metaphase, or in G_2 phase of the cell cycle using the premature chromosome condensation (PCC) technique. PCC can be chemically induced with Calyculin A and leads within minutes to the condensation of G_2 chromatin to distinct chromosomes without the need to progress to mitosis. This technique avoids analysis limitations generated by the IR induced cell cycle checkpoint and allows, cell cycle specific chromatid break frequency analysis, even after high IR doses (Shovman, et al. 2008). Previous experiments carried out in our laboratory were designed to advance our understanding regarding the repair pathways involved in CB processing in the G_2 – phase of the cell cycle. This cell cycle phase is particularly interesting as all three DSB repair pathways are operational and can engage in DSB processing.

CB repair was analyzed by exposing asynchronous cells to low IR doses (1 Gy) and damage analysis was carried out in the following metaphase. To this end a previously developed cytogenetic protocol was used, which allows cell cycle specific analysis by using a 1 h colcemid block to accumulate cells at metaphase. To analyze CB repair in cells that have been irradiated in the G_2 – phase, a colcemid block was directly applied after IR as well as 4 h post IR. Accumulating metaphases will represent cells that have been at the end of G_2 phase during IR (1 h post IR) or at the late S – phase/early G_2 – phase respectively (4 h post IR). In this way, the protocol

allows a cell cycle specific investigation of chromatid break processing, at a cytogenetic level.

With the above-mentioned procedure the interplay of the DSB repair pathways on the repair of IR induced CBs was investigated in different CHO wildtype and mutant cell lines.

Wildtype cells showed nearly complete repair of IR induced CBs by 5 h after IR. Next, CB repair kinetics was studied in cells with a HRR deficient background. Surprisingly, HRR mutants showed a strong deficiency in CB repair. On the other hand, cells mutated in components of c-NHEJ did show processing of CBs with similar kinetics to wildtype cells, although higher numbers of initial CBs were found (**Figure 11**).

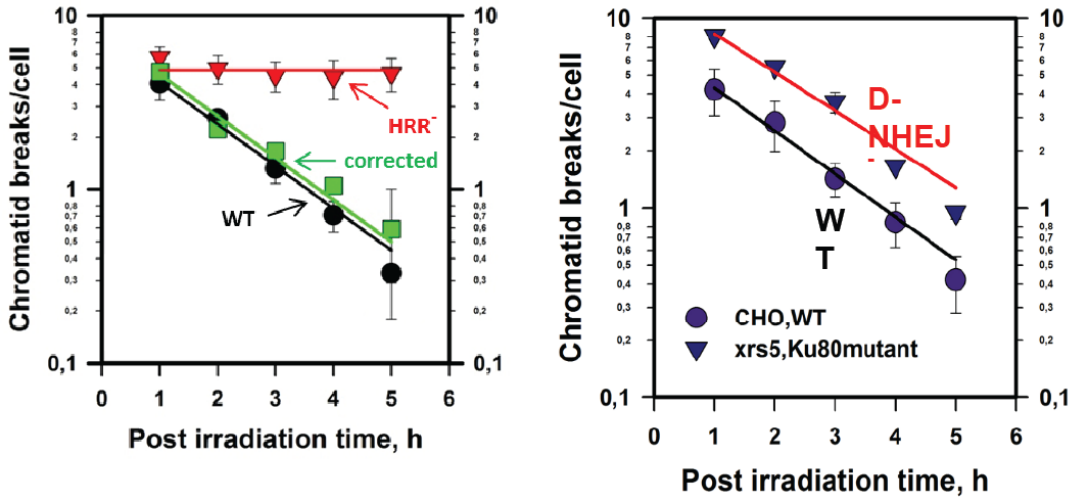

Figure 11: Repair of IR induced chromatid breaks in different CHO cell lines. HRR mutants show complete inhibition of CB repair after exposure to 1 Gy IR when analyzed in metaphase. Wildtype and c-NHEJ mutant cells lines show normal repair kinetics (Graphic adapted from (Soni 2010)).

The above-described observations suggested a crucial importance of HRR in chromatid break repair after exposure of cells to low doses of IR i.e. 1 Gy.

While PFGE based experiments suggested a dominant role of c-NHEJ in the removal of DSBs in G_2 – phase and almost no contribution of HRR after exposure to high IR doses, the situation is different after low doses of IR. Data on CB rejoining suggest that HRR has a more pronounced role in CB repair after exposure to low IR doses (1 Gy) going along with a strong repair defect, when compromised. On the other hand, deficiency in c-NHEJ does not result in CB repair inhibition after 1 Gy IR, suggesting that defects in c-NHEJ can be compensated by HRR.

In follow up experiments the contributions of DSB repair pathways to the repair of CB was further assessed in Chinese hamster wildtype cells and HRR mutant cells after exposure to high IR doses (5 Gy). CB repair was followed in the G_2 – phase of the cell cycle using the chemically induced PCC technique to avoid complications from the activation of the cell cycle checkpoints.

IR induced CB repair kinetics was analyzed within the first 8 h post IR. To prevent S – phase cells from entering G_2 – phase a nuclear replication inhibitor (Aphidicolin) was used to block cells in S – phase. Wildtype cells (V79) showed rapid repair of IR induced G_2 PCC breaks both after exposure to 1 Gy and 5 Gy IR (**Figure 12**).

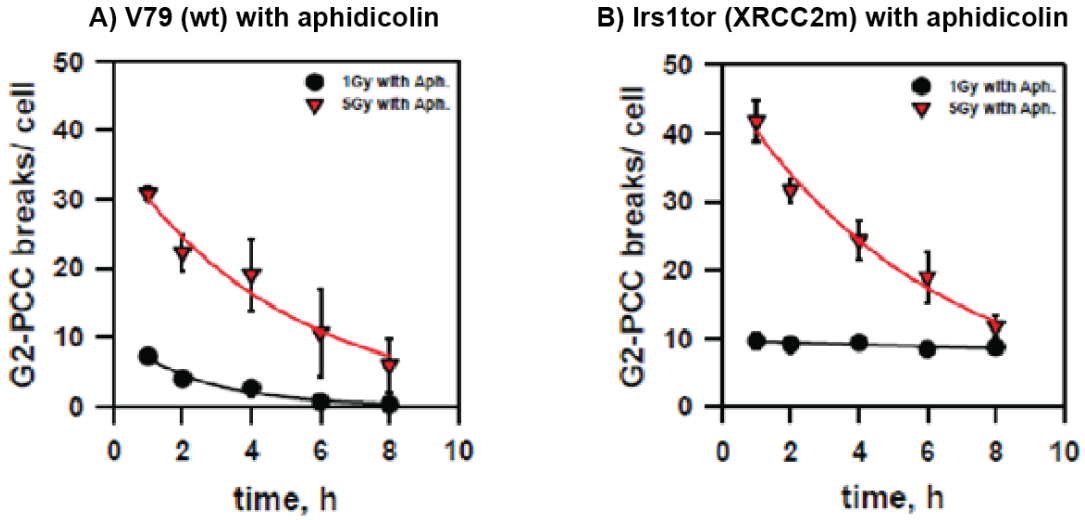

Figure 12: G_2 PCC break repair in V79 (wt) (A) and Irs1 – tor (HRR m) (B) cell lines. Cells were exposed to 1 Gy or 5 Gy IR and G_2 PCC break repair kinetics were measured till 8 h after IR (Graphic adapted from (Siemann 2013)).

For the HRR mutant cell line (irs1-tor) a strong G_2 PCC break repair abrogation was visible after exposure to 1 Gy IR, similar to previously obtained results using the classical cytogenetic protocol. More interesting however, was the observation that HRR mutant cells start to show CB processing when exposed to high IR doses (5 Gy) resulting in the repair of almost 70% of CBs (**Figure 12**).

In conclusion, these preliminary data generate solid foundation that justifies a thorough investigation of a possible dose – dependent DSB repair pathway regulation.

2. THESIS OBJECTIVE

In present thesis, the above-described findings are taken to the next level of investigation. The contributions of the different DSB repair pathways are studied primarily in the G_2 – phase of the cell cycle, by focusing on the repair of IR induced chromatid breaks. For this purpose different cell lines with mutations in key components of the different DSB repair pathways, as well as chemical inhibitors are employed and are exposed to a broad spectrum of ionizing radiation doses. Ultimate goal is to investigate, whether there is an IR dose dependent DSB repair pathway switch. To address these questions the experimental setup outlined above is applied, which allows to measure the contribution of all three DSB repair pathways in CB processing in the G_2 – phase. To investigate repair of chromosomal breaks after high IR doses and to avoid limitation arising from the G_2 checkpoint, the Calyculin A induced PCC technique is employed. PCC allows the visualization of interphase chromosomes in a condensed form, similar to that present in mitotic chromosomes, without the need to progress to mitosis. In this way, analysis of IR induced chromatid break repair becomes possible in G_2 – phase by collecting cells at fixed time points post IR. Assuming duration of 4 h for the G_2 – phase, analysis of PCC breaks is carried out within the first 4 – 6 h after irradiation to obtain mostly the response of cells that have been irradiated in the G_2 – phase. However, contaminations from cells coming from late S – phase cannot be excluded particularly at the later time points.

Throughout the thesis, we outline our efforts to develop approaches to improve the power of PCC technique in the form of analysis and to validate solutions we discovered. Goal is to improve the cell cycle specificity of the analysis.

In most experiments we chose Chinese hamster cell lines, as a model, since different mutants have been generated, allowing us to address DSB repair pathway specific questions.

3. MATERIALS & METHODS

3.1 Materials

3.1.1 Major laboratory apparatuses

Laboratory apparatus	Model	Provider
Cell and Particle Counter	Z2 Coulter Counter®	Beckman Coulter Inc., USA
Cell culture CO_2 incubators	MCO-18AV (UV)	Sanyo, Japan
Centrifuge	Multifuge ™3S-R	Hereaus, Germany
Confocal laser scanning Microscope	TCS SP5	Leica Microsystem, Germany
Firewire Camera	Marlin F-145C2	AVT Allied Vision Technologies, Germany
Flow cytometer	Gallios™	Beckman Coulter Inc., USA
Laminar flow cabinet	HERAsafe™	Hereaus, Germany
Leica Inverted Light Microscope	LEITZ DM RBE	Leica, Germany
Metafer Slide Scanning Plattform	MetaSystems	MetaSystems, Germany
pH meter	InoLab®	WTW GmbH, Germany
Water bath	Waterbath WNB	Memmert GmbH + Co. KG, Germany
Weighing Balance	Sartorius	Sartorius Germany
X-ray machine, Isovolt 320 HS		General Electric, Pantak/Seifert

3.1.2 Cell culture consumables

Consumable	Provider
Cell culture dishes (100mm and 60mm)	Greiner bio-on
Fetal bovine Serum (FBS)	GIBCO Life Science
Minimum essential medium (MEM)	Sigma-Aldirch
Non-essential amino acids (NEAA)	Merck Millipore
Penicillin	Sigma-Aldrich
Phosphate-buffered saline (PBS)	Roth
Serological plastic pipettes	Sarstedt
Streptomycin	Sigma-Aldrich

3.1.3 Cytogenetic consumables

Consumable	Provider
Buffer Tablets “GURR”	GIBCO
Entellan® (mounting medium)	Merck
Giemsa	Roth

High Precision Microscope Cover Glasses 24x60 mm	Roth
Immersion oil	SIGMA Life Science
Microscope Slides, 76x26 mm	Roth

3.1.4 Cell lines

Name	Characteristics	Cell type and biological source	Growth media
82-6 hTERT	wt	Human, fibroblast	MEM+ 1% NEAA, 10% FBS
CHOK1	wt	Ovary from Chinese hamster, epithelial	MEM+10% FBS
V79	wt	Lung from Chinese hamster, fibroblast	MEM+10% FBS
Irs-1 tor	XRCC2 m	Lung from Chinese hamster, fibroblast	MEM+10% FBS
Irs-2 tor	Rad51b m	Lung from Chinese hamster, fibroblast	MEM+10% FBS
IRS1 SF	XRCC3 m	Ovary from Chinese hamster, epithelial	MEM+10% FBS
XR-1	XRCC4 m	Ovary from Chinese hamster, epithelial	MEM+10% FBS

3.1.5 Software

Software	Provider	Application
Adobe® Creative Suite® 6	Adobe Systems Inc., USA	Graphic design
EndNote® X7	Thomson Reuters, USA	Reference management
Ikaros Karyotyping System	MetaSystems, Gemrany	Analysis of Giemsa Stained Metaphases/PCCs
Isis Fluorescence Imaging Platform	MetaSystems, Germany	Analysis of EdU stained PCCs and immunofluorescence in cytogenetics
ImageJ	Image Processing and Analysis in Java, USA	Analysis for cytogenetics
SigmaPlot® 12.5	Systat Software Inc., USA	Graphical Presentation of Data
Microsoft Office® 2010	Microsoft, USA	Word processing (Word), Data analysis and calculation (Excel)
Kaluza® 1.2 for Gallios	Beckman Coulter Inc., USA	Flow cytometry analysis

WinCycle AV	Phoenix Flow Systems, USA	Cell cycle analysis

3.1.6 Antibodies for immunofluorescence

Chemicals	Provider
4'.6-diamidino-2-phenylindole (DAPI)	SERVA
5-bromo-2‘-deoxyuridine (BrdU)	SERVA
5-Ethenyl-2’deoxyuridine (EdU)	Santa Cruz
Acetic Acid	Roth
Ascorbic Acid	Roth
Bovine Serum Albumin (BSA) fraction V	Roth
Calyculin A	LC Laboratories
Click-iT® EdU Alexa Fluor®647 Imaging Kit	Life Technologies
Colcemid	Calbiochem, Merck Millipore
Copper(II) sulfate pentahydrate	Sigma-Aldrich
Crystal Violet	Merck
Cy®5	ThermoFisher Scientific
Dimethyl sulfoxide (DMSO)	Sigma Aldrich
Ethanol	Sigma Aldrich
Ethylenediaminetetraacetic acid (EDTA)	Roth
Formaldehyde	Merck
KU5593 (ATM inhibitor)	Calbiochem
Methanol	J.T. Baker
NU7441 (DNA-PK inhibitor)	Tocri Bioscience
Olaparib	LC Laboratories
Paraformaldehyde (PFA)	Roth
Pepsin	Sigma-Aldirch
PJ34 (PARP inhibitor)	Merck Millipore
Potassium Chloride, KCl	Roth
PromoFluor Antifade Reagent	PromoKine
Propidium iodide	Sigma-Aldrich
RNase	
Sodium Chloride	Roth
Sulfo-Cyanine5 azide	Lumiprobe
TRIS PUFFERAN®	Roth
Triton X-100	Roth
Tween 20	Roth

3.2 Methods

3.2.1 General Cell culture

Cell lines were maintained as exponential cultures, through routine passaging, at 37°C and 5% CO_2 and 95% air. Chinese hamster cells were grown in minimal

essential medium (MEM) supplemented with 10% fetal bovine serum (FBS) and antibiotics. Human 82-6 hTERT cells were grown in MEM supplemented with 1% non-essential amino acids (NEAA) and 10% FBS. Routine passaging was carried out by removing the culture medium, washing the cells with 1x PBS, before trypsinization with 0.05% trypsin in EDTA. Trypsinization was stopped by adding fresh culture medium. Cells were counted with a cell and particle counter (Z2 Coulter Counter, Beckman Coulter) and appropriate numbers of cells were plated in fresh medium. Frozen cells were thawed and passaged 1 – 2 times before experiments.

3.2.2 X – ray irradiation

To induce double strand breaks cells were irradiated at various doses using a X-ray unit (Precision X-ray, North Branford, CT) operated at 320 kV, 10 mA with a 1.65 Al filter at a distance of either 50 cm (for irradiation of 60 mm dishes) or 100 cm (for irradiation of 100 mm dishes), at a dose rate of ~3.7 Gy/min or 1.68 Gy/min respectively.

3.2.3 Inhibitor treatments

To measure the contribution of different DSB repair pathways cells were treated with various inhibitors. **Table 1** gives an overview of these inhibitors, their mode of action and the protocols of their application in experiments.

Table 1: List of inhibitors applied in experiments.

Inhibitors Name	Inhibitor Description	Working concentration	Administration
Calyculin A	Inhibitor of serine/threonine phosphatase PP-1 and PP-2	100nM	30 min before time point collection
NU7441	Inhibitor of DNA-PKcs	5µM	1h before IR
Olaparib	Inhibitor for Parp1/2	5µM	1h before IR
PJ34	Inhibitor of Parp1/2	5µM	1h before IR

3.2.4 Calyculin A induced premature chromosome condensation technique

Premature chromosome condensation technique refers to the condensation of chromosomes outside of mitosis (condensation of interphase cells). Therefore, the PCC technique enables to assess IR induced chromatid breaks and aberrations in

interphase cells. The technique can further be applied after a broad spectrum of IR doses since it circumvents the G_2 checkpoint. Premature chromosome condensation was chemically induced, using 100 nM Calyculin A given to the cells 30 min before the time point of cell collection. Upon treatment with Calyculin A cells round up and detach from culture dishes. Cells were collected by centrifugation for 7 minutes at 1200 rpm at 4°C. Medium was discarded and cells were carefully resuspended. To allow visualization of prematurely condensed chromosomes, cells were treated for 10 min at RT with 10 ml hypotonic solution (75 mM KCl), which was added dropwise to the cells. Next, samples were again centrifuged for 7 min at 1200 rpm at 4°C. Hypotonic solution was discarded and the pellet was carefully resuspended. To preserve cells in their swollen state and to remove cell debris cells were fixed 3 times in Methanol-Acetic Acid in a 3:1 ratio. Spreads were prepared by dropping 15 µl of fixed cells on clean wetted glass microscope slides, which were then allowed to air dry overnight.

Slides were stained in 5% Giemsa prepared in “GURR” Buffer for 15 min. After staining, slides were rinsed with tap water and allowed to air dry before mounting them evenly with Entellan.

Slides were analyzed with an inverted light microscope. Per experiment, 50 – 100 PCCs were scored for each sample. Most of experiments were analyzed in a coded manner to avoid and minimize bias.

3.2.5 Classical Cytogenetics

Classical cytogenetics allows to investigate IR induced chromatid breaks and translocation for cells reaching metaphase. To prepare metaphase spreads the same protocol was followed as described for Calyculin A induced premature chromosome condensation, with the difference that metaphases were accumulated by adding colcemid 1 h before time point collection at a working concentration of 0.1 µg/ml. Cells were collected by trypsinization and processed as described under **3.2.4**.

3.2.6 EdU staining for fixed cytogenetic samples

In order to discriminate between G_2 PCCs coming from cells irradiated in S-phase and those of cells irradiated in G_2, an EdU pulse labelling was applied. EdU was administered to the cells at a working concentration of 10 µM 30 min before IR. After

IR, EdU was removed from the cells by aspirating the cell culture medium and washing cells 2 times with pre-warmed PBS and supplementing them with fresh pre-warmed growth medium. Time points were collected and the samples were treated as described for Calyculin A induced PCC technique (**3.2.4**). Spreads were prepared as described above. After overnight drying, slides were fixed for 15 min. at RT with 2% PFA. Next, slides were shortly washed with 1x PBS. Per slide 90 µl Click-iT reaction was prepared (**Table 2**). Slides were incubated with Click-iT reaction cocktail on Parafilm for ~1 h in the dark at RT. Afterwards, slides were washed for 5 min in 1x PBS and then counterstained with 50 ng/ml DAPI for 10 min in the dark. After DAPI staining slides were shortly rinsed with distilled water and allowed to air dry at RT in the dark. Slides were mounted with PromoFluor antifade reagent and covered with a cover slip. Slides were scanned with a predefined protocol using a MetaSystems working station and analysis was carried out with the Isis Fluorescence Imaging Platform.

Table 2: Click-iT reaction cocktail.

Solutions needed	Concentration Click-iT reaction
1M Tris pH 7.4	100 mM
1xPBS/MilliQ H_2O	
10 mM $CuSO_4$	1.25 mM
1 mM Azide dye	1.25 mM
500 mM Ascorbic Acid	1.25 mM

3.2.7 Flow cytometry

To assess the cell cycle distribution, cells were stained with propidium iodide (PI), which binds to the DNA proportionally to its mass and can be detected by fluorescence activated cell sorting. PI fluoresces red and is excited with an Argon laser at 488 nm.

For cell cycle analysis cells were previously harvested and fixed in cold 70% ethanol and stored at 4°C (longer storage was at -20°C), till the time of analysis. Before analysis, cells were centrifuged at 4°C for 5 min at 1500 rpm. Ethanol was discarded and the cell pellet was re-suspended in PI staining solution containing RNAase which clears all RNA, for 15 min at 37°C in a water bath. Cells were then subjected to flow cytometry. 10 000 – 20 000 events per condition were analyzed. To ensure that the cells of interest were measured, gating was monitored based on the side and forward

scattering. Cell cycle analysis was carried using Kaluza® Software or WinCycle® Software.

3.2.8 Clonogenic survival assay

To measure the capacity of cells to produce progeny after exposure to IR, clonogenic survival assays were conducted. To allow the formation of colonies from a single cell, cells to be tested were plated in low numbers aiming towards 30 – 150 colonies/dish. The number of plated cells was adopted according to the IR dose. Before experiments cells were plated to obtained exponential cultures. At the day of experiment cells were exposed to different IR doses and plated immediately. Cells were incubated for ~7 days at a humidified atmosphere at 37°C and 5% CO_2. Colonies were stained with 1% Crystal Violet in 70% Ethanol and counted. Only colonies that comprised 50 or more cells were scored.

3.2.9 BrdU Assay

BrdU is a nucleoside analogue, which can be used in order to detect S-phase cells. BrdU is incorporated into the DNA during DNA replication instead of thymidine. To measure the progression of S-phase cells through the cell cycle the BrdU assay was used. Exponentially growing cells were pulse-labelled with 10 µM BrdU 30 min before IR. BrdU was washed out directly after IR, using pre-warmed 1x PBS and cells were supplemented with fresh pre-warmed growth medium. Time points were collected by harvesting of cells and centrifugation for 5 min at 1500 rpm. Medium was discarded and cells were fixed in cold 70% ethanol. Samples were stored at -20°C till the time of analysis.

At the time of analysis, samples were centrifuged for 5 min at 1500 rpm and ethanol was discarded. Cell pellet was washed with 1 ml NaCl (0.9%) and again centrifuged for 5 min at 1500 rpm and NaCl was discarded. Cell pellet was incubated in 1 ml Pepsin solution for 10 min in a water bath at 37°C. Another 3 ml of NaCl (0.9%) was added and samples were centrifuged for 5 min at 2500 rpm. Solution was discarded, pellet was vortexed and 1 ml of 2N HCl was added for 30 min at RT. 3 ml of NaCl (0.9%) was added and samples were centrifuged at 2500 rpm for 5 min. Solution was discarded and cell pellet was washed with 1 ml PBS-Tween 20 (0.05%) and samples were again centrifuged at 2500 rpm for 5 min. Anti-BrdU Antibody as diluted 1:50 in

PBS-Tween 20 (0.05%) and added to the cell pellet for 90 min at 4°C. After Antibody incubation 1 ml of PBS was added and samples were centrifuged for 5 min at 2500 rpm. Cell pellet was washed with 1 ml PBS-Tween 20 (0.05%) – BSA (1%) and centrifuged for 5 min at 2500 rpm. After centrifugation solution was discarded and secondary antibody AF488® was added diluted 1:300 in PBS for 30 min at 4°C, in the dark. At last, 3 ml PBS was added and samples were centrifuged for another 5 min at 1500 rpm.

Cell pellet was diluted in 1 ml PI solution and incubated for 15 min, at 37°C in a water bath and measured in a flow cytometer using appropriate gating to discriminate between BrdU positive and negative cells.

3.2.10 Statistical analysis

Graphs were created using SigmaPlot 12.5. Mean and standard deviation was calculated from results obtained in independent experiments. The statistical significance was calculated using two tailed Students *t*-test. The following asterix designation is used: $P < 0.001$ ***, $P < 0.01$ **, $P < 0.05$ *.

4. RESULTS

PART I: VALIDATION OF PREMATURE CHROMOSOME CONDENSATION TECHNQIUE

4.1 Premature Chromosome Condensation (PCC): Attempts towards Assay validation

Premature chromosome condensation (PCC) is a technique used since the 1970s for the analysis of IR induced chromosome damages. Throughout the years, the PCC technique was further optimized and today PCCs can be induced chemically by Calyculin A (Johnson and Rao 1970; Miura and Blakely 2011).

Its beauty is that it allows the investigation of IR induced chromatid breaks in interphase cells. In this way, cells do not need to progress to metaphase and lack of proliferation or G_2 – checkpoint issues are circumvented, allowing analysis of more cell types even after high IR doses.

Most of the experiments, described throughout this thesis, employ the PCC technique. Our main point of interest is to shed light on the contribution of the different DSB repair pathways to the processing of IR induced PCC breaks for cells that have been irradiated in the G_2-pahse of the cell cycle, where all DSB repair pathways can engage.

For most experiments, we use Chinese hamster cells, as a model to study IR induced chromatid break repair. Different Chinese hamster mutant cell lines have been generated before, which allows us to address DSB repair pathway specific questions. Another advantage of Chinese hamster cells is their karyotype, encompassing only 19-22 chromosomes, making the analysis straightforward (Wurm and Hacker 2011).

In **Figure 13**, examples of the different morphologies of chemically induced PCCs, using Calyculin A, are presented.
It can be clearly differentiated between early-, middle, and late S – phase PCCs (**Figure 13, A, B, C**), which are characterized by their “pulverized” appearance. G_2 PCCs in contrast present as condensed chromatids that lie parallel to each other (**Figure 13, D**). Metaphases (**Figure 13, E**) can be distinguished from G_2 PCCs by

their centromeric constriction, which is absent in G_2 PCCs. Taken into consideration, that each chromatid contains a single DNA molecule, chromatid breaks are thought to represents unrepaired DSBs. After IR, a subset of DSBs is converted to chromatid breaks, which can be visualized with Giemsa staining. PCC breaks can be scored and quantified as shown in **Figure 13 F**. By definition, a PCC break is a discontinuity in the chromatid that is larger than the width between the chromatids (Savage 1975). Yet, chromatid exchanges (**Figure 13, G**) can also be visualized and scored.

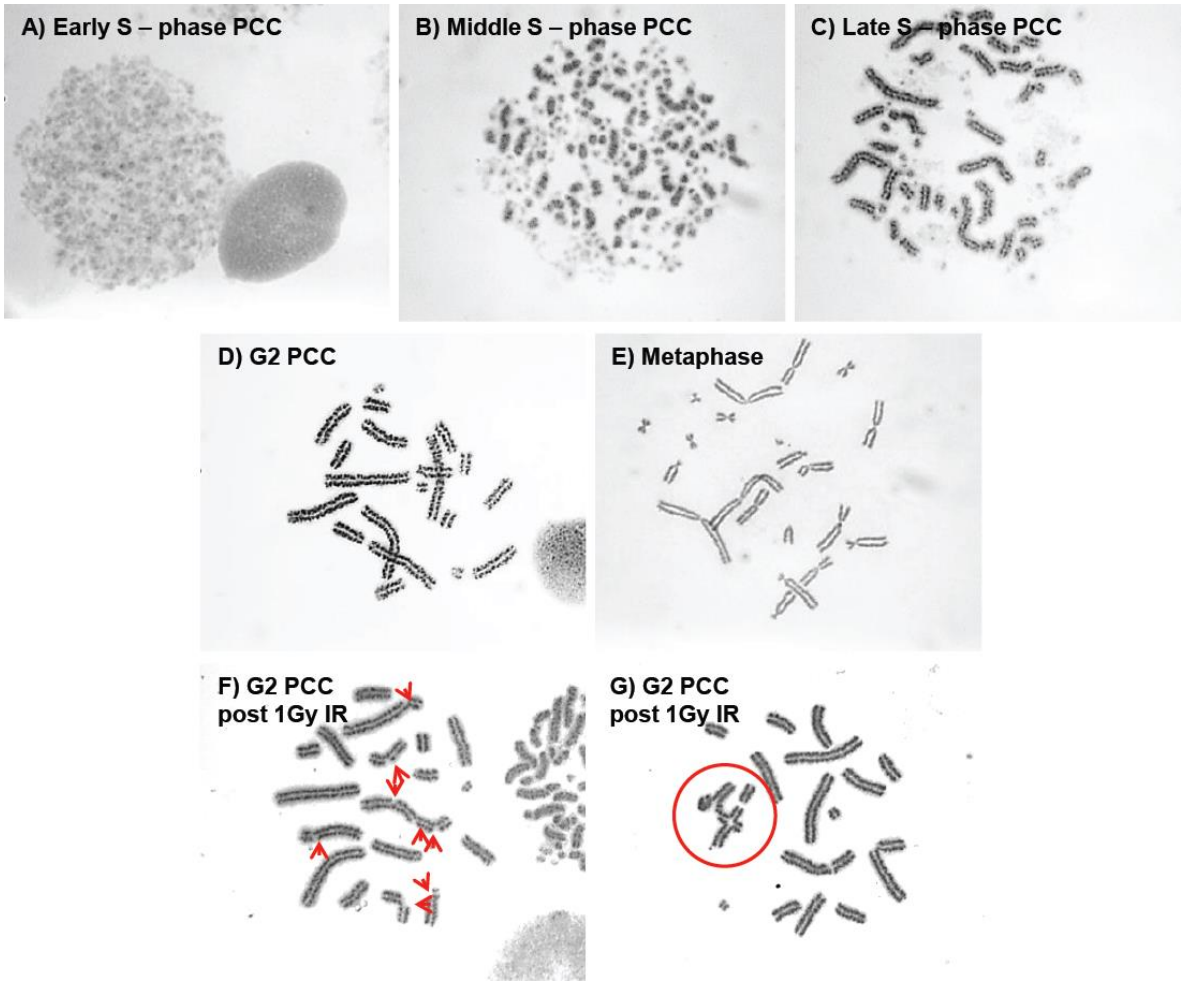

Figure 13: Morphology of Calyculin A induced PCCs in Chinese hamster cells. It can be distinguished between early-, middle-, and late S-phase PCCs (A, B, C), which are characterized by their pulverized appearance. G_2 PCCs (D) present as parallel chromatid threads lacking the centromeric constriction, which is characteristic for metaphases (E). Upon IR chromatid breaks become visible (F) as indicated with the red arrows. In additions, chromatid exchanges (G) can form as indicated by the red circle.

Before progressing to experiments, we need to provide sound validation of the PCC technique for the intended type of analysis.

A question often raised when the PCC technique is used for experiments, is whether there is contamination with S-phase cells. At early time points such cells may be

mistaken as cells containing CB, whereas at the late time points we will analyze cells irradiated in S-phase and therefore possibly showing a different response. Both complications will bias the results obtained and may mislead to erroneous interpretations.

Generally, PCC leads to the condensation of cells that are in the G_2-phase of the cell cycle. Yet, the PCC technique does not exclude, cells which are in the late S-phase during the time of irradiation and would arrive in G_2-phase at later times and present as G_2-PCCs, which will be indistinguishable to real G_2-PCCs.

One approach to circumvent this issue of S-phase cells coming to G_2 – phase includes the addition of DNA-synthesis (S-phase) inhibitors. Previous PCC experiments carried out in our lab included therefore aphidicolin, which is a specific DNA polymerase inhibitor and blocks S-phase cells from progressing to G_2 – phase (Siemann 2013).
Drawback of this approach, however, is that such inhibitors may interfere with normal cell cycle progression upon irradiation and greatly influence the experimental outcome. Moreover, it is known that aphidicolin increases the number of PCC breaks on its own, rendering the addition of aphidicolin less favorable.

Consequently, we sought new approaches for PCC technique validation. Here we describe our attempts towards validation of techniques circumventing the use of S-phase inhibitors.

4.1.1 BrdU pulse labelling reveals contaminations of S-phase cells that reach G_2-phase after IR

In a first attempt to check, whether S-phase cells reach G_2-phase after different doses of IR and at different time points, we carried out Bromodeoxyuridine (BrdU) staining in Chinese hamster cell lines, V79 (wt) and Irs2 (HRR m). Next, we measured the fraction of BrdU positive and negative G_2-phase cells, via flow cytometry.

BrdU is a nucleoside analog to thymidine. Thus, BrdU is actively incorporated during replication into newly synthesized DNA substituting thymidine and is detectable via antibody staining (Duque and Rakic 2011).

To stain only those cells, that have been in S-phase during the time of IR, we pulse labelled the cells with BrdU around 30 min before IR and washed BrdU out directly after IR. Next, samples were processed for the detection of BrdU positive cells via flow cytometric analysis. From the results obtained, it was possible to calculate the percentage of BrdU negative and positive G_2 cells. G_2 cells, which are BrdU negative, were in G_2 at the time of IR, while BrdU positive G_2 cells were in S-phase during the time of IR and reached G_2 phase during the postirradiation incubation period (see **Figure 14**).

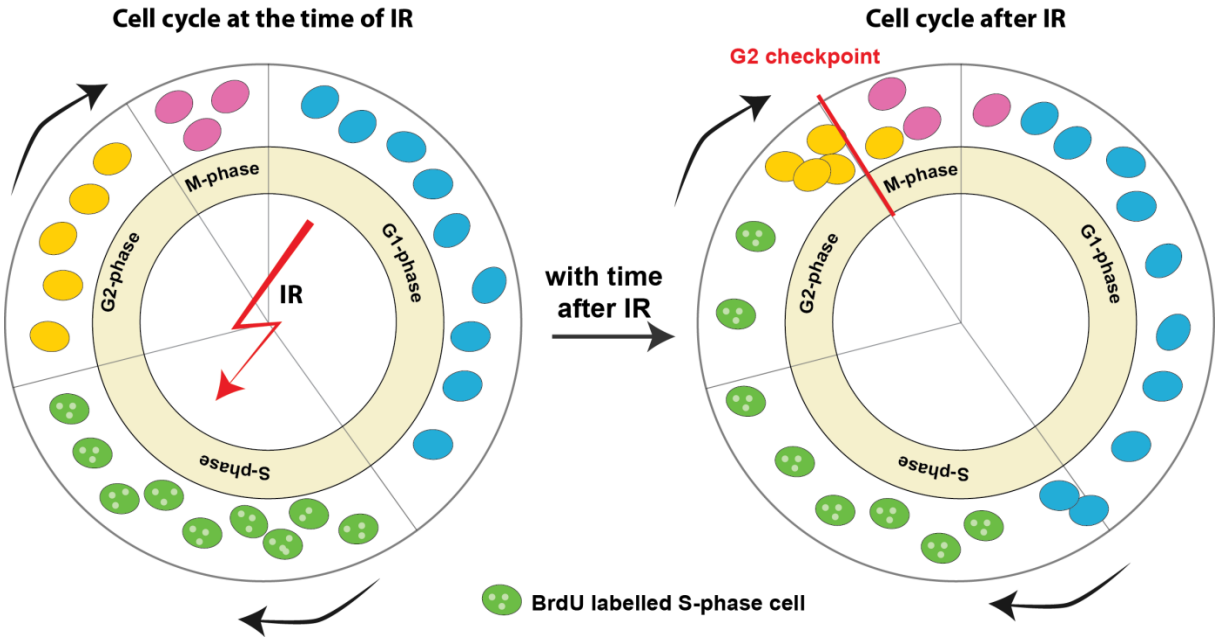

Figure 14: Cell cycle progression of BrdU pulse labelled S-phase cells. Cells are irradiated as asynchronous cultures. S-phase cells have BrdU incorporated through pulse labelling. Note that with time after IR S-phase cells reach to G_2-phase.

Time points were collected 1 h and 4 h post IR. Results obtained are depicted in **Figure 15** (for flow cytometry histograms refer to **Supplementary Figure 4** and **Supplementary Figure 5**).

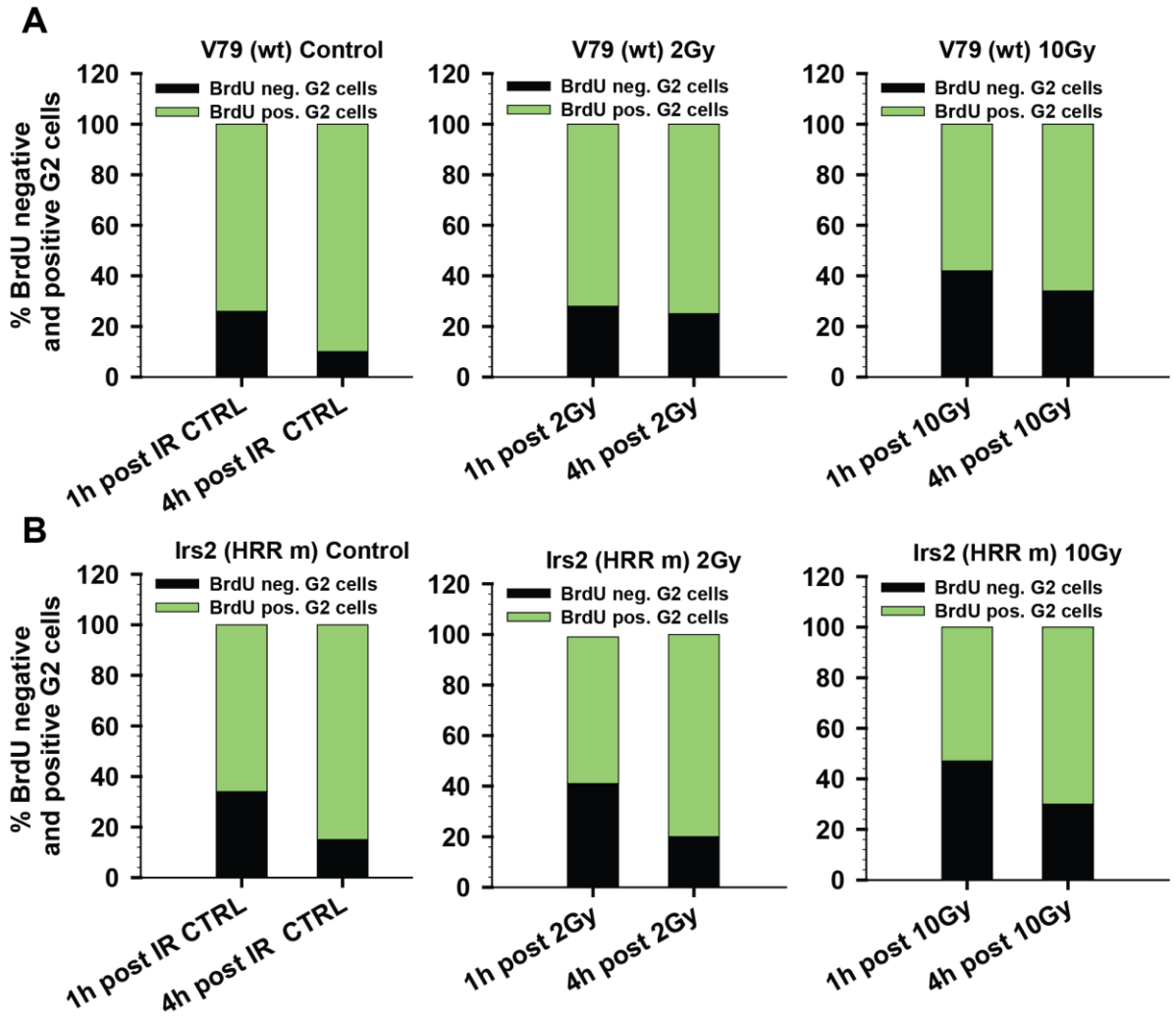

Figure 15: Determination of BrdU positive and negative G2-phase cells in V79 (wt) and irs2 (HRR m) cells after exposure to different IR doses. (A) V79 (wt) and (B) irs2 (HRR m) cells were pulse labelled with BrdU, 30 minutes before exposure to different IR doses. Time points were collected 1 h and 4 h post IR and the percentage of BrdU negative and positive G_2-phase cells was determined by flow cytometry measurements.

Data show, that S-phase cells reach G_2-phase already 1 h post IR. For V79 (wt) cells flow cytometry analysis measured 60% BrdU positive G_2 cells (reflecting cells that have been in S-phase during IR) and 80% BrdU positive G_2 cells 4 h after BrdU pulse labelling. Exposure of V79 (wt) to 2 Gy and 10 Gy IR led to a slight increase in the fraction of real (BrdU negative) G_2 cells 1 h post IR. The fraction of cells in G_2-phase (real G_2 cells) during IR stayed about the same 4 h post IR. The reason behind the slower progression of S-phase cells after exposure to IR is most likely due to the activation of the DNA damage checkpoint.

Similar results were also obtained for irs2 (HRR m) cells. Here again, the fraction of real G_2 cells increased with increasing IR dose, both after 1 h and 4 h post IR (**Figure 15**, **B**).

The above-described results show a contamination of S-phase cells that reach G_2-phase, within the measured timeframe. Yet, the experiment lacks information based on the appearance of prematurely condensed chromosomes.

4.1.2 Development and validation of an EdU staining method to identify S-phase cells on cytogenetic preparations

Since antibody staining with BrdU is not compatible with protocols of classical cytogenetics, or the PCC technique, we sought new approaches and tested combining Click-iT EdU chemistry with a protocol previously described by P. Jeppesen (Jeppesen 2000), which allows immunofluorescence detection on non-denatured cell preparations.

Testing this approach, we were able to discriminate between EdU positive and EdU negative G_2 PCCs as presented in **Figure 16**. However, poor maintenance of PCC morphology, the associated difficulty in scoring, as well as the high cost of the reagents and the laborious protocol rendered the method impractical.

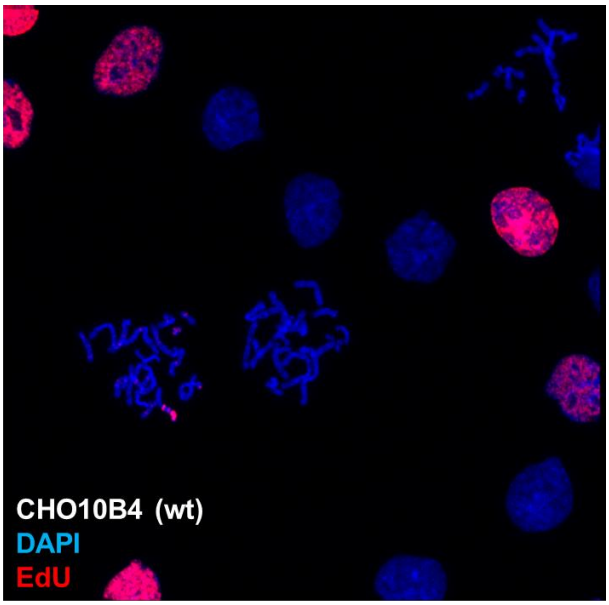

Figure 16: Click-iT labelling for CHO10B4 (wt) cells to allow discrimination between EdU negative and EdU positive G_2 PCCs. This preparation uses the protocol described by P. Jeppesen (Jeppesen 2000). Note that the spreading as well as the form of PCCs was suboptimal for scoring of PCC breaks.

To overcome these limitations we adapted click chemistry using commercially available reagents and tested it in preparations of PCCs. In this way, PCC morphology was maintained and staining with EdU was possible.

In the developed protocol, exponentially growing cells were pulse labelled for 30 min with EdU just before irradiation. Immediately after IR, EdU was washed out and cells were supplied with fresh pre-warmed medium. PCC was induced 30 min before collection of each time point, and cells were processed according to the conventional PCC protocol. Cell spreads on microscope slides were stained with Click- chemistry and counterstained with DAPI. EdU was detected using a Metasystem station. In this procedure EdU negative PCCs reflect cells that have been irradiated in G_2-phase, while EdU positive PCCs are from cells that were in S-phase at the time of irradiation and have since progressed into G_2-phase. Examples for EdU stained PCCs collected after different time points are presented in **Figure 17**.

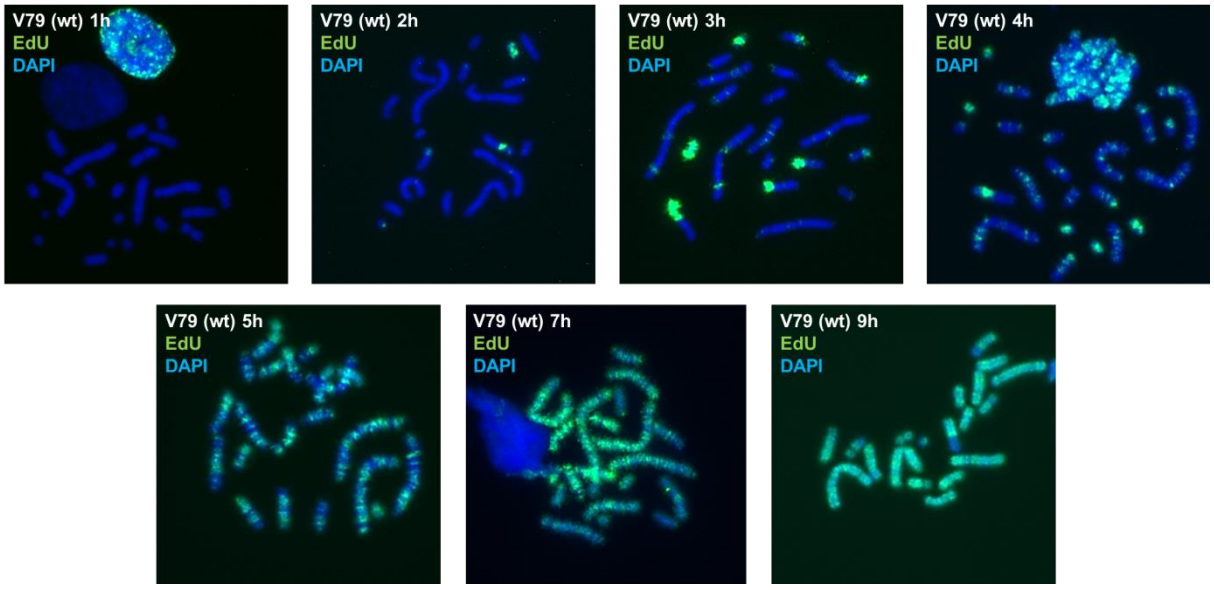

Figure 17: EdU incorporation in PCCs of V79 (wt) cells. V79 (wt) cells were pulse labelled with EdU. PCCs were collected at different time points and samples were processed for EdU staining as described in the text. A Metasystem station was used to detect EdU negative and positive PCCs.

As expected, the fraction of EdU positive PCCs increases with time after EdU labelling. Another interesting observation is that the amount of EdU incorporated differs, depending on the time point at which PCCs are collected. Thus, cells that have been in late S-phase (presented by PCCs at 2 h, 3 h and 4 h), have less EdU incorporated, while cells that have been in earlier stages of the S-phase, incorporated more EdU (5 h, 7 h and 9 h). This observation is in line with the known well-timed replication of the DNA. Furthermore, we could discriminate between the

different PCC types as we have described for Giemsa stained preparations in **Figure 13**.

Using this approach we were able to identify PCCs from cells irradiated in the S-phase and distinguish them from those of cells irradiated in G_2–phase (see **Figure 18**).

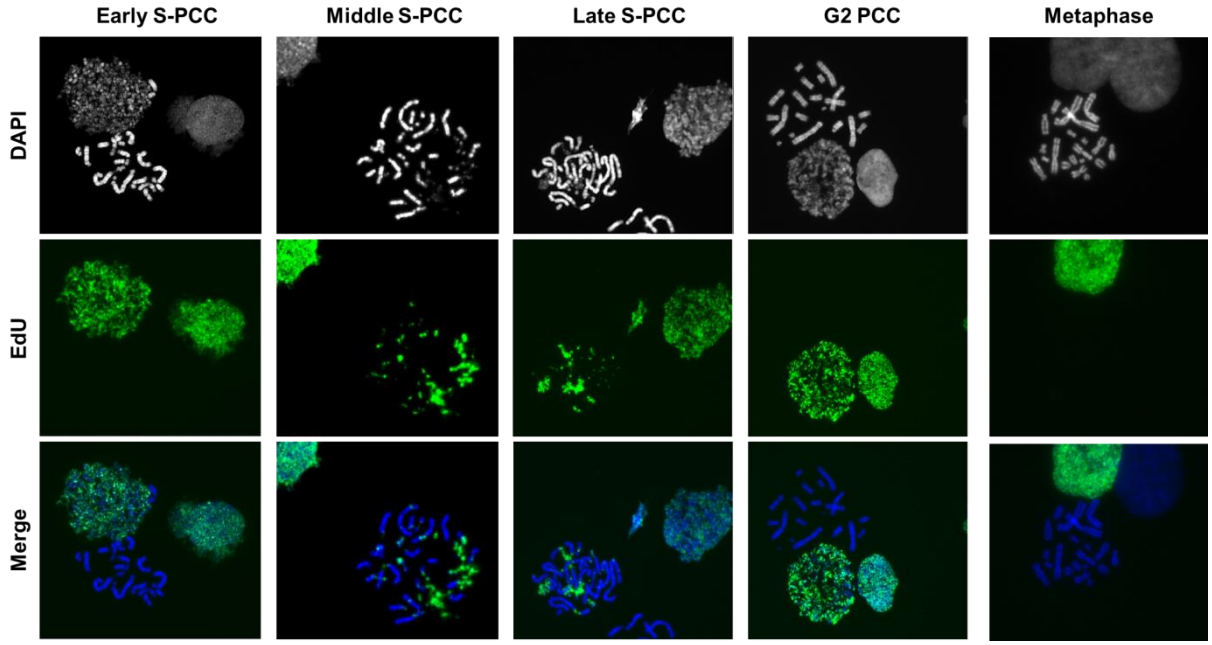

Figure 18: G_2 PCCs with DNA replication regions stained with EdU. These cells incorporated EdU in S-phase and progressed to G_2-phase during the post treatment incubation period. Shown are V79 (wt) cells.

Early S-phase PCCs show high amounts of pulverization and EdU foci distributed homogenously in those structures. Middle S-phase PCCs show more condensed regions and the size of EdU foci is increased, while the number of EdU foci is decreased. Late S-phase PCCs show mostly condensed mitotic like chromosomes, and less and bigger EdU foci, as well as less pulverization. G_2 PCCs appeared as EdU negative and are fully condensed. Metaphases are also EdU negative and distinguishable from G_2 PCCs by their centromeric constriction. Examples are given in **Figure 18**.

To further validate our newly developed method, we also had to confirm that EdU pulse labelling does not exert a toxic effect, which could contribute to chromosomal breakage. We chose to test toxicity employing classical cytogenetics. V79 (wt) cells were pulse labelled with EdU for 30 min and cells were collected at metaphase using a 1 h colcemid block. We collected time points till 12 h post EdU pulse labelling.

Without IR, V79 (wt) cells show a fast progression through the cell cycle, reflected by a fast increase in the fraction of EdU positive metaphases (see **Supplementary Figure 6**). Scoring of chromatid breaks in metaphases revealed an average number of 0.15 chromatid breaks per cell, which is within the range of control, Giemsa-stained metaphases. Thus, a toxic effect of EdU could be excluded within the measured timeframe of 12 h.

Yet, we had another very interesting observation during the above-described metaphase experiment. We detected a frequent appearance of EdU banding patterns, meaning that EdU was visible on confined chromosome regions. Examples are illustrated in **Figure 19**.

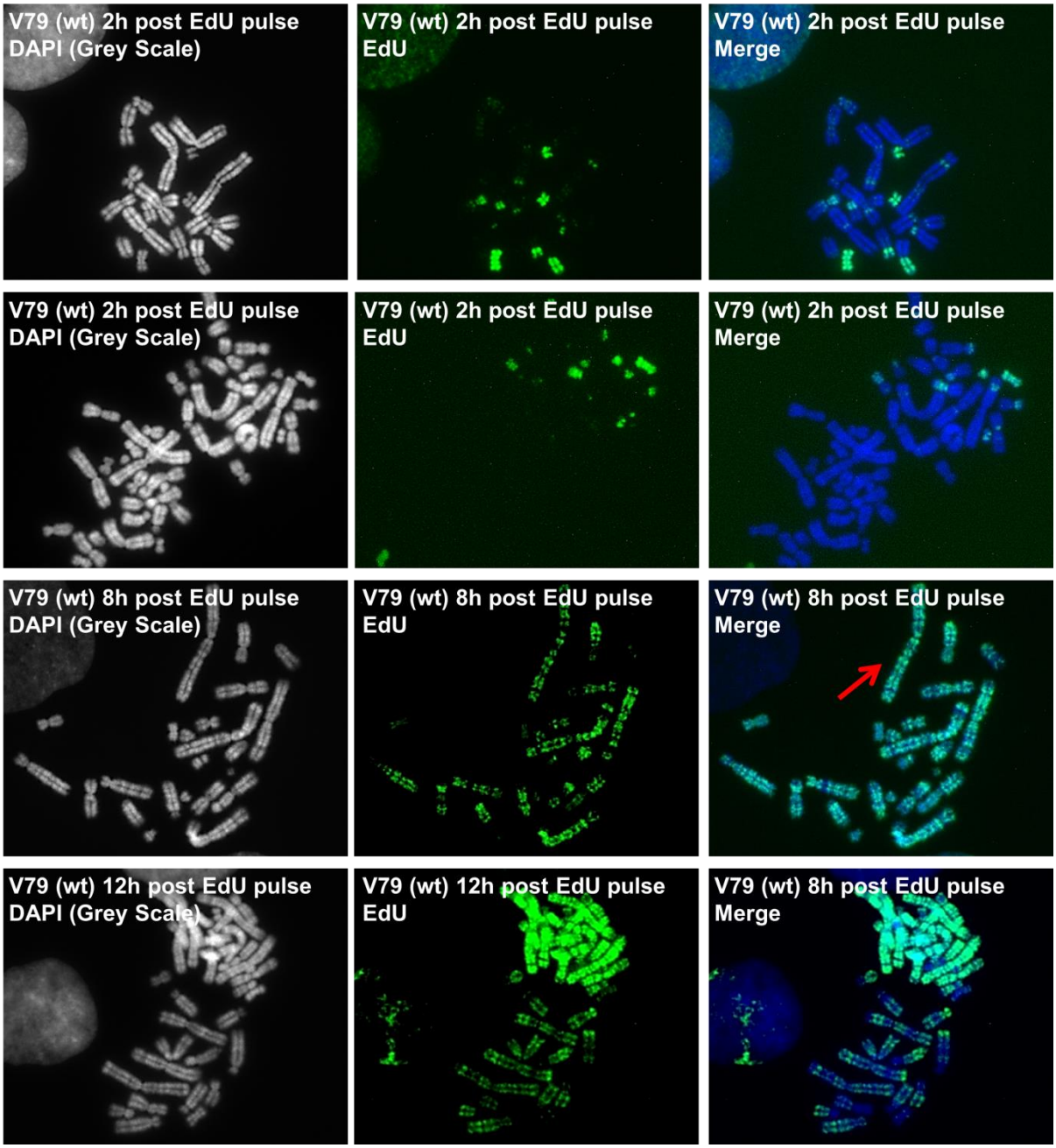

Figure 19: EdU banding patterns observed at different times post EdU pulse labelling in V79 (wt) cells. V79 (wt) cells showed discrete EdU banding patterns conferred to particular regions of the chromosome. The red arrow points toward Chinese hamster Chromosome 1 and its banding pattern coincides with G-banded chromosomes (See **Figure 20**).

In one case the EdU banding pattern coincided with G-banding regions for Chinese hamster chromosome 1 as represented in **Figure 20**.

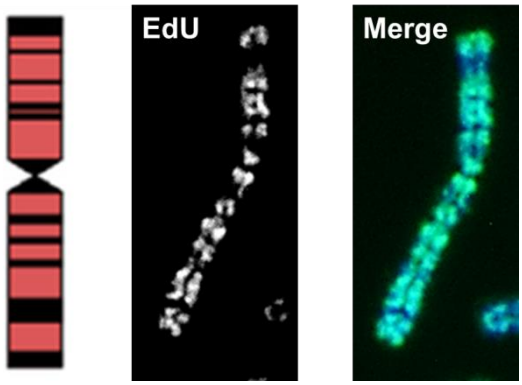

Figure 20: EdU banding pattern coinciding with G-banded regions of Chinese hamster Chromosome 1. Illustration of G-banded regions of Chinese hamster Chromosome 1 on the left was adapted from (Wurm and Hacker 2011)).

This observation offers new means for investigating replication timing of different chromosome regions based on EdU pulse labelling and will be discussed later.

We now have established a methodology which allows us to distinguish between EdU negative PCC (truly representing cells irradiated in the G_2-phase of the cell cycle) and EdU positive PCC (representing cells irradiated in the S-phase of the cell cycle that have progressed to G_2 during the incubation period).

Based on this, we determined the percentage of EdU negative and positive G_2 PCCs in Chinese hamster cells including, V79 (wt), irs2 (HRR m) and irs1 (HRR m), after EdU pulse labelling alone or in combination with 1 Gy or 5 Gy.

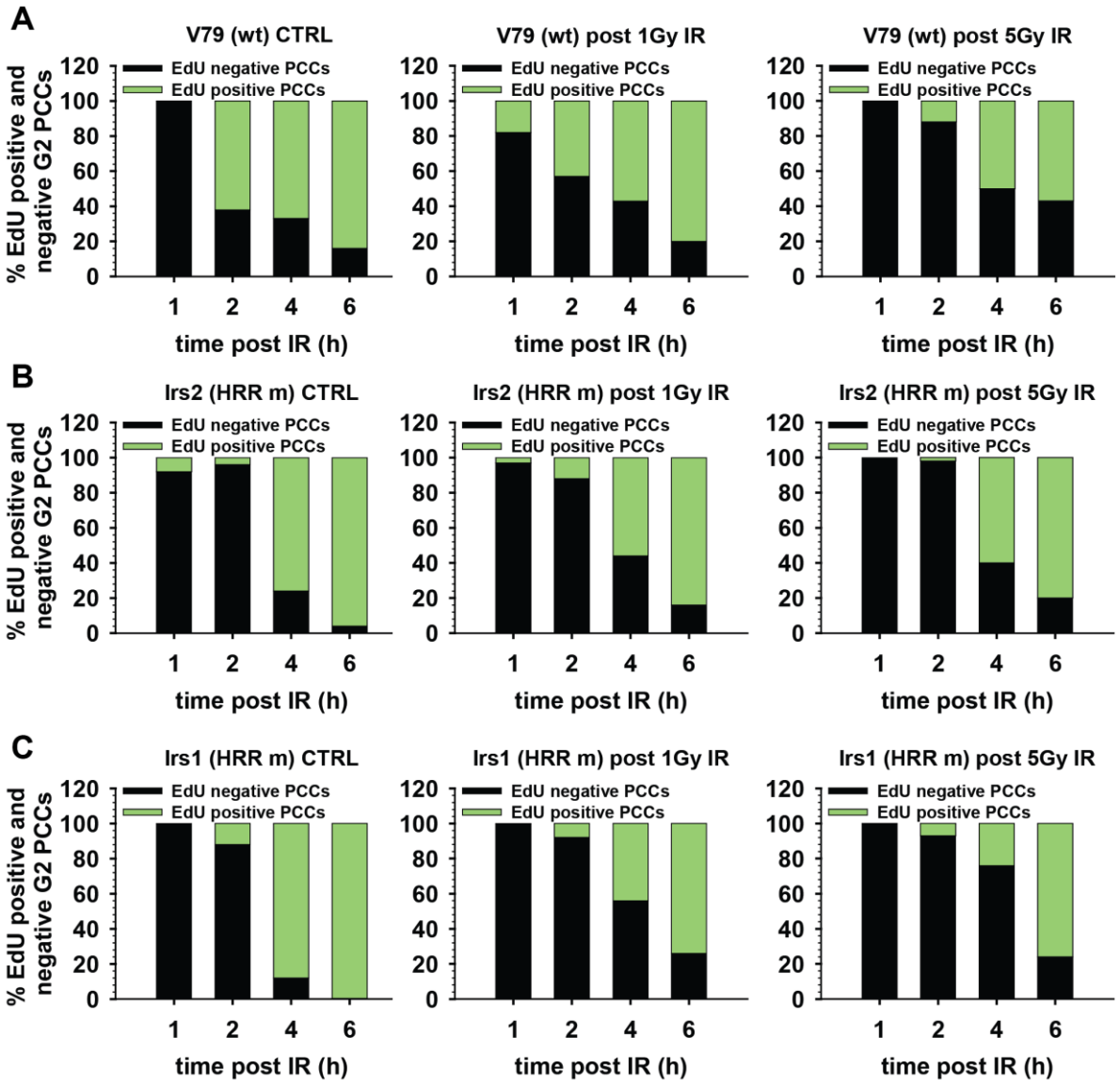

Figure 21: Percentage of EdU negative and positive PCCs in different Chinese hamster cell lines exposed to different doses of IR. A) V79 (wt), B) irs2 (HRR m) and C) irs1 (HRR m) cells were pulse labelled with EdU before IR and time points were collected after IR and cells were processed for EdU detection in PCCs.

Results presented in **Figure 21** show a steady increase in the fraction of EdU positive G_2 PCCs with increasing time post EdU pulse labelling. 1h after EdU pulse labelling the fraction of EdU negative PCCs (real G_2 cells) is around 98 – 100%. However, already 4 h later, the fraction of these EdU negative cells decreased to 20 – 40%, while the fraction of EdU positive PCCs increased. 6 h after EdU pulse labelling, mainly EdU positive PCCs are detected, indicating that the original G_2-phase cells had progressed to mitosis.

A clear difference was observed in the fraction of EdU negative and positive PCCs upon exposure of cells to 1 Gy or 5 Gy IR. For V79 (wt) cells (**Figure 21, A**), the

fraction of EdU negative PCCs is still 50% at 4h post IR and 30% at the 6h time point. Slower progression of irradiated S-phase cells is more evident after 5 Gy IR, with 50% of EdU negative PCCs being present 6 h after IR. These trends hint towards a delay in cell cycle progression upon IR, which was also to some extent measured in the BrdU experiments, described before (**Figure 15**).

Similar tendencies were also seen with the HRR mutant cell lines irs2 and irs1 (**Figure 21**, **B** and **C**). Here again, a higher fraction of EdU negative PCCs is detected 4 h and 6 h post exposure to 1 Gy or 5 Gy as compared to unirradiated controls. Thus, 4 h after IR, 50-60% of the PCCs are EdU negative (real G_2 PCC). The pronounced cell cycle delay, observed in V79 (wt) cells, is less pronounced in irs2 and irs1 cells.

We next inquired, whether there is a difference in PCC break repair in EdU negative and EdU positive PCCs. Answering this question is very important, since the experiments carried out in this thesis, study PCC break repair using conventional Giemsa staining, where discrimination between G_2 PCCs coming from late S- or G_2 –phase irradiated cells is not possible.

With the established protocol and the use of a Metasystem station, we scored PCC breaks in EdU/DAPI stained preparations. **Figure 22** demonstrates an example of an EdU positive and negative PCC lying next to each other, 4 h after exposure to 5 Gy IR.

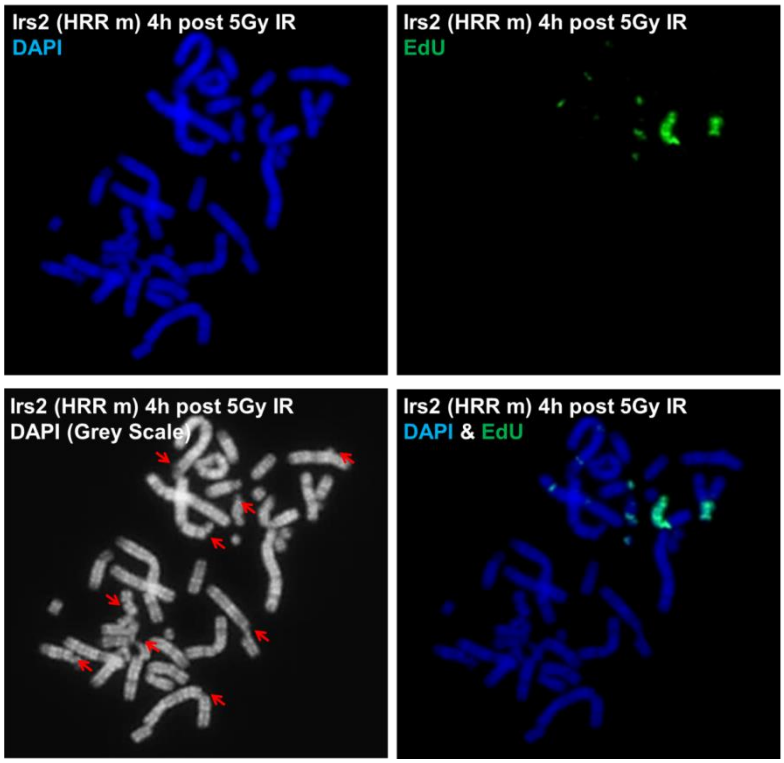

Figure 22: Representative image for an EdU negative and positive G_2 PCC in irs2 (HRR m) cells. Irs2 cells have been EdU pulse labelled, exposed to 5 Gy and collected 4 h post IR and processed for EdU detection. Red arrows indicated PCC breaks in both the EdU positive and the EdU negative PCCs.

PCC break repair kinetics in EdU negative and positive PCCs were examined for V79 (wt), irs2 (HRR m) and irs1 (HRR m) cells exposed to 1 Gy IR and 5 Gy IR and analyzed till 6 h post IR. Quantitative data are summarized in **Figure 23**. Within the measured timeframe, we could not detect any significant differences in the repair of IR induced PCC breaks in EdU negative PCCs compared to EdU positive PCCs for all three cell lines examined.

Taken together these results show that even if there is contamination with S-phase cells that have come to G_2 at the later time points, PCC break repair kinetics are not influenced by this contamination. This adds another level of validation to the PCC technique used to analyze PCC break repair via the conventional Giemsa staining method.

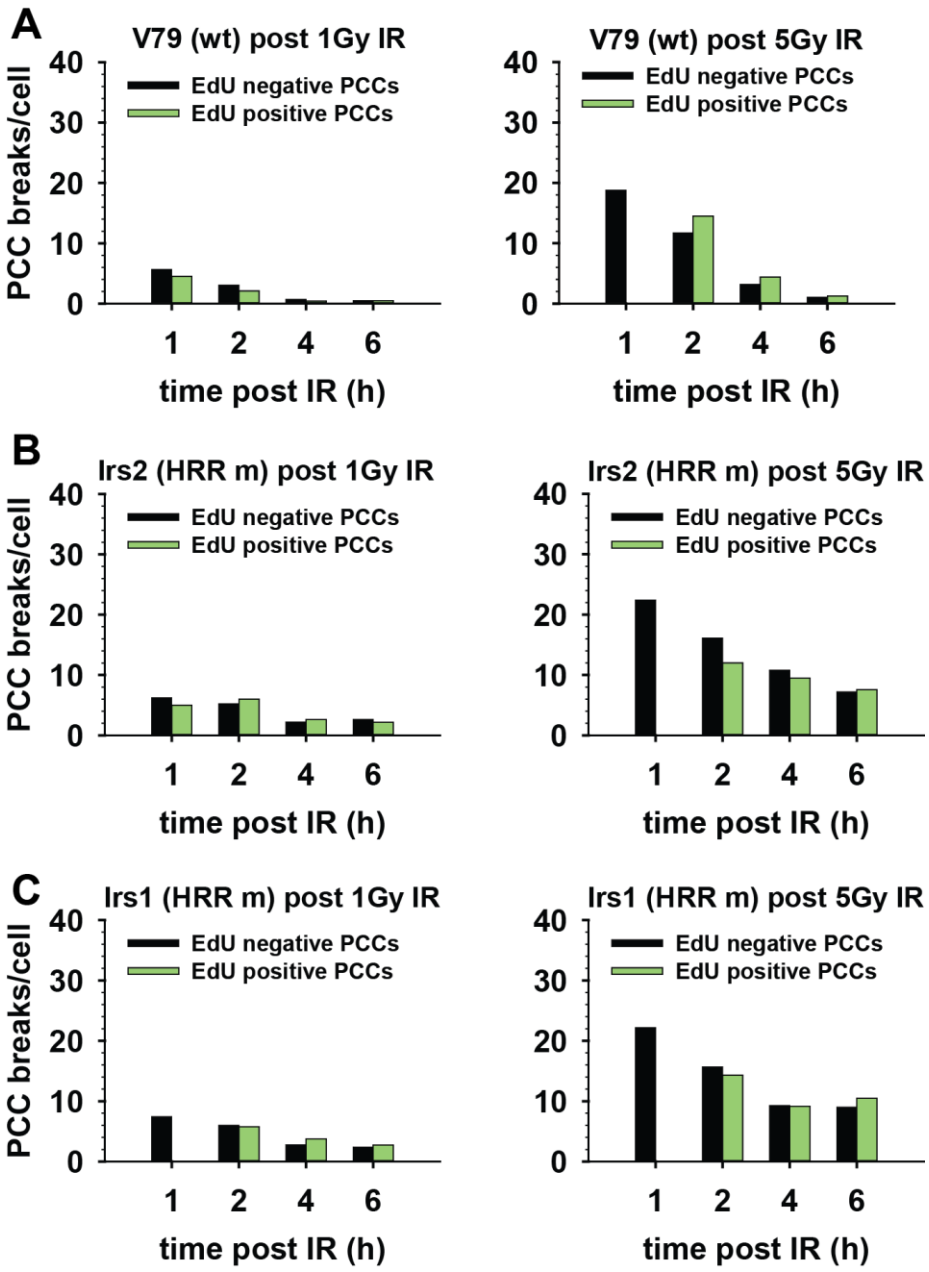

Figure 23: Quantitative analysis of PCC breaks in EdU negative and positive PCCs. A) V79 (wt), B) irs2 (HRR m) and C) irs1 (HRR m) cells were exposed to different IR doses immediately after EdU pulse labelling. PCC breaks were scored separately for EdU positive and negative PCCs and plotted against the time. Data are from one experiment.

4.1.3 Do all G_2 phase cells condense to G_2 PCC upon treatment with Calyculin A?

A further point, which needed validation, was whether all G_2 phase cells are condensed to PCCs after treatment with Calyculin A. We decided to approach this question by an indirect experiment and determined the PCC index on Giemsa stained slides and compared this value to the fraction of G_2-phase cells as measured by flow cytometry. Graphs presented in **Figure 24,** show the quantitative analysis of this experiment.

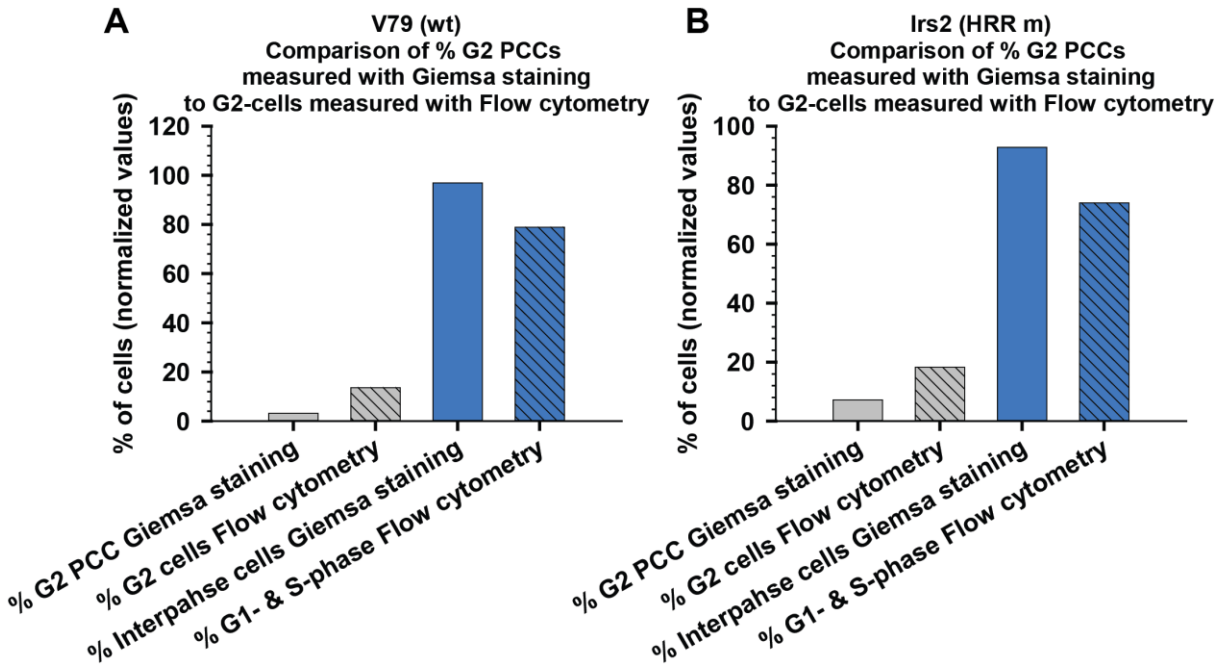

Figure 24: Comparison of G_2 PCC index with the fraction of G_2 cells measured by flow cytometry. A) V79 (wt) and B) irs2 (HRR m) cells were used to determine the G_2 PCC index via Giemsa staining and by flow cytometry. Data are representative from one experiment.

Acquired data display a 4 fold difference in the amount of G_2 PCCs as compared to the fraction of G_2-phase cells measured by flow cytometry in case of V79 (wt) cells. Also for irs2, only around 40% of total G_2 cells (as measured by flow cytometry) are converted to G_2 PCCs. Based on these results, we could come to the conclusion that not all G_2 cells are condensed to G_2 PCCs.

Yet, we have to keep in mind that the fraction of G_2 cells determined by single flow cytometry includes late S-phase cells. With the help of two-parameter flow cytometry, using BrdU and PI co-staining, we could provide a more reliable estimate here. Thus, the fraction of real G_2-phase cells for V79 (BrdU neg. G_2 cells, refer to

Supplementary Figure 4, 0Gy Results) revealed that the percentage of real G_2 cells was 7.2% (1 h post BrdU pulse labelling) and 3.66% (4 h post BrdU pulse labelling), respectively. Comparing this to the PCC index (**Figure 24**, **A**), we can conclude that more than 50% of G_2 cells are condensed to G_2 PCCs.

For Irs2 cells, two-parameter flow cytometry (refer to **Supplementary Figure 5**, 0Gy Results) showed that around 11.15% (1 h post BrdU pulse labelling) and 4.99% (4 h post BrdU pulse labelling) are real G_2 cells (BrdU neg. G_2). Hence, we conclude that more than 60% of G_2 cells are condensed to G_2 PCCs for Irs2 cells (**Figure 24**, **B**).

Nevertheless, we have to be aware that we may need to find out even more precise approaches in order to determine the real fraction of G_2 cells that are condensed to G_2 PCCs since both; flow cytometry as well as the G_2 PCC technique are fundamentally different methods and a direct comparison may not be that detailed.

In summary: In this first part of the thesis, we validated the PCC technique by developing a protocol, which allows discrimination between G_2 PCCs coming from irradiated G_2 cells and those coming from cells that have been in S-phase during IR using EdU staining.
We further demonstrated that within the measured timeframe of 6 h post IR PCC break repair kinetics are not significantly different in EdU negative PCCs and EdU positive PCCs. This observation is particularly important, since it adds validation to the experiments, which will be described in the next sections.
Moreover, we could show that the progression of S-phase cells (and consequently the fraction of EdU positive and negative PCCs) is dependent on the IR dose to which cells have been exposed, the corresponding cell cycle delays as well as the genetic background of the cell line tested.
Furthermore, acquired data give interesting information regarding the incorporation patterns of EdU in chromosomes during S-phase.
Last but not least the experiment outlined above suggests that depending on the cell line 50 – 60% of G_2 cells are condensed to PCC upon chemical PCC induction. Yet, further careful investigation needs to be carried out.

PART II: THE CONTRIBUTION OF DSB REPAIR PATHWAYS TO THE PROCESSING OF PCC BREAKS

4.2 Chemical inhibition of DNA-PK reveals a dose-dependent repair pathway switch in irradiated Chinese hamster cells

As outlined in the introduction, previous work suggests that defects in HRR do not affect DSB processing as measured by PFGE after exposure of cells to high IR doses (Wu, et al. 2008). Furthermore, unpublished work from our laboratory provided evidence that defects in HRR, compromises the rejoining of metaphase chromatid breaks after exposure of cells in G_2 – phase to low doses of IR like 1 Gy (Siemann 2013; Soni 2010). Finally, more recent experiments hint towards a saturation of HRR with increasing radiation dose (Demond 2016).

Collectively, these observations suggest a model according to which HRR dominates at low doses of IR but becomes progressively saturated at high IR doses giving way to e.g. c-NHEJ.

We wished to test this hypothesis following chromatid breaks as a model form of DNA damage still reflecting the formation and processing of DSBs. If indeed CB repair reflects some form of DSB repair, we can make the following prediction:

At low IR doses CB repair will depend on HRR and will therefore, be slow. At higher doses, CB repair will increasingly depend on c-NHEJ and will therefore pickup speed. We tested this hypothesis using CBs as detected by PCC. As described in **Part I**, PCC will allow us to study IR induced chromatid breaks in G_2 – phase without requiring cells to progress from G_2- to M – phase, circumventing thereby the G_2-checkpoint or any other form of cell cycle progression arrest.

4.2.1 PCC break repair kinetics in V79 cells exposed to a broad spectrum of IR doses

In a first set of experiments, we were interested in measuring the contribution of c-NHEJ to the repair of IR induced PCC breaks. To this end we employed NU7441, a potent inhibitor of DNA-PK, to chemically inhibit DNA-PK, a key component in c-NHEJ.

We exposed exponentially growing V79 wildtype cells to a broad spectrum of IR doses ranging from low doses like 0.2 Gy, to high doses like 10 Gy. Induction of PCC breaks was measured 1 h after irradiation to obtain a dose response curve.

The 1 h time point after IR was taken as the initial time point, since earlier time points proved to be less informative, as they were confounded by artefacts that made them irreproducible. We compared the induction of PCC breaks to the expected number of DSBs in an irradiated G_2-phase cell. It is known that DSB induction increases linearly with IR dose (Barnard, et al. 2013). A G_2 cell is known to sustain about 40 DSBs upon exposure to 1 Gy of IR, 80 after 2 Gy of IR and so on. On this basis, we calculated the fraction of DSBs that convert to chromatid breaks as measured by PCC (Table 3**, Figure 25**).

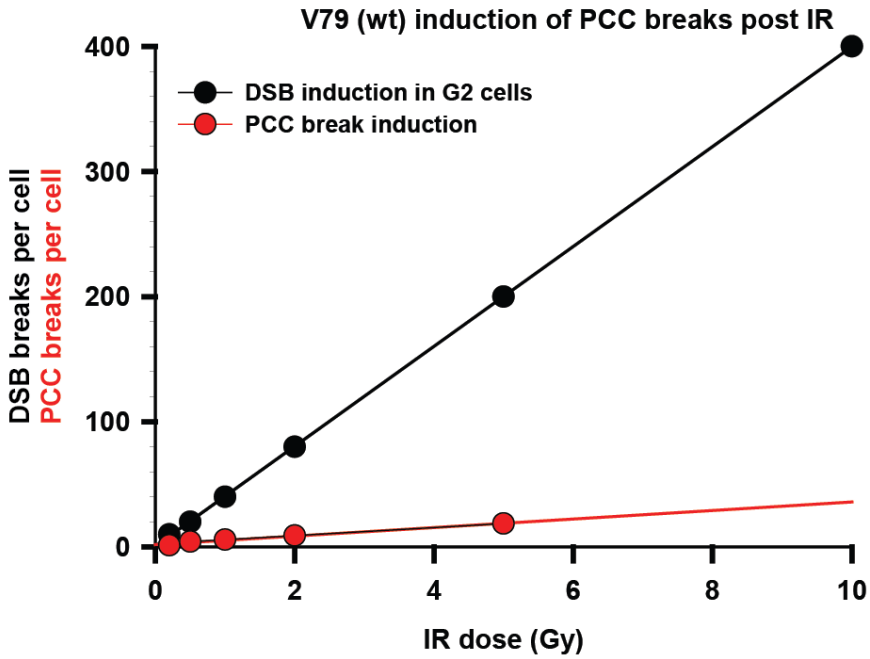

Figure 25: Induction of PCC breaks compared to the induction of DSB breaks in G_2-cells.

Similar to DSBs, PCC breaks increase linearly with increasing radiation dose. We found that 10 – 20% of DSBs are maximally translated to PCC breaks for V79 (wt) cells (Table 3).

Table 3: Fraction of DSBs maximally translated to PCC breaks. The percentage of DSBs breaks that are converted to PCC breaks was calculated by dividing the number of PCC breaks at a given dose by the number of DSBs at the same dose multiplied by 100 to determine the percentage.

IR dose (Gy)	DSB/cell	PCC breaks/cell	DSBs converted to PCC breaks
0.2	10	1.27	13%
0.5	20	4.29	21%
1	40	5.81	15%
2	80	9.09	11%
5	200	18.67	10%

Next, the dose response curve was determined for cells exposed to IR in the presence of the DNA-PK inhibitor (NU7441), to investigate, whether the inhibition DNA-PK has an effect on PCC break induction. The results obtained are plotted in **Figure 26**.

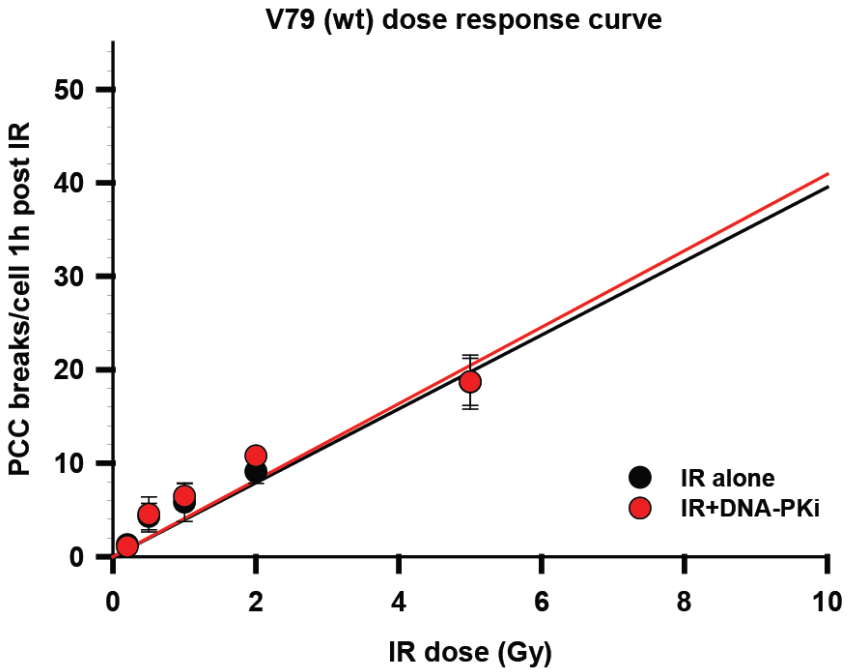

Figure 26: V79 (wt) Dose response curve. PCC breaks were scored 1 h post IR and are plotted against the IR dose. Results are presented for PCC break induction after exposure of V79 cells to IR alone and IR with DNA-PKi (NU7441). Shown is the mean of three independent experiments ± SD.

PCC breaks 1 h post IR could be scored up to 5 Gy. For doses higher than 5 Gy an accurate scoring was impossible. Since high-dose results (10 Gy) were important for the following analysis of PCC break repair kinetics, we extrapolated the dose response curve up to 10 Gy, to estimate the number of PCCs breaks and use them in the analysis presented later.

Figure 26 illustrates that the induction of PCC breaks in the presence of the DNA-PK inhibitor is indistinguishable from that measured in its absence.

In an effort to attain a more detailed look, at the contribution of the DSB repair pathways to the processing of PCC breaks, after different IR doses we performed whole repair kinetic experiments. To this end, we exposed V79 wildtype cells to IR doses ranging from 0.2 Gy to 10 Gy. We followed PCC breaks up to 6 h post IR. Within this timeframe, we mainly focused on the response of cells that have been irradiated in the G_2-phase, where all DSB repair pathways can engage.

The number of PCC breaks was scored in the presence or absence of the DNA-PK inhibitor and plotted against the time of postirradiation incubation (**Figure 27**, Table 4).

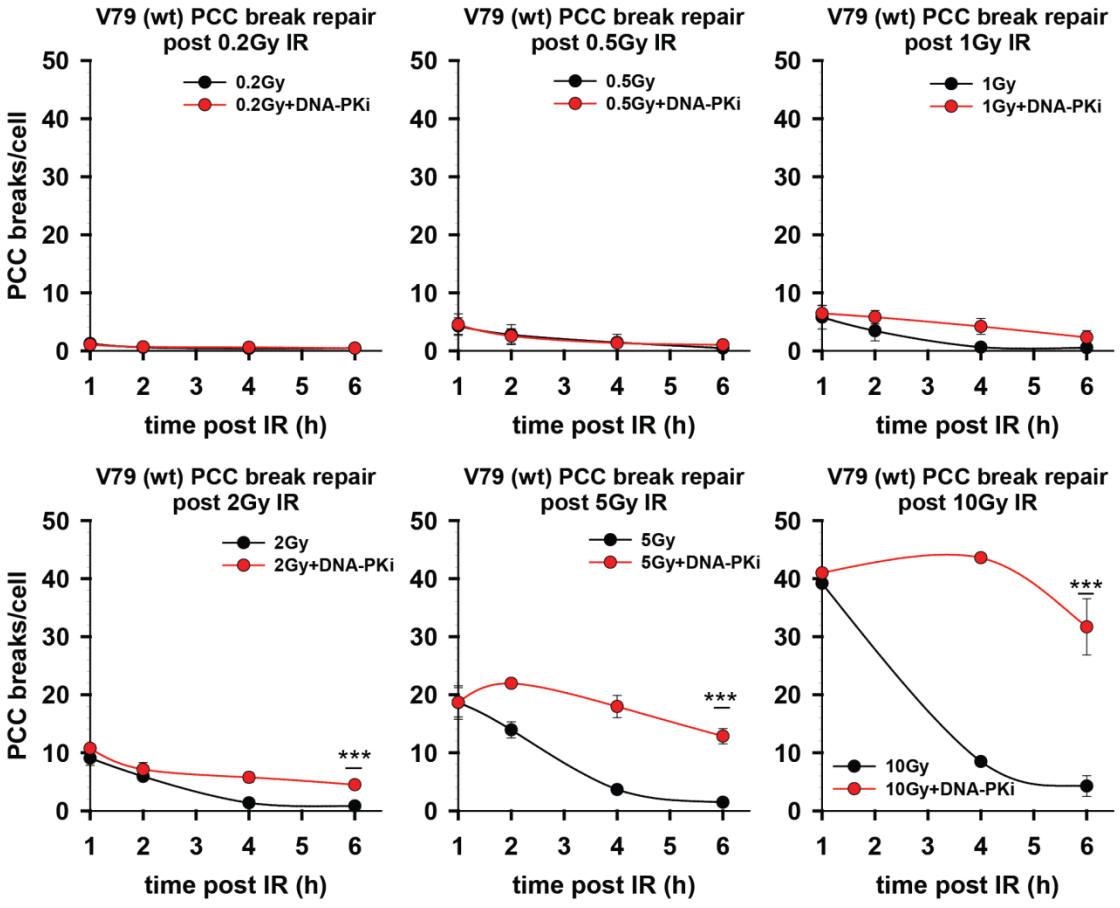

Figure 27: PCC break repair kinetics in V79 (wt) cells after exposure to IR ± DNA-PK inhibitor. Exponentially growing V79 (wt) cells were exposed to a broad range of IR doses and PCC break repair was measured 1 – 6 h post IR. P-values were determined for the 6 h time points between IR alone and IR+DNA-PKi, to compare residual damage. A two tailed student t-test (asterix designation $p<0.001$ ***, $p<0.01$ **, $p<0.05$ *) was used for this purpose. Data represent the mean of three independent experiments ± SD.

Figure 27 shows PCC-break repair-kinetics in V79 cells. It is evident that 80 – 90% of initial PCCs breaks are repaired in V79 cells exposed to IR alone at all IR doses measured (Table 4). Furthermore, when $t_{1/2}$ was calculated, we observed only slight changes at different doses; PCC breaks are resolved to 50% within 2 - 2.7 h (Table 4)**.**

Table 4: Determination of $t_{1/2}$ and the percentage of residual damage for V79 (wt) cells. The residual damage was calculated by comparing the number of initial PCC breaks (1 h post IR) to the number of residual PCC breaks (6 h post IR). $T_{1/2}$ is determined as the time point where 50% of initial breaks are rejoined (see also **Figure 30**).

IR dose (Gy)	$t_{1/2}$ IR alone (h)	$t_{1/2}$ IR+DNA-PKi (h)	% Residual damage post IR	% Residual damage IR+DNA-PKi
0.2	1.8	5	36	41
0.5	2.6	2.2	11	23
1	2.2	5	9	36
2	2.5	4.7	9	41
5	2	N.a*	8	96
10	2.7	N.a*	11	77

*N.a $t_{1/2}$ not obtained in the measured timeframe

We inhibited DNA-PK, with the aim to inhibit c-NHEJ. Hence, the repair pathways left for wildtype cells to resolve PCC breaks are HRR and alt-EJ.

The inhibition of DNA-PK after irradiation with doses like 0.2 Gy, 0.5 Gy and 1 Gy (**Figure 27**, upper row) does not affect PCC break repair significantly. 60 – 80% of PCC breaks are resolved 6 h after IR. Yet, after irradiation with 2 Gy, 5 Gy and 10 Gy (**Figure 27**, lower row) a significant fraction of PCC breaks remained un-rejoined (Table 4). This observation indicates preferential abrogation of PCC break processing by c-NHEJ at higher IR doses.

Furthermore, chemical inhibition of DNA-PK renders the repair of IR induced PCC breaks slower (Table 4). While 50% of breaks are repaired within 3 – 5 hours after IR with 0.2 Gy, 0.5 Gy, 1 Gy and 2 Gy, the $t_{1/2}$ for PCC breaks after 5 Gy and 10 Gy exceeded 6 h. This suggests that a slow repair pathway compensates for inhibited c-NHEJ, after exposure of cells to 0.2 Gy, 0.5 Gy and 1 Gy IR. At doses greater than 2 Gy however, this pathway cannot compensate any longer and repair becomes inefficient. In other words, c-NHEJ plays a greater role at high than at low radiation doses. This puts c-NHEJ to the front for the repair of PCC breaks after exposure of cells to doses higher than 2 Gy and points towards an IR dose dependent regulation of DSB repair pathway as uncovered by measuring the processing of PCC breaks.

Collectively, these results allow us to conclude that c-NHEJ processes most of IR induced PCC breaks. Inhibition of c-NHEJ (by chemical inhibition of DNA-PK) uncovers a slow repair component at doses lower than 2 Gy that carried most of the PCC break processing. Furthermore, after exposure of cells to IR doses greater than 2 Gy, neither HRR nor alt-EJ is able to compensate efficiently for abrogated c-NHEJ at the level of PCC break repair.

4.2.2 Whole PCC break repair kinetics for Irs2 (HRR m) cells after exposure to a broad spectrum of IR doses

In the above described experiment, PCC break rejoining was investigated in wildtype cells after IR alone, or in the presence of the DNA-PK inhibitor. Thus, the connection to HRR was only indirect since HRR could engage under all measured conditions.

For a more direct analysis of the role of HRR we analyzed IR induced PCC break repair in the Chinese hamster cell line irs2. Irs2 cells have a mutation in Rad51b, one of the paralogues of Rad51. Rad51 paralogues are essential in aiding Rad51 for homology search and strand invasion (Suwaki, et al. 2011).

Similar to V79 (wt) cells, we first looked at the induction of PCC breaks after IR alone or IR in the presence of the DNA-PK inhibitor (**Figure 28**).

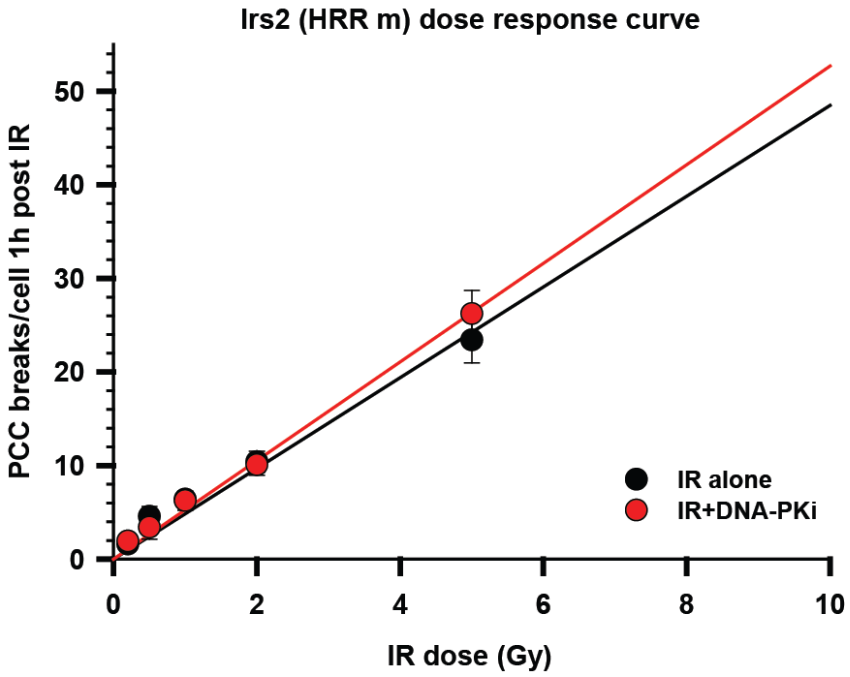

Figure 28: Dose response curve in irs2 (HRR m) cells. PCC breaks were scored 1 h post IR and plotted against the IR dose. Results are presented for PCC break induction after exposure of irs2 cells to IR alone and IR with DNA-PKi (NU7441). Shown is the mean of three independent experiments ± SD.

Irs2 cells show a linear induction of PCC breaks with increasing radiation dose. Yet, the fraction of DSBs converted to chromatid breaks was slightly higher (1.2 fold) for irs2 (HRR m) than V79 (see Table 3), suggesting that mutations in HRR renders cells more prone to chromosomal breakage.

Table 5: Fraction of DSBs maximally translated to PCC breaks (irs2 HRR m). The percentage of DSBs breaks that are maximally converted to PCC breaks was calculated by dividing the number of PCC breaks at a given dose by the number of DSBs at the same dose multiplied by 100 to determine the percentage.

IR dose (Gy)	DSB/cell	PCC breaks/cell	DSBs maximally converted to PCC breaks
0.2	10	1.61	16
0.5	20	4.57	23
1	40	6.4	16
2	80	10.41	13
5	200	23.41	12

Next, we examined PCC break repair kinetics in irs2 cells. The results are summarized in **Figure 29**.

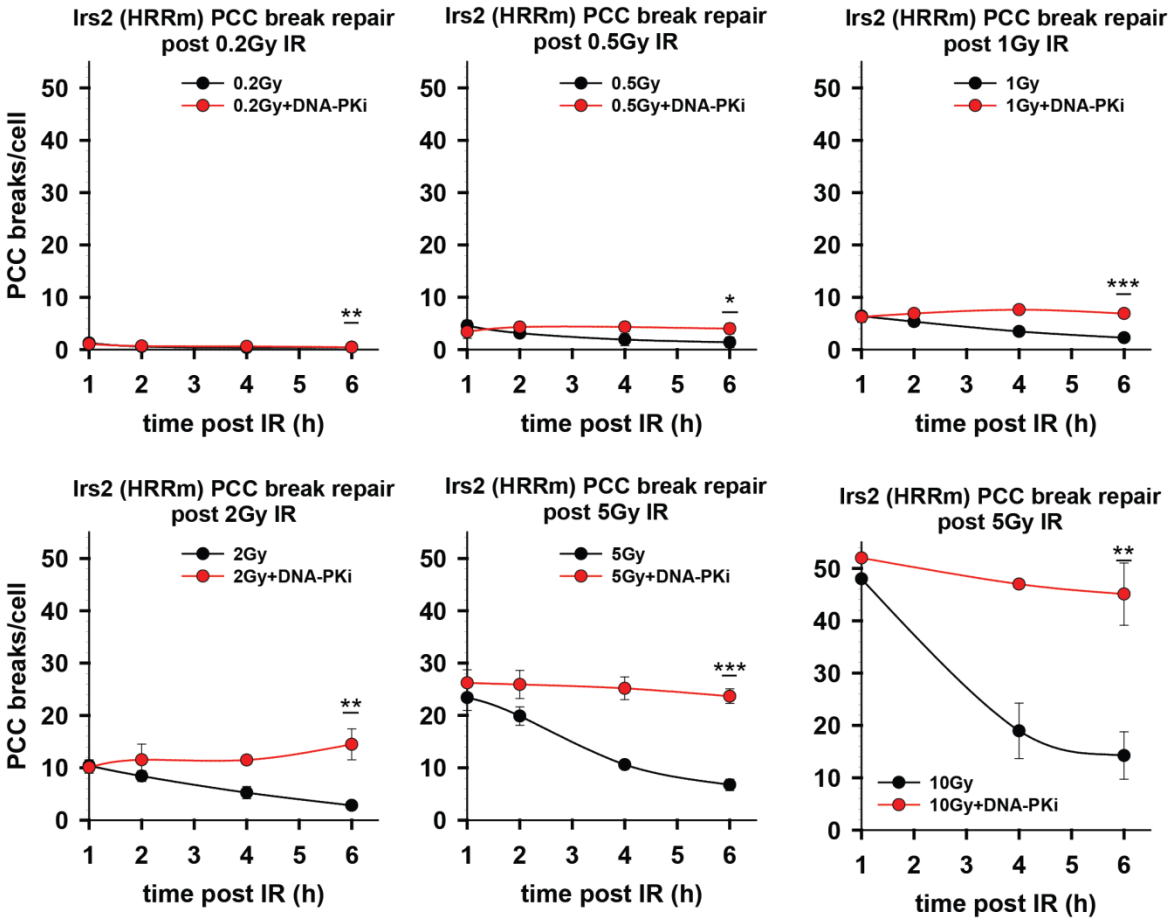

Figure 29: PCC break repair kinetics in irs2 (HRR m) cells after exposure to IR ±DNA-PK inhibitor. Exponentially growing irs2 (HRR m) cells were exposed to a broad range of IR doses and PCC break repair was measured 1 – 6 h post IR. Significances of differences were determined for the 6 h time points between IR alone and IR+DNA-PKi, to compare residual damages. A two tailed student t-test (asterix designation $p<0.001$ ***, $p<0.01$ **, $p<0.05$ *) was used. Data present the mean of three independent experiments ± SD.

Upon exposure to 0.2 Gy, 0.5 Gy and 1 Gy, 50 – 60% of the initial breaks are repaired, within the measured time frame of 6 h (Table 6).

After exposure to 2 Gy, 5 Gy and 10 Gy IR, we observed more efficient repair of PCC breaks, with 70 – 80% of PCC breaks being re-joined within 6 h post IR (Table 6**, Figure 29**). Looking at $t_{1/2}$ we found, that irs2 needs in between 3.2 – 4.8 h to repair 50% of the initial PCC breaks, after IR alone. If we compare the $t_{1/2}$ after exposure to 2 Gy (around 4 h) we observed a slightly faster repair of PCC breaks upon exposure to 5 Gy and 10 Gy with $t_{1/2}$ of 3.7 down to 3.3 h respectively.

Table 6: Determination of $t_{1/2}$ and the percentage of residual damage in irs2 (HRR m) cells. The residual damage was calculated by comparing the number of initial PCC breaks (1 h post IR) to the number of residual PCC breaks (6 h post IR). $t_{1/2}$ is determined as the time point where 50% of initial breaks are rejoined (see also **Figure 30**).

IR dose (Gy)	$t_{1/2}$ IR alone (h)	$t_{1/2}$ IR+DNA-PKi (h)	% Residual damage IR alone	% Residual damage IR+DNA-PKi
0.2	4.8	N.a*	37	88
0.5	3.21	N.a*	30	117
1	4.29	N.a*	35	110
2	4	N.a*	27	122
5	3.7	N.a*	28	90
10	3.3	N.a*	29	86

*N.a $t_{1/2}$ not obtained in the measured timeframe

Interestingly, the inhibition of c-NHEJ led to total PCC break repair abrogation at all doses examined (**Figure 29**). After 0.5 Gy, 1 Gy and 2 Gy the residual damage even exceeded the initial damage (Table 6).

These results suggest a backup role for c-NHEJ, when HRR is mutated. Even further, data suggest that alt-EJ, which should be still able to engage in repair when both c-NHEJ and HRR are abrogated, cannot backup at the level of PCC break repair under the conditions tested.

To directly compare PCC break repair kinetics acquired for V79 (wt) and Irs2 (HRR m) cells, the number of PCC breaks was normalized to the initial (1 h value) number of PCC breaks (**Figure 30**).

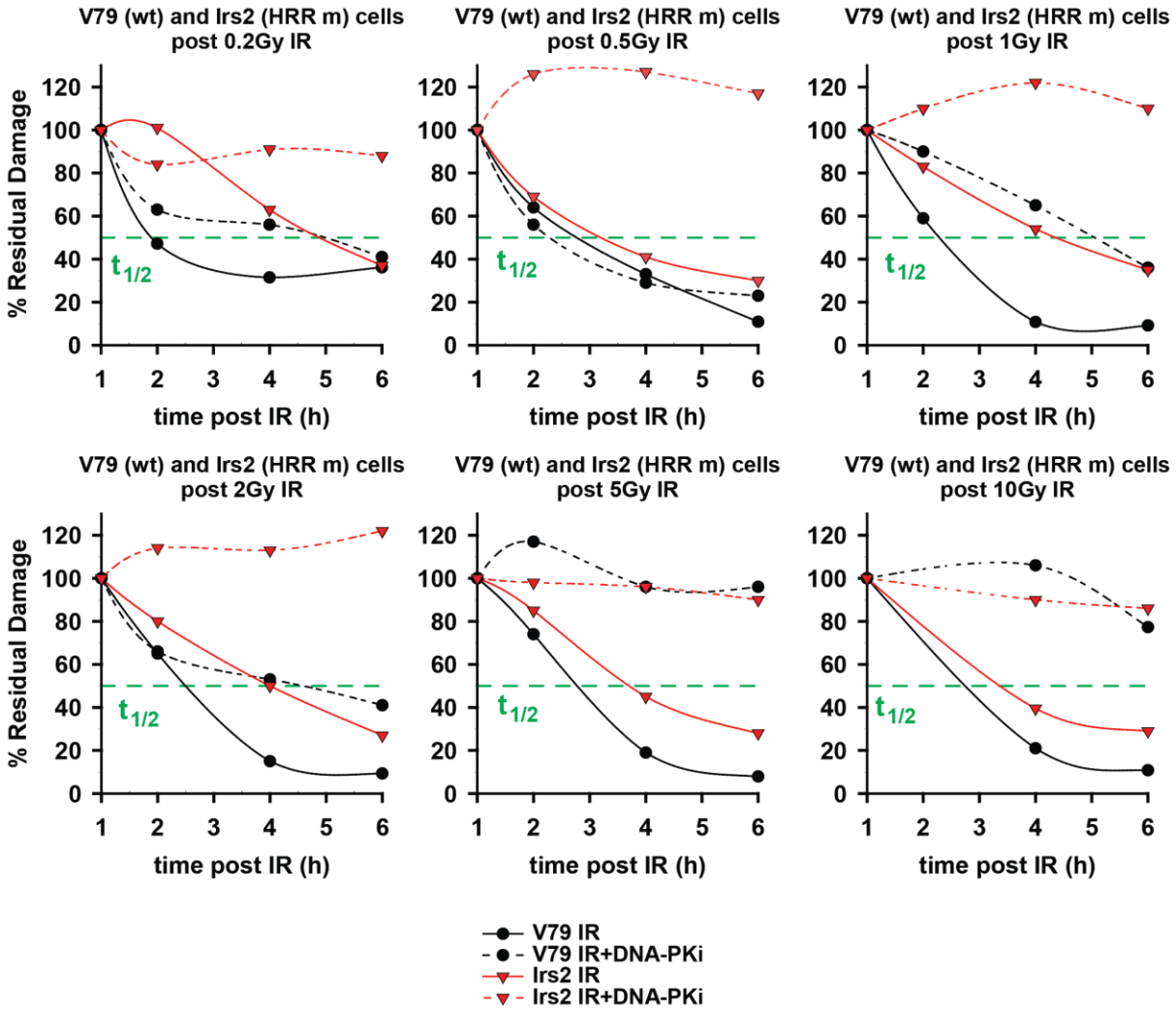

Figure 30: Comparison of % residual damage in V79 (wt) cells and irs2 (HRR m) cells after exposure to IR alone or IR+DNA-PKi. Mean values from three independent experiments are normalized to the number of PCC breaks measured at 1 h. The green dotted line serves the orientation for the determined $t_{1/2}$ values.

Figure 30 clearly shows that irs2 (HRR m) cells do need more time to repair PCC breaks after IR alone as compared to V79 (wt) cells at all doses measured. Moreover, the residual damage at 6 h, is higher for irs2 (HRR m) than for V79 (wt) cells. Hence, mutations in HRR cannot fully be compensated by c-NHEJ, in terms of efficiency of rejoining of PCC breaks. Furthermore, the results suggest that HRR, particularly at low doses (0.2 Gy and 0.5 Gy), compensates for deficient c-NHEJ (chemical inhibition), since V79 (wt) cells repair IR induced PCC breaks in the presence of DNA-PKi, almost as efficient as the IR alone control.

At higher doses however (2 Gy, 5 Gy and 10 Gy), HRR saturates giving way to c-NHEJ. Its chemical inhibition therefore causes PCC break repair abrogation.

These experiments in aggregate demonstrate a dose dependent regulation of DSB repair pathway engagement to IR induced PCC breaks.

4.2.3 IR dose dependent repair pathway switch is not restricted to V79 (wt) and irs2 (HRR m) cell lines

Is the dependence on c-NHEJ for PCC break repair after exposure of cells to high IR doses specific to V79 and irs2 cells? Can a similar trend be observed in other wildtype and HRR defective cell lines?

To answer this question, we tested three additional Chinese hamster cell lines. We scored initial breaks (1 h post IR) and residual breaks (4 h post IR) after different IR doses alone, or after IR in the presence of the DNA-PK inhibitor NU7441.

Among the three cells lines tested one is wildtype (CHOK1) and two are mutants in Rad51 paralogues XRCC2 (irs1-tor) and XRCC3 (irs1SF).

First, PCC break induction was determined at 1 Gy, 2 Gy and 5 Gy in the presence or absence of the DNA-PK inhibitor, NU7441.

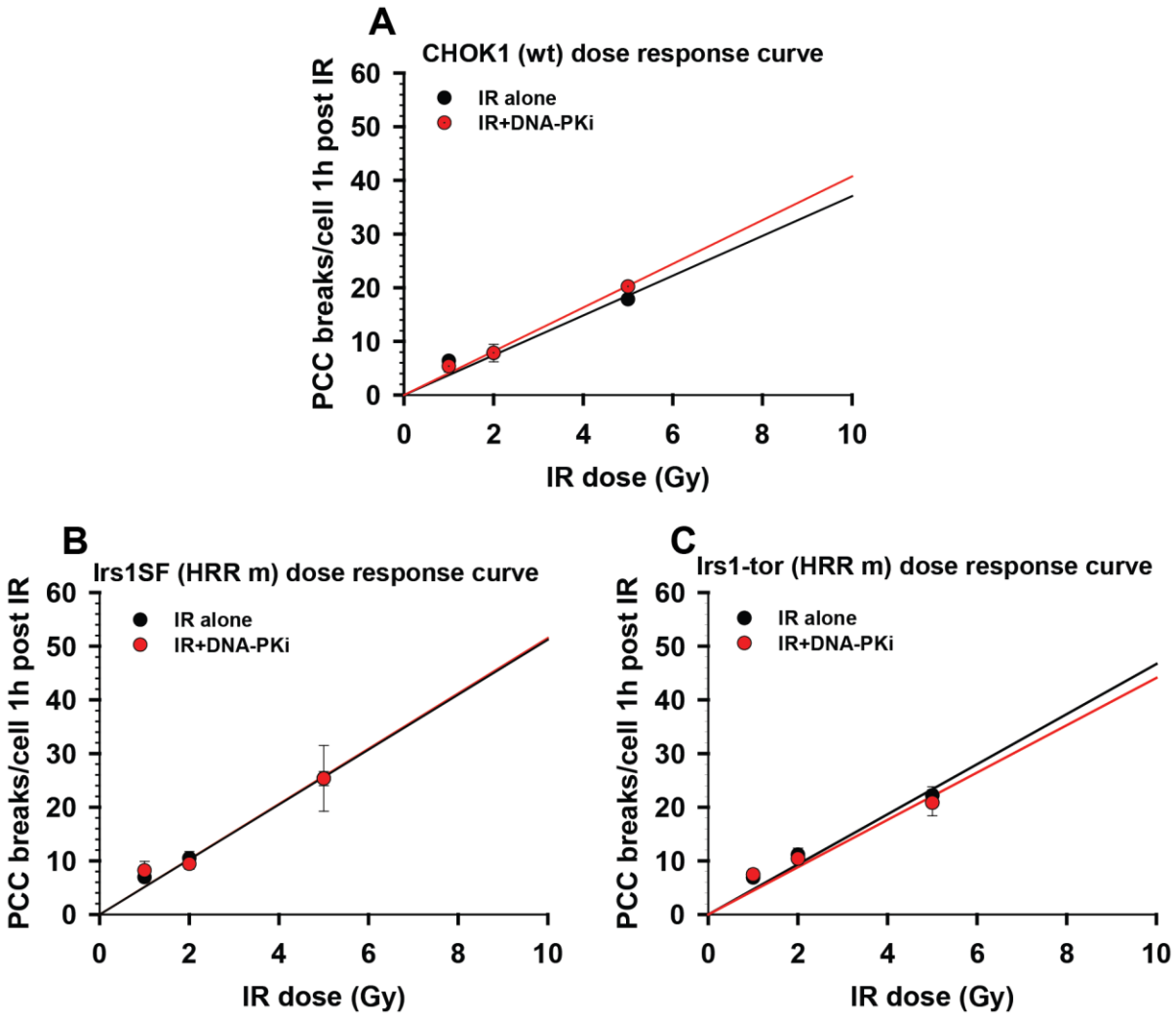

Figure 31: Dose response curve for the induction of PCC breaks in indicated Chinese hamster cell lines measured in the presence or absence of DNA-PKi. Chinese hamster cell lines were exposed to different doses of IR alone or in the presence of DNA-PK inhibitor NU7441. Dose response for A) CHOK1 (wt), B) Irs1SF (XRCC3 m), and C) Irs1-tor (XRCC2 m). The induction of PCC breaks was measured 1 h post IR. Results are obtained from three independent experiments and ± SD was determined.

All three cell lines show a linear induction of PCC breaks that remains unchanged in the presence of DNA-PKi (**Figure 31**).

The induction of PCC breaks was slightly lower in CHOK1 (wt) cells as compared to irs1-tor and irs1-SF cells (see **Supplementary Figure 1**), suggesting again that mutations in HRR render cells more prone to chromosomal breakage.

We next analyzed PCC breaks 1 h (initial damage) and 4 h (residual damage) after exposure to IR alone, or IR in the presence of DNA-PK inhibitor. Doses of 1 Gy, which we considered as a low dose, 2 Gy and 5 Gy (high doses) were selected since we saw significant changes in repair pathway contribution at those doses in the previous experiments. Obtained results are presented in **Figure 32** and Table 7.

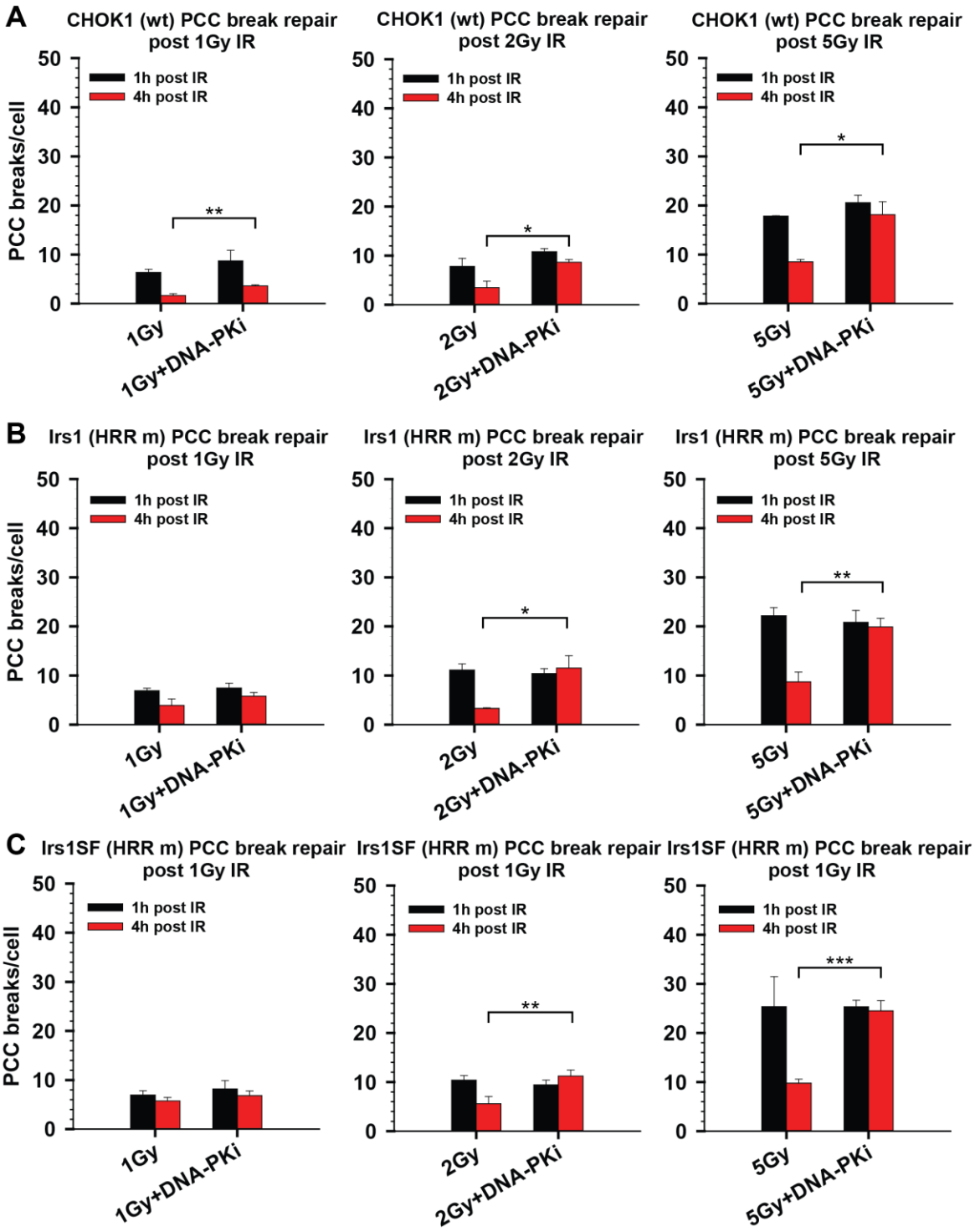

Figure 32: PCC break repair after exposure of different Chinese hamster cell lines to different doses of IR alone or IR+DNA-PK inhibitor NU7441. Cells were exposed to 1 Gy, 2 Gy and 5 Gy IR alone or in the presence of the DNA-PK inhibitor. PCC breaks were determined 1 h post IR (initial breaks) and 4 h post IR (residual breaks). Data are obtained from 2 – 3 independent experiments and ± SD was determined. The significance of differences was determined by comparing cells after IR alone to cells after IR+DNA-PKi using a two tailed student t-test (asterix designation $p<0.001$ ***, $p<0.01$ **, $p<0.05$ *).

Table 7: Residual damage 4 h post IR for Chinese hamster cell lines exposed to different IR doses alone or in the presence of DNA-PKi. The residual damage was calculated by comparing PCC breaks scored 1h post IR to PCC breaks scored 4h post IR.

Cell lines	IR Dose	% Residual damage after IR alone	% Residual damage after IR+DNA-PKi
CHOK1 (wt)	1 Gy	26	41
	2 Gy	44	80
	5 Gy	47	88
Irs1-tor (HRR m)	1 Gy	57	78
	2 Gy	30	111
	5 Gy	39	96
Irs1-SF (HRR m)	1 Gy	83	83
	2 Gy	54	119
	5 Gy	39	97

Acquired results show that CHOK1 (wt) cells repair 70% of PCC breaks within 4 h post 1 Gy IR. Inhibition of DNA-PK renders repair less efficient, with only 60% of breaks rejoining at 4 h post IR (**Figure 32**, **A**). Although, the calculated difference is significant, CHOK1 cells are still able to resolve 60% of initial PCC breaks indicating that other pathways can compensate for PCC break repair. Exposure of CHOK1 cells to 2 Gy and 5 Gy IR reduced repair speed and only 50 – 60% of breaks were resolved (Table 7) within 4 h.

Chemical inhibition of DNA-PK caused repair abrogation after exposure of CHOK1 cells to 2 Gy and 5 Gy IR. 10 – 20% of initial PCC breaks are rejoined by 4 h, which is significantly different to cells exposed to IR alone. Observations for CHOK1 cells are in line with the findings for V79 (**4.2.1**). Also for CHOK1, inhibited c-NHEJ can be compensated by other repair pathways like HRR or alt-EJ after low doses of IR (1 Gy). Correspondingly, a switch to c-NHEJ is evident at doses higher than 2 Gy.

Irs1 (HRR m) cells repaired about 40% of initial breaks after exposure to 1 Gy. Inhibition of DNA-PK caused another decrease of repair to only 20% 4 h post IR. The calculated difference was not significant.

More interesting was the observation, that PCC break repair became more efficient after irs1 (HRR m) cells are exposed to 2 Gy and 5 Gy IR. While after 1 Gy only 40% of breaks are resolved a clear increase in PCC break repair, to 70%, was detected upon exposure to 2 Gy and 5 Gy IR. After exposure to 2 Gy and 5 Gy in the presence of the DNA-PK inhibitor, PCC breaks remained un-rejoined. This observation once

more supports a predominant role of c-NHEJ in PCC break repair after exposure of cells to high IR doses (**Figure 32 B,** Table 7).

Similar tendencies are also observed in irs1SF cells (**Figure 32, C**). Only 20% of initial PCC breaks were resolved 4 h after 1 Gy IR, as well as after 1 Gy in the presence of the DNA-PK inhibitor. Yet, repair gained speed after 2 Gy and 5 Gy IR with 50 – 70% of breaks being resolved at 4 h post IR; hinting again towards an increasing role of c-NHEJ (Table 7). Similar to the irs1 cells, in irs1SF cells PCC breaks remained un-rejoined after exposure to 2 Gy and 5 Gy, when c-NHEJ was chemically inhibited.

The results of CHOK1, irs1SF and irs1 support the results obtained in V79 (wt) and irs2 (HRR m) cells (**4.2.2**). Although, c-NHEJ does play an important role in PCC break repair at all IR doses, c-NHEJ seems to be more crucial after high IR doses. In particular, the experiments carried out with HRR mutant cell lines support this conclusion. Furthermore, results for the CHOK1 (wt) cells show a role of HRR or alt-EJ in compensating for failures in c-NHEJ after 1 Gy IR.

4.2.4 C-NHEJ mutant cell lines confirm an IR dose dependent repair pathway switch

The above outlined experiments estimate the contribution of c-NHEJ via chemical inhibition of DNA-PK. We inquired whether similar conclusion could be drawn using mutants of c-NHEJ – similar to the use of HRR mutants above.

If there is a switch to c-NHEJ at high IR doses and a saturation of HRR, we would expect abrogated PCC break repair, when c-NHEJ mutant cells are exposed to high IR doses, like 5 Gy. To test this idea, we choose Chinese hamster XR1 cells. XR1 cells show a mutation in XRCC4, a cofactor for DNA Ligase 4, which in a complex with XLF aids the re-joining of DSBs via c-NHEJ (Ahnesorg, et al. 2006). Using a similar protocol, we exposed XR1 cells to 1 Gy, 2 Gy and 5 Gy and measured PCC breaks 1 h (initial breaks) and 4 h (residual breaks) post IR (**Figure 33, B**). Furthermore, dose response curves were generated to compare the induction of PCC breaks in XR1 cells to CHOK1 (wt) and irs1SF (HRR m) cells (**Figure 33, A**).

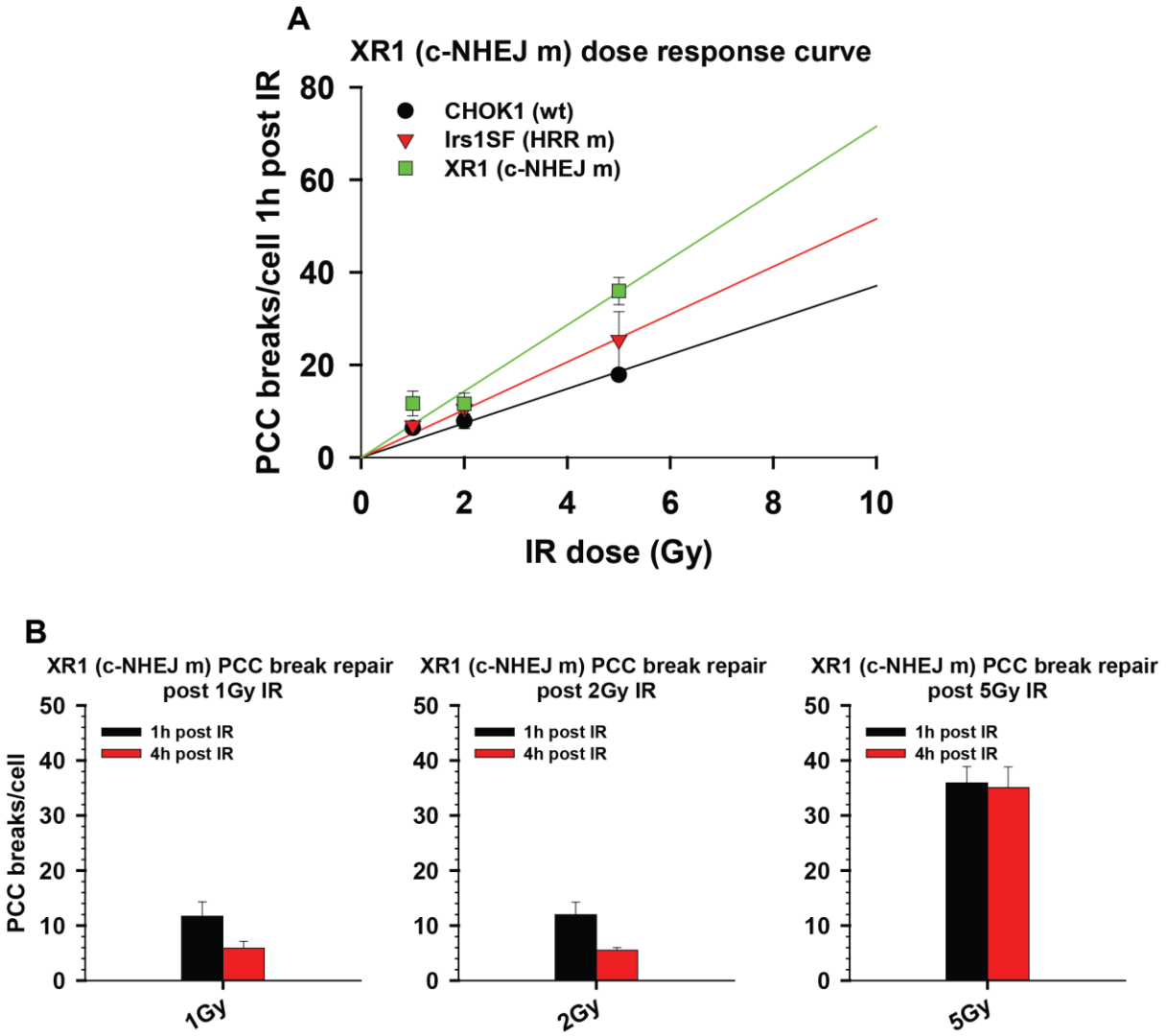

Figure 33: Dose response and PCC break repair for XR1 (c-NHEJ) cells after exposure to different IR doses. XR1 (XRCC4 m) cells were exposed to different IR doses and dose response curve (A) was created comparing the induction of PCC breaks in XR1 cells to wildtype CHOK1 cells and HRR mutated irs1SF cells. B) PCC break repair for XR1 cells after different doses of IR measured 1 h (initial breaks) and 4 h (residual breaks) after IR. Data obtained from 2-3 independent experiments ± SD.

The induction of PCC breaks in XR1 cells is clearly elevated as compared to CHOK1 (wt) and irs1SF (HRR m) cells. XR1 cells show a twofold higher number of initial PCC breaks as compared to CHOK1 (wt) cells. In comparison to irs1SF (HRR m) cells a 1.5 fold increase in the number of PCC breaks was detected for XR1 cells (**Figure 33**). Hence, intact c-NHEJ is of critical importance for genomic stability and mutations in key components of c-NHEJ renders cells more prone to chromosome breakage. Data also indicate that it makes a difference, whether the cell has a mutation in c-NHEJ or if c-NHEJ is chemically inhibited, since we were not able to detect significant differences in the induction of PCC breaks in wildtype or HRR mutated cells upon exposure to IR in the presence of the DNA-PK inhibitior.

With regard to PCC break repair in XR1 cells, 50% of initial PCC breaks are repaired within 4 h post 1 Gy and 2 Gy IR. After exposure to 5 Gy IR, PCC breaks remain un-rejoined reinforcing the importance of c-NHEJ at high IR doses.

Thus, results obtained with XR1 cells strengthen our hypothesis that after high IR doses mainly c-NHEJ is involved in the repair of PCC breaks, while after exposure of cells to lower doses other pathways can partly compensate for defects in c-NHEJ. In addition results show that not only the inhibition of DNA-PK but also mutations in other key components of c-NHEJ significantly influence PCC break repair.

4.2.5 Chemical inhibition of DNA-PK abrogates PCC break repair in a human fibroblast cell lines in a dose dependent manner

Are the above-observed trends only true for rodent Chinese hamster cells?

We decided to measure PCC-break repair-kinetics in the human wildtype, fibroblast cell line 82-6, which is immortalized with h-tert (human telomerase reverse transcriptase). 82-6 cells present a clean karyotype (46 chromosomes) and form good PCCs, which can be distinguished from metaphases as illustrated in **Figure 34**.

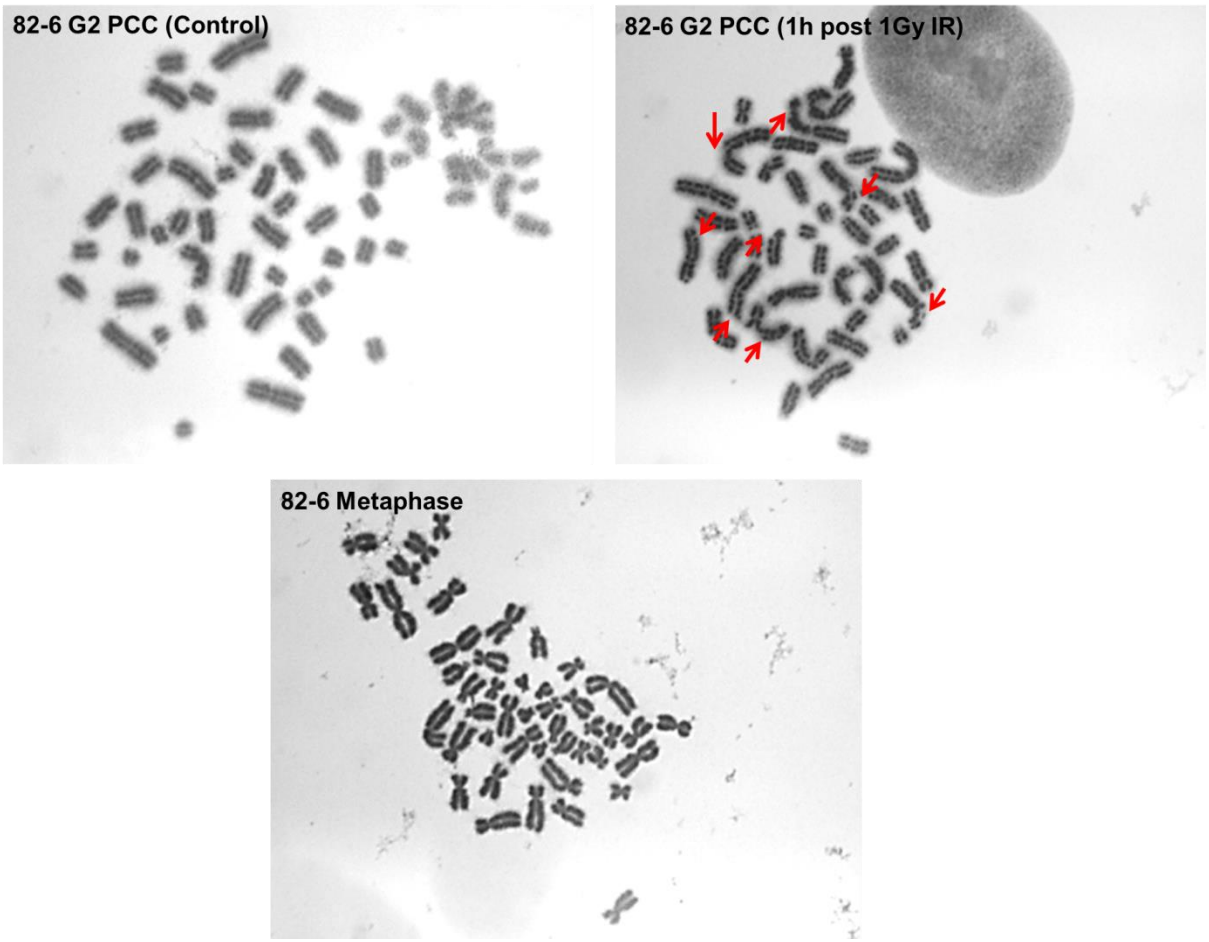

Figure 34: Representative Image for G2 PCCs and metaphases in 82-6 cells. Note that PCC breaks generated upon exposure to IR can be visualized and scored also in 82-6 cells. The morphology of a G_2 PCC is clearly distinguishable from that of a metaphase chromosome.

Experiments in 82-6 cells used protocol similar to those described for the rodent cells. Repair was followed 1 h, 2 h as well as 4 h post 1 Gy, 2 Gy and 5 Gy IR. The results obtained are summarized in **Figure 35**.

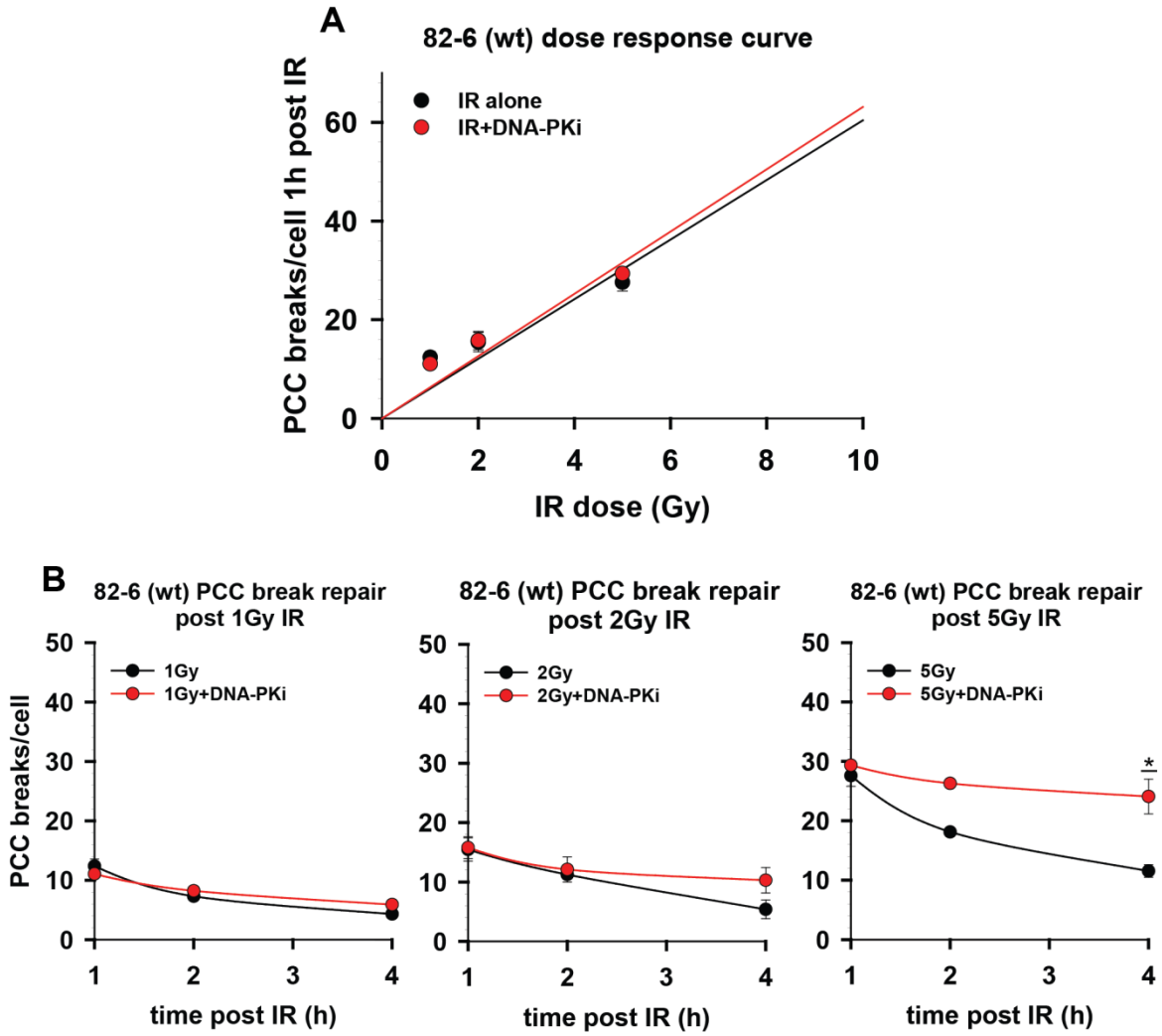

Figure 35: Dose response curve and PCC break repair kinetics for human 82-6 (wt) cells after exposure to IR ±DNA-PK inhibitor. Exponentially growing 82-6 (wt) cells were exposed to different IR doses alone, or in the presence of DNA-PK inhibitor NU7441 and the (A) dose response curve and (B) PCC break repair kinetics were determined. Significance of differences was determined for the 4 h time points between IR alone and IR+DNA-PKi, to compare residual damages. A two tailed student t-test (asterix designation $p<0.001$ ***, $p<0.01$ **, $p<0.05$ *) was used. Data represent the mean of two independent experiments ± SD.

Induction of PCC breaks in human 82-6 cells increases linearly with IR dose. Inhibition of DNA-PK does not change the number PCC breaks scored (**Figure 35, A**).

With respect to PCC break repair (**Figure 35, B)**, 82-6 (wt) cells repair around 70% of breaks after 1 Gy and 2 Gy IR (refer also to **Supplementary Figure 2**). After 2 Gy IR only 60% of breaks are repaired within the covered timeframe. We further observed a decrease in repair speed with increasing radiation dose. While 50% of breaks are rejoined after 2.5 h post 1 Gy IR, $t_{1/2}$ after 2 Gy and 5 Gy corresponded to 3 h (see also **Supplementary Figure 2** and Table 8).

Table 8: Determination of $t_{1/2}$ and % residual damage for 82-6 cells. $t_{1/2}$ was determined from the normalized repair kinetics graph. The residual damage represents the breaks remaining 4 h post IR in comparison to the initial breaks (See also **Supplementary Figure 2**).

IR dose (Gy)	$t_{1/2}$ IR alone (h)	$t_{1/2}$ IR+DNA-PKi (h)	% Residual damage post IR	% Residual damage IR+DNA-PKi
1	2.44	4	35	53
2	3.1	N.a*	35	65
5	3.1	N.a*	41	81

*N.a $t_{1/2}$ not obtained in the measured time frame

The chemical inhibition of DNA-PK compromised PCC break repair speed and increased the residual damage after 1 Gy, 2 Gy and 5 Gy. Specifically, after 1 Gy IR only 47% of PCC breaks are repaired 4 h post IR. $t_{1/2}$, upon exposure to 1 Gy, in the presence of DNA-PKi, exceeded the measured timeframe of 4 h, suggesting that a slow DSB repair pathway e.g. HRR is engaged in PCC break repair. After 2 Gy IR only 37% of initial PCC breaks are rejoined 4 h post IR and also here, $t_{1/2}$ was not within the measured time frame (Table 8). After 5 Gy IR in the presence of DNA-PKi, 80% of PCC breaks remained un-rejoined which is significantly different for PCC breaks post IR alone.

The results obtained demonstrate an IR dose dependent contribution of c-NHEJ. Similar to the Chinese hamster cells, human 82-6 cells show that inhibition of c-NHEJ can be better compensated at low doses (1 Gy) than at high doses (5 Gy).

Summarizing the results obtained under **4.2** for Chinese hamster cell lines and human cells; we are able to draw the following conclusions:

First, after exposure of cells to low doses of IR (0.2 Gy, 0.5 Gy and 1 Gy) slow pathways are actively involved in the repair of PCC breaks and can compensate (although at a lower repair speed) for abrogated c-NHEJ.

Second, with increasing radiation dose c-NHEJ becomes the main repair pathway taking care of PCC break repair. This is mainly supported by data obtained in wildtype cell lines upon exposure to IR+DNA-PKi which leads to significantly higher residual damages (see V79, CHOK1 and 82-6 results). This conclusion is also supported by results obtained using HRR mutants, which show total abrogation of PCC break repair after exposure to 2 Gy, 5 Gy and 10 Gy IR in the presence of the DNA-PK inhibitor (see irs2, irs1SF and irs1).

Third, not only the inhibition of DNA-PK, but also mutations in other key components of c-NHEJ, leads to PCC break repair abrogation after high (>2 Gy) IR doses as demonstrated for XR1 (XRCC4 m) cells.

Fourth, we can note that mutations or chemical inhibition of key components of c-NHEJ give different results. This is particularly obvious for the induction of PCC breaks. While the chemical inhibition of DNA-PK did not cause significant differences in the induction of PCC break, as seen for V79 (wt), irs2 (HRR m), irs1 (HRR m), irs1SF (HRR m), 82-6 (wt) and CHOK1 (wt), the induction of PCC breaks in the c-NHEJ mutated XR1 cell lines showed 1.5 to two fold increase in the initial PCC breaks.

Finally, c-NHEJ seems to be the main repair pathway taking care of PCC break repair post IR and can partially compensate for defects in HRR, which is supported by results collected for the HRR mutants.

Thus, coming back to our hypothesis stated at the beginning, of this second part, we have good proof for the presence of an IR dose dependent regulation of DSB repair pathways in the processing of PCC breaks.

PART III: THE ROLE OF ALT-EJ TO IR INDUCED PCC BREAK REPAIR PROCESSING

4.3 Alt-EJ does not show a clear contribution to the repair of PCC breaks in Chinese hamster cells

In **4.2** we mainly focused on investigating the contribution of c-NHEJ and HRR to the repair of IR induced PCC breaks.

However, several studies report an involvement of alt-EJ, as a backup in the processing of IR-induced DSBs (Ceccaldi, et al. 2015; Chiruvella, et al. 2013; Wu, et al. 2008) - particularly, when other repair pathways fail to engage (Frit, et al. 2014; Mladenov, et al. 2016).

One molecule, which has been repeatedly implicated to play crucial roles in alt-EJ is Parp-1 (Iliakis, et al. 2015b; Mansour, et al. 2010; Soni, et al. 2014).

We reasoned that inhibition of Parp-1 should uncover eventual contributions of alt-EJ to PCC break repair.

To this end, we carried out experiments in which wildtype, HRR mutant and c-NHEJ mutant Chinese hamster cells were exposed to IR alone in the presence or absence of the Parp-1 inhibitor, PJ34. The initial number of PCC breaks (1 h post IR), as well as the residual number of PCC breaks (4 h post IR) were determined.

First, we analyzed PCC break processing in repair proficient V79 and CHOK1 wildtype cell lines.

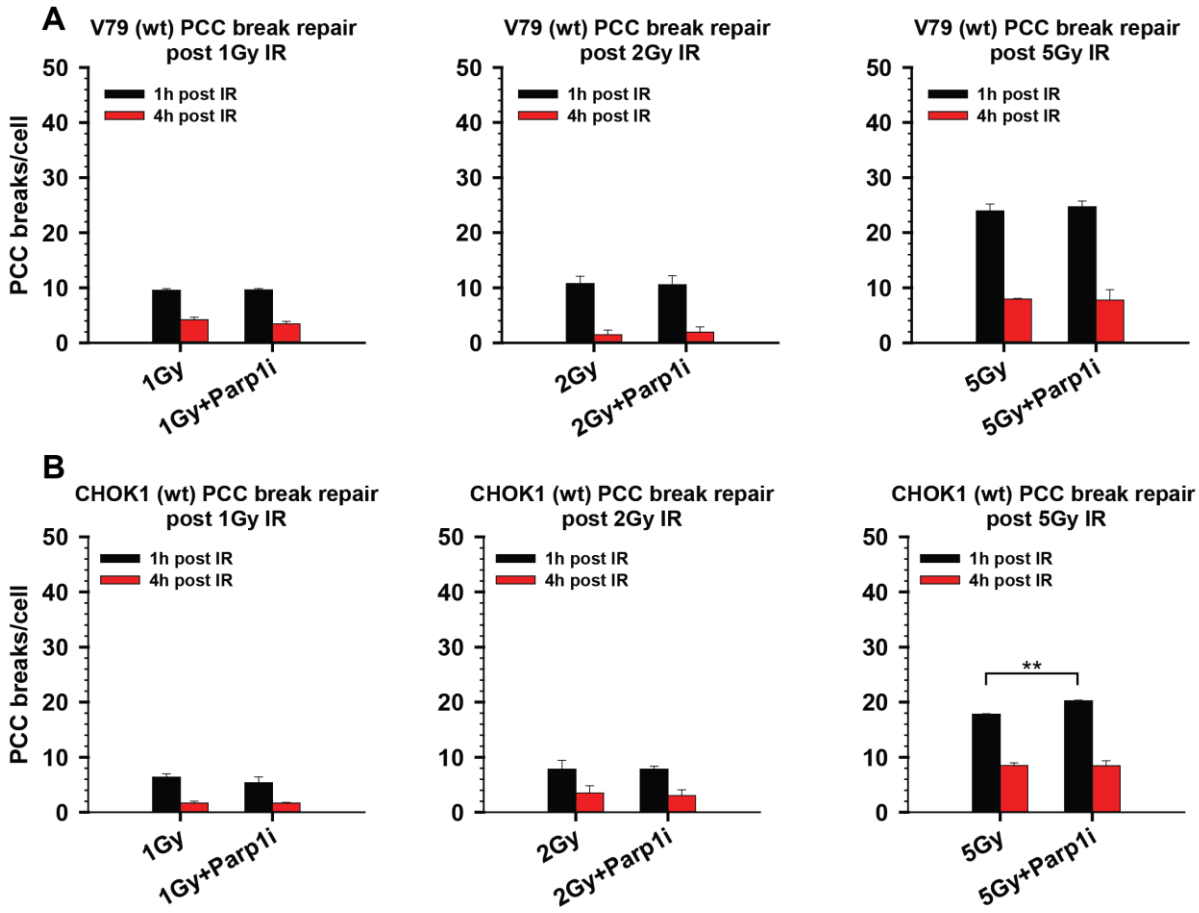

Figure 36: PCC break repair after exposure of wildtype Chinese hamster cells to IR alone, or in the presence of Parp-1 inhibitor PJ34. A) V79 (wt) and B) CHOK1 (wt) cells have been exposed to different IR doses alone or in the presence of Parp-1 inhibitor PJ34. PCC breaks were scored 1h and 4h post IR and significant differences between IR alone and IR+Parp-1i were determined employing a two tailed student t-test (asterix designation $p<0.001$ ***, $p<0.01$ **, $p<0.05$ *). Results present the mean of 2 – 3 independent experiments ± SD.

The results obtained show (**Figure 36**), that inhibition of Parp-1 does not detectably affect PCC break repair. The residual damage measured for CHOK1 and V79 cells after exposure to 1 Gy, 2 Gy and 5 Gy alone and in the presence of Parp-1 inhibitor, is very similar (for the calculated residual damage see **Supplementary Table 1**). Only for CHOK1 cells a significant difference could be detected for the initial breaks 1 h post 5 Gy IR (**Figure 36, B**), but PCC break re-joining is not affected. Based on these results in repair proficient cells we conclude that alt-EJ is not significantly involved in the processing of PCC breaks.

In a next experiment we inquired, whether alt-EJ is involved in IR induced PCC break repair, when one of the main DSB repair pathways is abrogated through mutations in key proteins. To this end, we studied the rejoining of IR induced PCC breaks in irs1

(XRCC2 m), irs2 (Rad51B m) and irs1SF (XRCC3 m) cell lines.

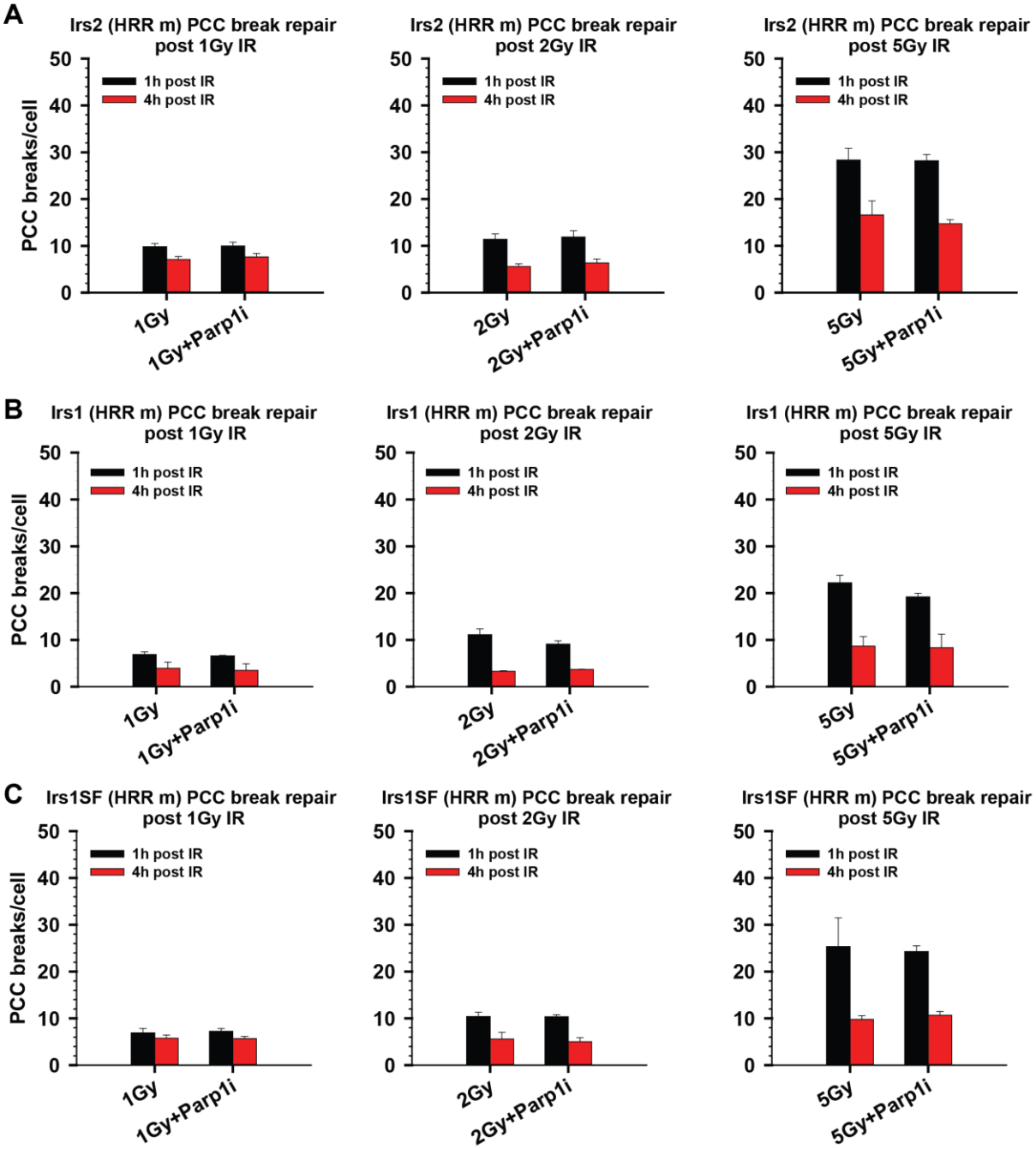

Figure 37: PCC break repair for different Chinese hamster HRR mutants after exposure to IR alone or in the presence of Parp-1 inhibitor PJ34. A) Irs2 (Rad51B m), B) irs1 (XRCC2 m), C) irs1SF (XRCC3 m). PCC breaks were scored 1 h (initial breaks) and 4 h (residual breaks) post IR. Data obtained represent the mean of 2 – 3 independent experiments ± SD.

Also in HRR mutant cell lines, inhibition of Parp-1 did not uncover a role of alt-EJ to PCC break repair (**Figure 37**). The residual damage measured, for cells exposed to IR in the presence of Parp-1 inhibitor is similar to that measured in cells exposed to IR alone. Thus, although HRR is abrogated in irs2, irs1 and irs1SF cells, the defect is

compensated by c-NHEJ (for the calculated residual damage see **Supplementary Table 1**).

In same manner we studied PCC break repair upon inhibition of Parp-1 in c-NHEJ deficient XR1 (XRCC4 m) cells. This experiment was of particular interest since earlier studies, investigating repair of DSBs as by PFGE showed a contribution of alt-EJ to DSB repair when c-NHEJ is abrogated (Iliakis 2009; Mladenov and Iliakis 2011).

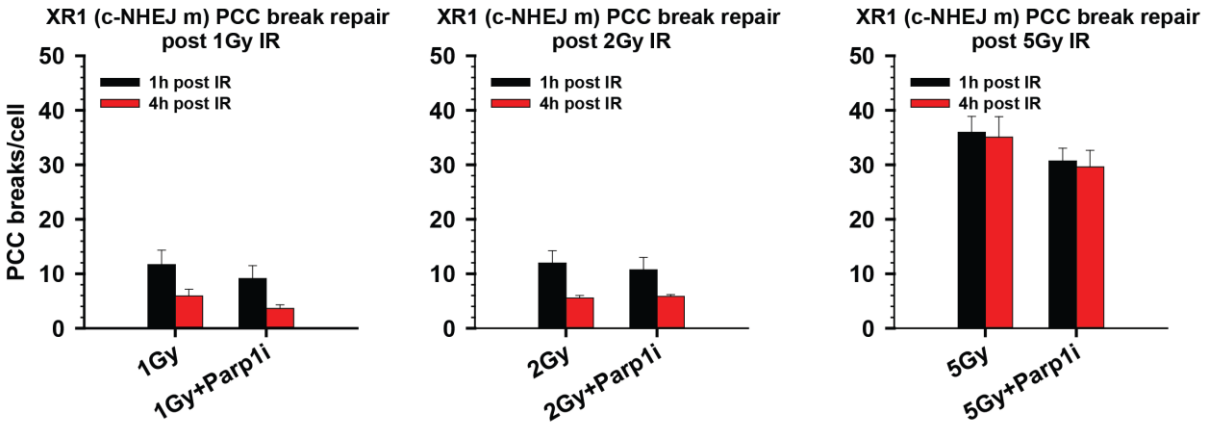

Figure 38: PCC break repair in Chinese hamster XR1 (XRCC4 m) cells post IR and in the presence of Parp-1 inhibitor PJ34. Initial PCC breaks (1 h post IR) and residual PCC breaks (4 h post IR) were measured. Data represent the mean of 2 – 4 independent experiments ± SD.

But even in XR1 cells, Parp-1 inhibition failed to show a contribution of alt-EJ to PCC break rejoining under the conditions employed (**Figure 38,** for the calculated residual damage see **Supplementary Table 1**).

In a last attempt to uncover a contribution of alt-EJ to PCC break repair, we carried out experiments employing the combined inhibition of DNA-PK and Parp-1 in irs2 cells and quantified initial and residual PCC breaks (**Figure 39**).

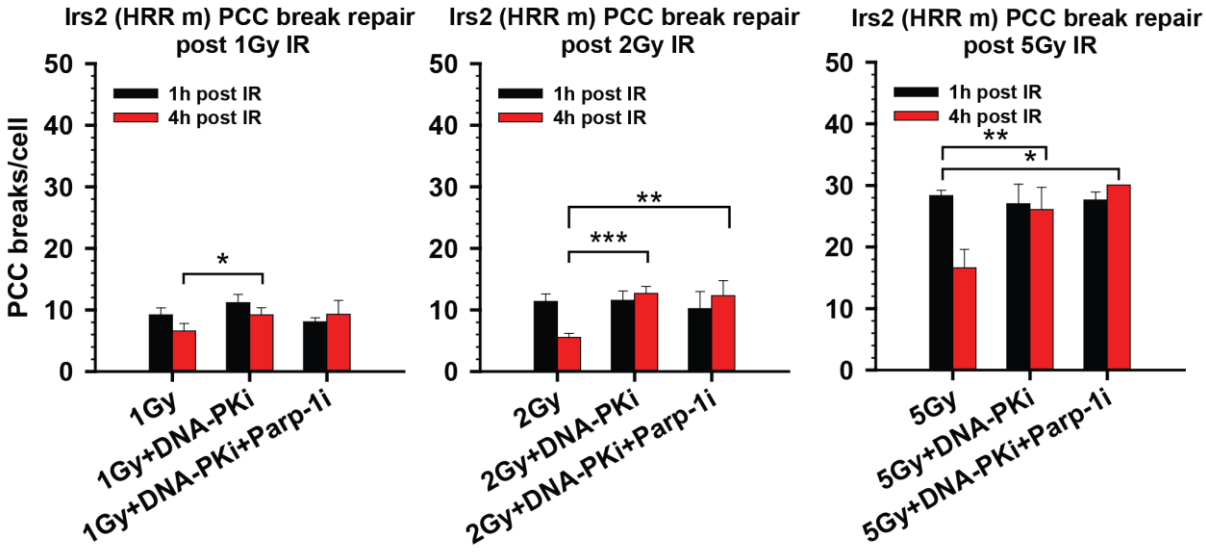

Figure 39: PCC break repair in irs2 (HRR m) cells upon exposure to IR and combined inhibition of DNA-PK and Parp-1. Initial (1 h) and residual (4 h) PCC breaks were quantified. Data represent the mean of 2 – 3 independent experiments. Significance of differences was calculated employing a two tailed student t-test (asterix designation $p<0.001$ ***, $p<0.01$ **, $p<0.05$ *).

The number of PCC breaks scored upon combined inhibition of DNA-PK and Parp-1 are substantially higher as compared to cells exposed to IR alone. The data after combined inhibition are very similar to the data obtained for DNA-PK inhibition alone. Thus, the observed effect can most likely be attributed to inhibited c-NHEJ and any additional effects, which could hint towards an involvement of alt-EJ are not detectable.

We conclude that alt-EJ (as measured by Parp-1 inhibition) does not contribute to PCC break repair, at least under the conditions examined.

PART IV: THE CONTRIBUTION OF DSB REPAIR PATHWAYS TO THE FORMATION OF CHROMOSOMAL EXCHANGES (CE)

PCC does not only allow the investigation of PCC breaks, but also the visualization and quantification of chromatid type exchanges (CEs). Studying the formation of CEs and the DSB repair pathways involved in their formation is of significant importance, since chromosomal exchanges have been implicated in tumorigenesis, genomic instability as well as cell killing (Lengauer, et al. 1998).

In the fourth part of the present Thesis, we will therefore focus on the contribution of the DSB repair pathways, to the formations of CEs. As before we were interested in the G_2-phase of the cell cycle, where all DSB repair pathways can engage.

CEs are miss-rejoining events which require at least two double strand breaks. CEs are thought to form by potentially error prone DSB processing pathways like c-NHEJ and alt-EJ. As outlined in the Introduction, both repair pathways cannot ensure that the original DNA ends or DNA sequence will be restored at the break site (Agarwal, et al. 2006; Ferguson and Alt 2001; Richardson and Jasin 2000).

Figure 40 shows an image of typical CEs observed, via PCC, after exposure of Chinese hamster cells to IR.

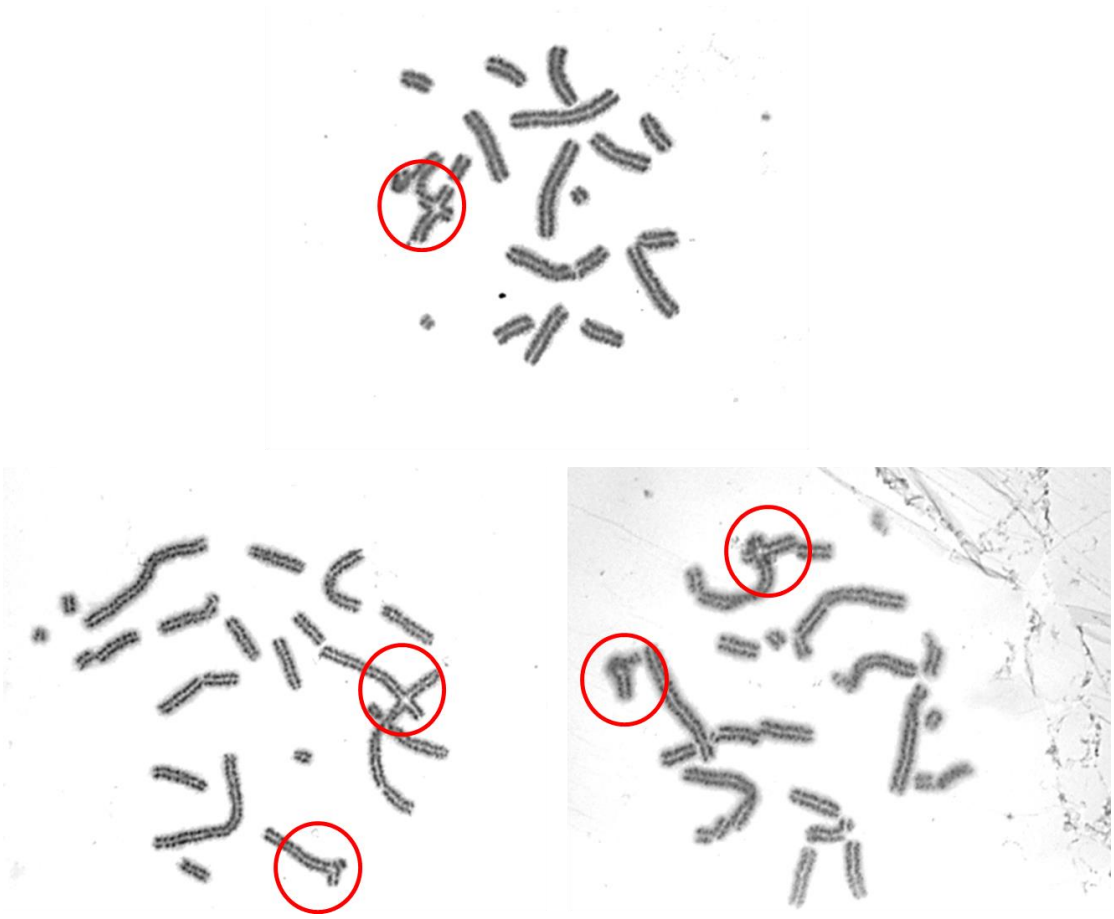

Figure 40: Representative images of typical chromatid type exchanges formed upon exposure to IR and visualized by premature chromosome condensation. Note that CEs formed in G_2 PCC are mainly of the chromatid type involving two different chromosomes. Images obtained using Chinese hamster cells.

4.4 Mutations in key components of HRR and c-NHEJ renders cells prone to the formation of chromosomal exchanges after exposure to IR

In the first set of experiments, we executed a comprehensive analysis of CE formation for rodent V79 (wt) as well as for irs2 (HRR m) cells. Both cell lines were exposed to a broad spectrum of IR doses and CE formation was analyzed 1 h, 2 h and 4 h post IR. The results obtained are shown in **Figure 41**.

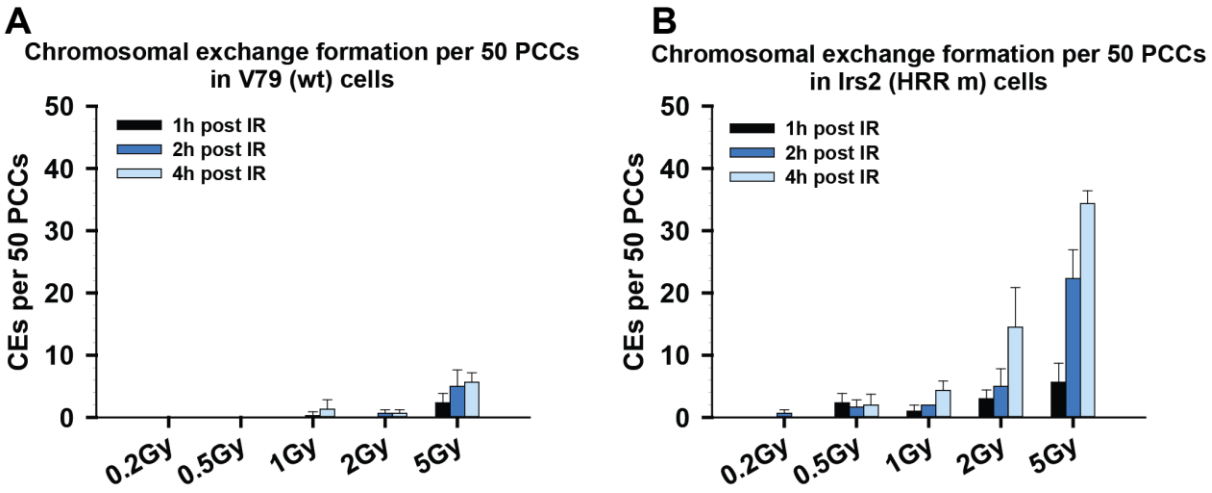

Figure 41: Formation of chromosomal exchanges as measured by PCC after exposure of indicated Chinese hamster cell lines to different doses of IR. CE formation was scored in A) V79 (wt) and B) Irs2 (HRR m) cells. Data represent the mean of three independent experiments ± SD.

Comparing the number of CEs measured in V79 (wt) cells to those obtained for irs2 (HRR m) cells, we confirm significantly lower levels of CEs in V79 cells. Furthermore, the results illustrate a dose dependent increase in CE formation. In V79 (wt) cells, disproportionally more CEs form with increasing radiation dose. This increase with dose is less pronounced in irs2 (HRR m) cells. Another important observation is that the formation of CEs takes time and maximal numbers of CEs are reached 4 h post IR. This suggests that the formation of CEs depends on DSB repair pathways that operate with slow speed. Finally, the results demonstrate a crucial role for HRR in suppressing the formation of CEs.

To further refine our findings, we measured the formation of CEs in four additional Chinese hamster cell lines, 1 h as well as 4h after exposure to 1 Gy, 2 Gy and 5 Gy of IR (**Figure 42**).

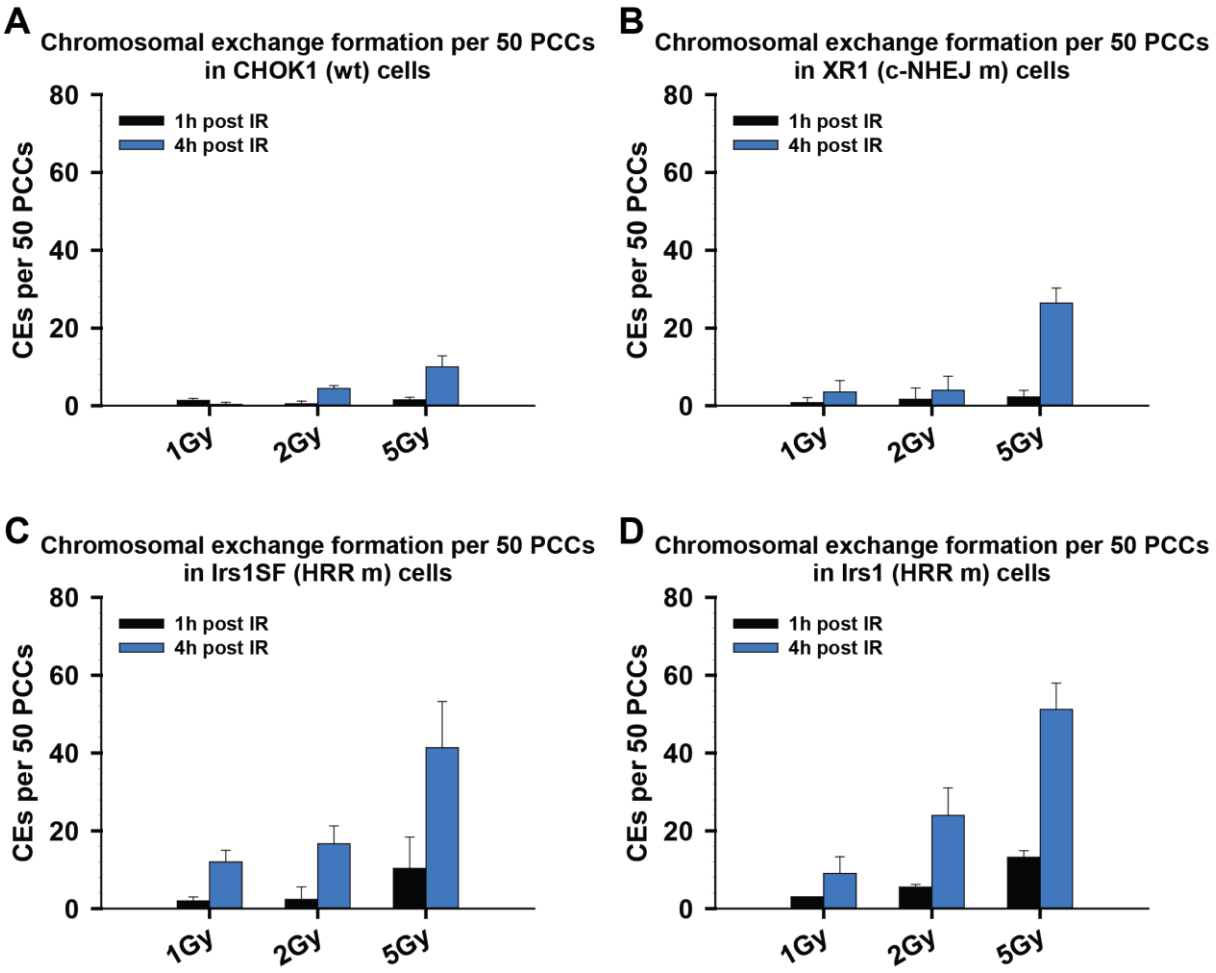

Figure 42: Formation of Chromosomal exchanges as measured by PCC after exposure of the indicated Chinese hamster cell lines to different doses of IR. CE formation was scored in A) CHOK1 (wt) and B) XR (XRCC4 m), C) Irs1SF (XRCC3 m) and D) Irs1 (XRCC2 m) cells. Data represent the mean of two to three independent experiments ± SD.

Also here, we could observe similar trends in the formation of CEs, as noted above for V79 and irs2 cells. For CHOK1 (wt) cells we saw, in contrast to V79 (wt) cells, a more proportional increase in the number of CEs with increasing radiation dose (**Figure 42, A**).

For both HRR mutant cell lines, irs1 and irs1SF, a 2 – 2.5 fold increase in the number of CEs was noted when the radiation dose increased from 1 to 2 Gy and from 2 to 5 Gy, underscoring the importance of HRR in CE suppression. Even more interesting is the observation that the c-NHEJ mutant (XR1) showed very low numbers in CEs, after exposure to 1 Gy and 2 Gy, but a 10 fold increase in the number of CEs upon exposure to 5 Gy (**Figure 42, B**).

Many published studies (Sasai, et al. 1994; Schipler, et al. 2016) implicate the formation of chromosome exchanges to radiation-induced cell killing. To investigate this point, we carried out clonogenic survival experiments and compared the results obtained to the formation of CEs.

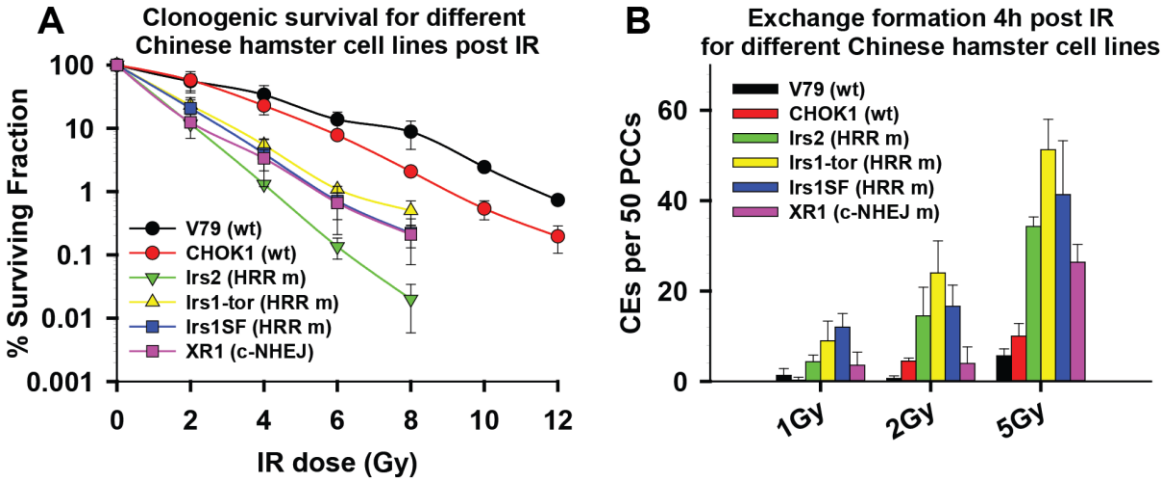

Figure 43: Clonogenic survival and CE formation, as measured by PCC, in the indicated Chinese hamster cell lines, exposed to different doses of IR. A) Chinese hamster cells were exposed to different IR doses and immediately plated for clonogenic survival. B) CE formation as measured by premature chromosome condensation, 4h after exposure of different Chinese hamster cell to various IR doses. Data represent the mean of 2 – 3 independent experiments ± SD.

The results obtained confirm that mutations in either of HRR or c-NHEJ sensitize cells to IR, and correlate this endpoint to the formation of CEs (**Figure 43, A and B**). First, data for V79 and CHOK1 wildtype cell lines are analyzed: Both cell lines do have intact DSB repair pathways and are resistant to IR exposure. Yet, CHOK1 (wt) cells are overall more radiosensitive than V79 (wt) cells. Accordingly, we observed more CEs for CHOK1 (wt) cells as compared to V79 (wt) cells, supporting the idea that increased CE formation contributes to IR induced cell killing.

Comparing the formation of CEs to IR induced cell killing for the HRR mutants a clear correlation is observed again. Both, irs1 (XRCC2 m) and irs1SF (XRCC3 m) show radiosensitivity and the number of CEs is also very similar between the two cell lines, but clearly higher than that measured in the corresponding wildtype cell lines.

Likewise, XR1 (XRCC4 m) cells show greater radiosensitivity towards IR. However, although radiosensitization of XR1 cells is very similar to irs1 and irs1SF cells, we failed to observe a corresponding increase in the number of CEs. Thus, the number of CEs for XR1 cells remains comparatively low.

In contrast to the other HRR mutant cell line, irs2 were most sensitized by IR. We would have expected that irs2 cells would therefore present with the highest numbers of CEs. This however is not the case as shown in **Figure 43 B.** The number of CEs is lower as compared to irs1 and irs1SF cells.

Summarizing the data presented in **4.4** we can conclude that increasing doses of IR renders cells more prone to CE formation. Mutations in key molecules of HRR or c-NHEJ contribute to the formation of CEs and result in significantly higher numbers of CEs as compared to wildtype cells at all IR doses. The clonogenic survival experiments further allow us to correlate cell killing with the formation of CEs.

4.4.1 The inhibition of Parp-1 does not affect the formations of CEs as measured by premature chromosome condensation

Previous experiments, carried out in our laboratory, using classical cytogenetic approaches evaluated the formation of CEs in G_2 cells that reached metaphase after exposure to 1 Gy IR. These experiments revealed that suppression of Parp-1 leads to decreases in CE formation, rendering alt-EJ the main culprit of their formation (Soni, et al. 2014).

We asked, whether we see similar contributions of alt-EJ to CE formation using PCC. More generally, we asked how DSB repair pathways actually contribute to CE formation. To this end, we designed experiments, measuring CE formation after different IR doses via the PCC technique. And here again we employed pathway specific inhibitors, as well as different Chinese hamster cell lines.

First, we analyzed the induction of CEs in V79 (wt) and CHOK1 (wt) cells, after exposure to different IR doses alone or in the presence of the Parp-1 inhibitor PJ34. CE formation was measured 1 h and 4 h post IR.

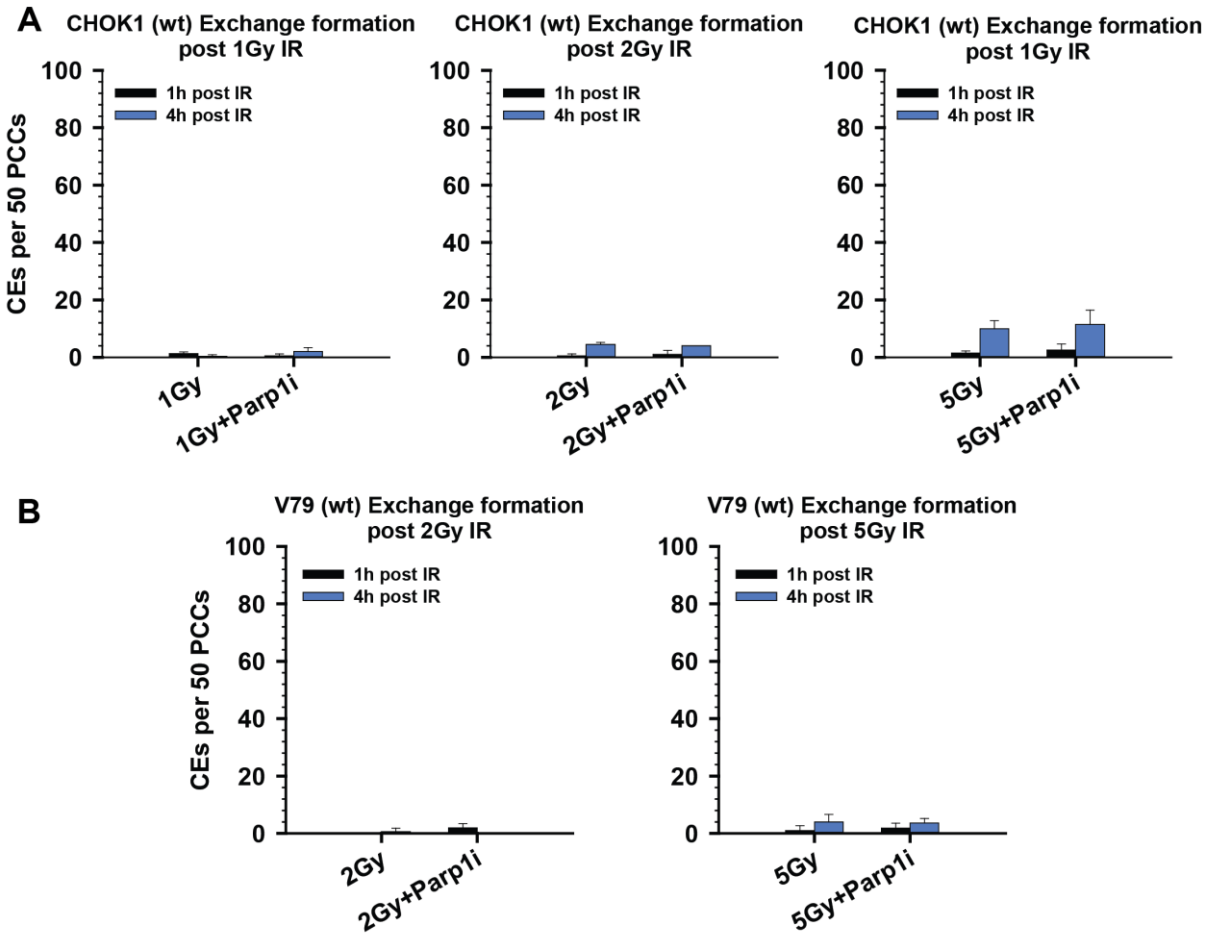

Figure 44: CE formation in the indicated Chinese hamster wildtype cell lines after exposure to different IR doses ± Parp-1 inhibition using PJ34. A) CHOK1 (wt) and B) V79 (wt) cells. The formation of chromosomal exchanges was measured 1 h and 4 h post IR. Results represent 2 – 3 independent experiments ± SD.

The results show that chemical inhibition of Parp-1 in combination with IR has no effect on the formation of CEs both in V79 (wt) and CHOK1 (wt) cells as represented in **Figure 44**.

Previous studies have implicated that alt-EJ can backup failures in HRR, but at the cost of an increased formation of CEs as measured by classical cytogenetics (Soni, et al. 2014). Consequently, we tested this assumption by measuring the formation of CEs in HRR mutants (irs2, irs1 and irs1SF). **Figure 45** summarizes the results obtained.

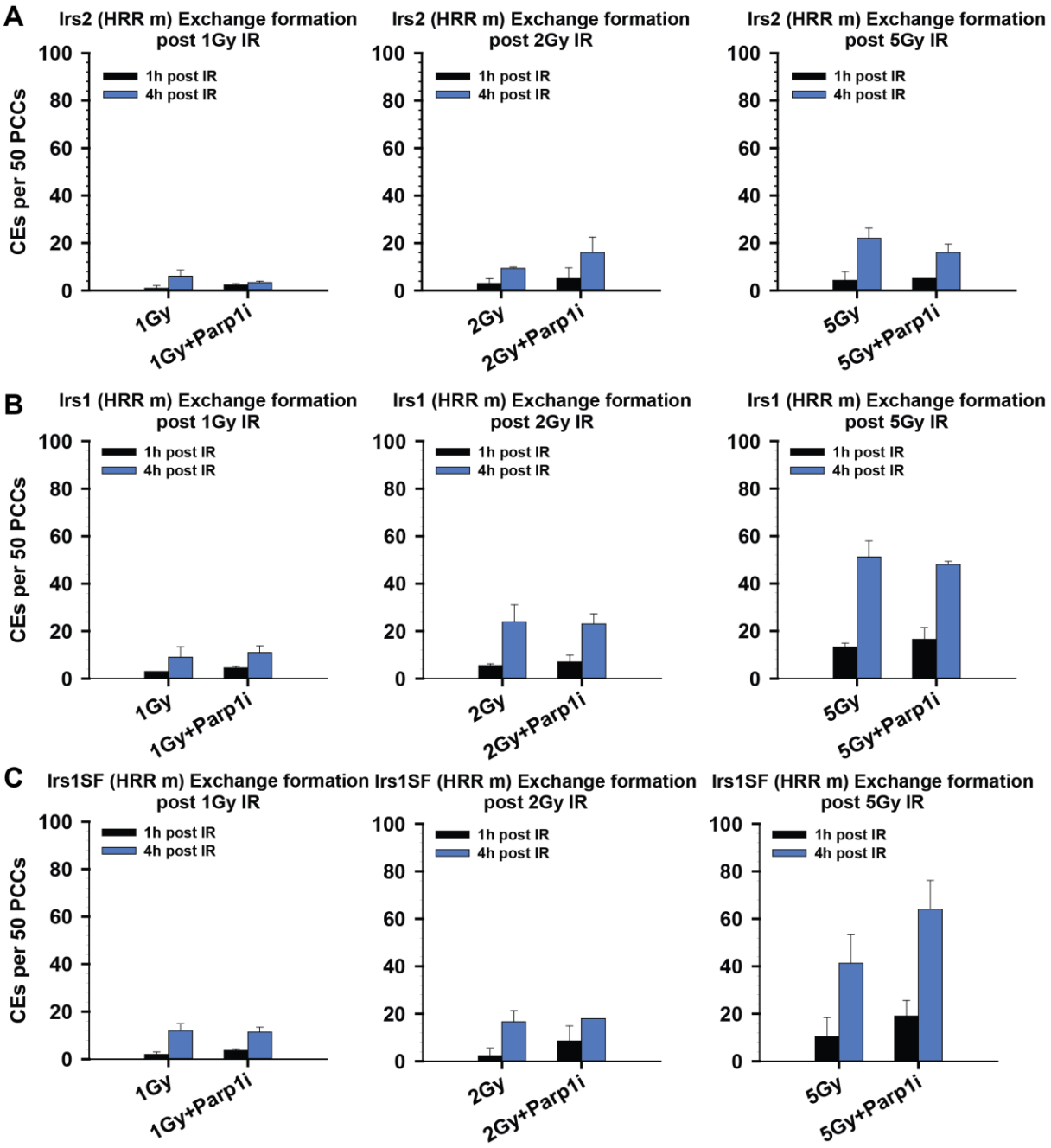

Figure 45: CE formation in indicated Chinese hamster HRR mutant cell lines after exposure to different IR doses ± Parp-1 inhibition with PJ34. A) Irs2 (Rad51B m), B) Irs1 (XRCC2 m), C) Irs1SF (XRCC3 m) cells. The formation of chromosomal exchanges was measured 1 h and 4 h post IR. Results represent 2 – 3 independent experiments ± SD.

Although, significant differences, as determined by student t-test, could not be detected, we nonetheless observe that for example irs2 cells (**Figure 45**, **A**) form slightly less CEs after Parp-1 inhibition, 4 h post 5 Gy IR. Additionally, a slight decrease in the formation of CEs was also observed, 4 h post 1 Gy IR. Exposure to 2 Gy in the presence of Parp-1 inhibitor however led to slightly more CEs.

The results with irs1 cells, suggest that Parp-1 inhibition does not have measurable effects on the formation of CEs under the conditions examined. Similar responses were also observed in irs1SF cells. After exposure of irs1SF cells to 1 Gy and 2 Gy IR, the number of CEs measured for cells exposed to IR alone as compared to that measured in the presence of Parp-1 inhibitor is very similar. Exposure to 5 Gy IR in the presence of Parp-1 inhibitor let to slightly more CEs. So, a clear contribution of alt-EJ to the formation of CEs could not be detected for HRR mutant cell lines under the tested conditions of Parp-1 inhibition.

We wondered whether, inhibition of Parp-1 using different Parp-1 inhibitor would uncover an effect on CE formation. To this end, we measured CE formation after inhibition of Parp-1 with Olaparib in selected Chinese hamster cells. Notably, Parp-1 inhibition with Olaparib also fails to uncover a clear contribution of alt-EJ to CE formation (results are presented in **Supplementary Figure 3**).

Although, a contribution of alt-EJ to PCC break rejoining in XR1 (c-NHEJ m) cells was not detected, we were able to show a significant contribution of alt-EJ to CE formation after exposure of XR1 cells to 5 Gy IR (**Figure 46**). These results are in line with previous findings where alt-EJ has been shown to backup c-NHEJ.

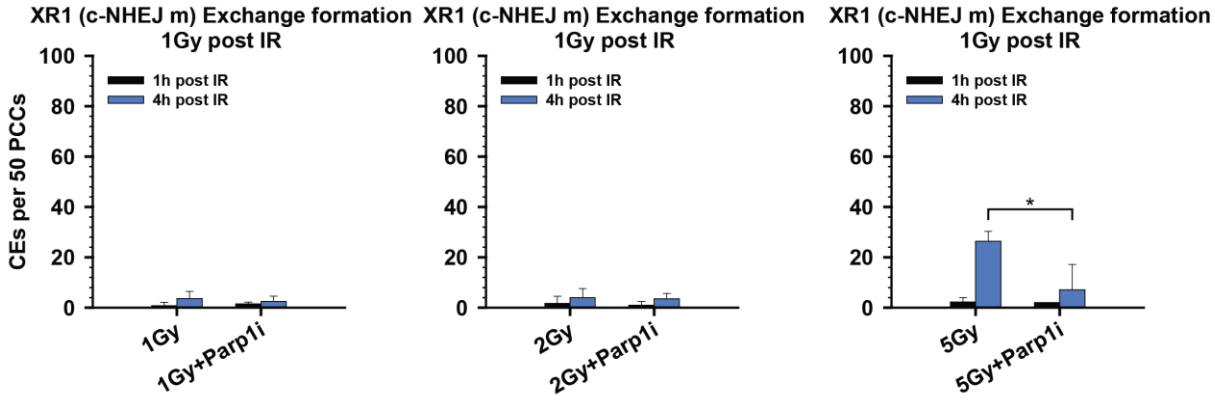

Figure 46: CE formation in indicated c-NHEJ mutated Chinese hamster cell line XR1 after exposure to different IR doses ± Parp-1 inhibition with PJ34. XR1 (XRCC4 m) cells were exposed to different IR doses as exponential cultures with or without Parp-1 inhibition by PJ34. The formation of chromosomal exchanges was measured 1 h and 4 h post IR. Results represent 2 – 3 independent experiments ± SD. Significance was calculated using a two tailed students t-test (asterix designation $p<0.001$ ***, $p<0.01$ **, $p<0.05$ *).

This result indicates a contribution of alt-EJ to CE formation after high IR doses.

Summarizing the above findings, we can say that in wildtype cells as well as in HRR mutant cells; alt-EJ does not show a clear contribution to CE formation, at least with

the PCC assay. However, when c-NHEJ is abrogated and after exposure of cells to high IR doses (5 Gy), alt-EJ seems to backup for failed c-NHEJ at the cost of an increased CE formation, which is sensitive to Parp-1 inhibition.

4.4.2 C-NHEJ contributes to the formation of chromosomal exchanges after exposure of cells to high IR doses

Not only alt-EJ has been implicated in the formation of CEs. Several studies have also implicated c-NHEJ in the formation of CEs. C-NHEJ is by nature error prone, since it lacks proofing mechanisms that would ensure the joining of original ends at a DSB.

We examined the role of c-NHEJ to CE formation via DNA-PK inhibition in different Chinese hamster cell lines. **Figure 47** shows results obtained for wildtype V79 and CHOK1 cells.

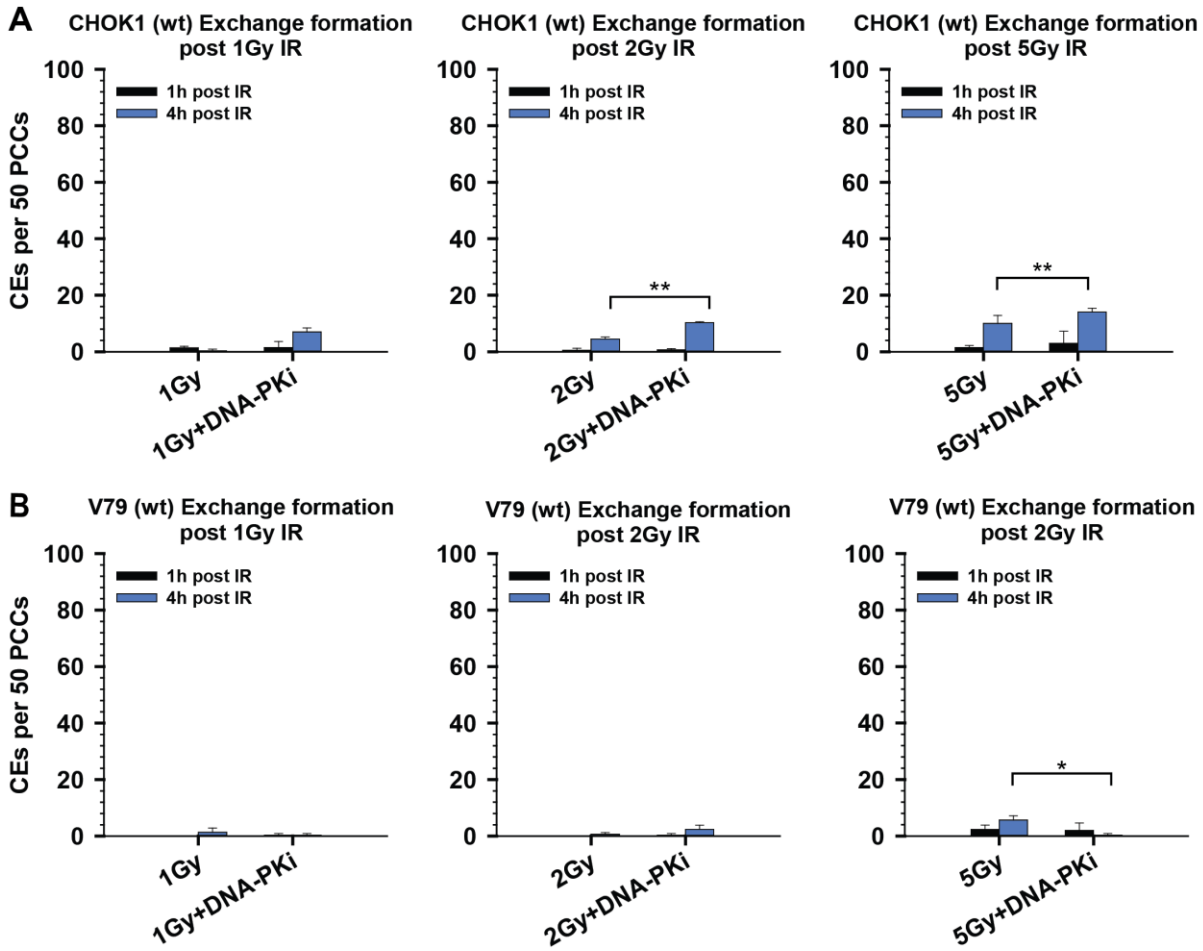

Figure 47: CE formation in different V79 (wt) and CHOK1 (wt) cells upon exposure to IR ± DNA-PK inhibition. Exponentially growing A) CHOK1 and B) V79 cells were exposed to different IR doses alone or in the presence of DNA-PK inhibitor NU7441. CE formation was measured 1 h and 4 h post IR. Significant differences were calculated using a two tailed student t-test (asterix designation $p<0.001$ ***, $p<0.01$ **, $p<0.05$ *). Shown is the mean of 2 – 3 independent experiments ± SD.

Inhibition of DNA-PK in V79 and CHOK1 cells showed interesting trends. The inhibition of DNA-PK in CHOK1 cells resulted in a significant increase in the number of CEs 4 h post 2 Gy and 5 Gy IR. This suggests that upon c-NHEJ inhibition a more error prone pathway (e.g. alt-EJ) contributes to CE formation. Furthermore, this result also proposes a role of c-NHEJ in the suppression of CEs. A converse trend was observed for V79 cells. For V79 cells, we detected a decrease in CEs upon c-NHEJ inhibition, which puts c-NHEJ more towards the promotion of CEs.

Next, we checked the contribution of c-NHEJ to CE formation in HRR mutant cell lines (**Figure 48**).

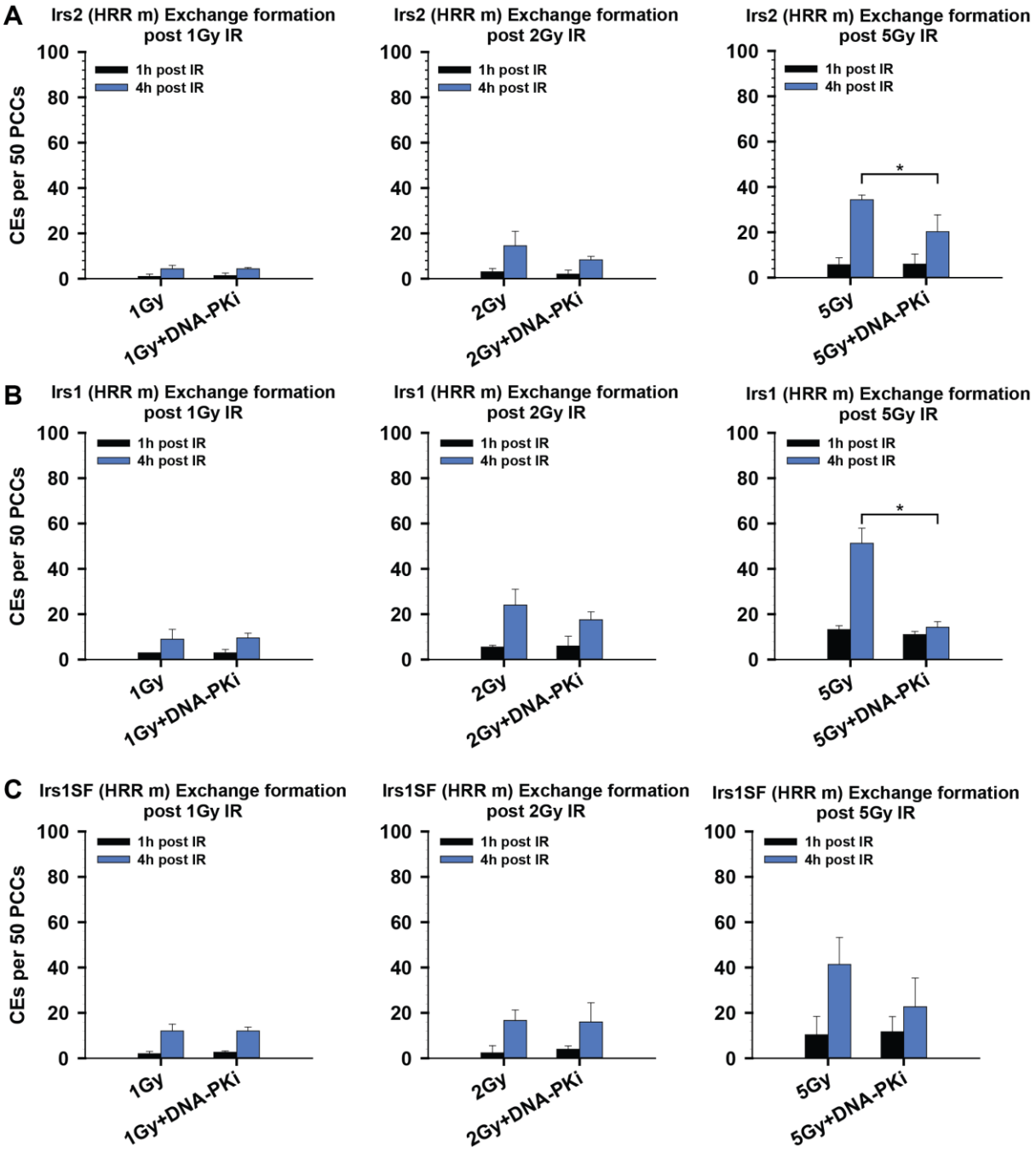

Figure 48: CE formation in indicated Chinese hamster HRR mutant cell lines, upon exposure to IR ± DNA-PK inhibition. Exponentially growing A) Irs2 (Rad51B m), B) Irs1 (XRCC2 m) and C) Irs1SF (XRCC3 m) cells were exposed to different IR doses alone or in the presence of DNA-PK inhibitor NU7441. CE formation was measured 1 h and 4 h post IR. Significant differences were calculated using a two tailed students t-test (asterix designation $p<0.001$ ***, $p<0.01$ **, $p<0.05$ *). Represented is the mean of 2 – 3 independent experiments ± SD.

While, the inhibition of c-NHEJ after exposure of all three HRR mutant cell lines to 1 Gy and 2 Gy IR does not show a measurable differences in CE formation, significant decreases in CE formation are observed after exposure of cells to 5 Gy IR (4 h time point) (**Figure 48, A, B and C**). The number of CEs decreased to half in all HRR

mutant cells lines, tested at 4 h post IR. Thus, a clear contribution of c-NHEJ to CE formation is noted after exposure of these mutants to high IR doses (5 Gy).

In a last experiment, we inquired how combined inhibition of Parp-1 plus DNA-PK would change the formation of CEs. For this purpose we exposed V79 (wt) and irs2 (HRR m) cells to 1 Gy, 2 Gy and 5 Gy in the presence of both DNA-PK as well as the Parp-1 inhibitor and scored the formation of CEs.

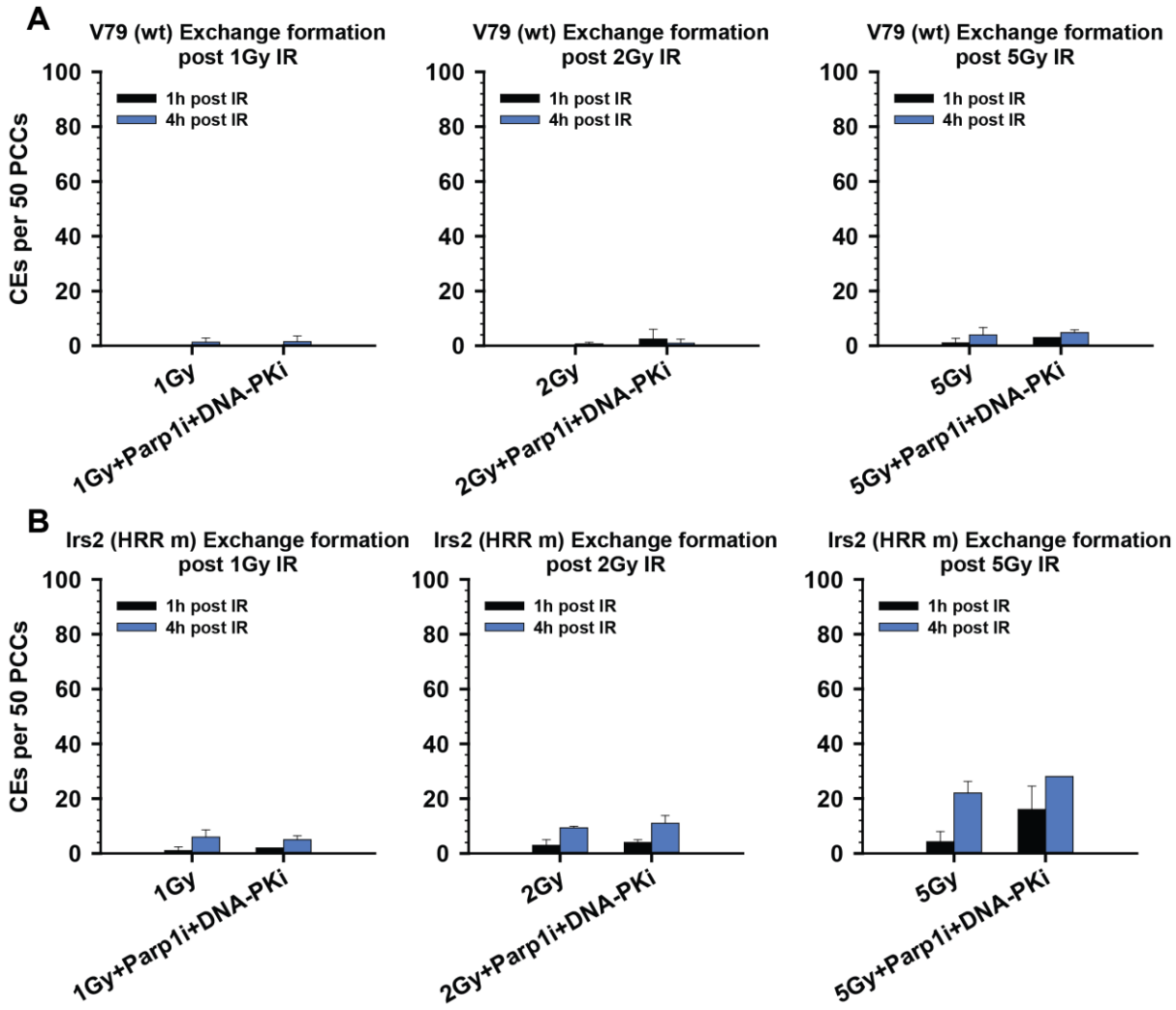

Figure 49: CE formation upon exposure of Chinese hamster cells to different IR doses in the presence of DNA-PK inhibitor and Parp-1 inhibitor. A) V79 (wt) cells and B) Irs2 (HRR m) cells were exposed to different IR doses in the presence or absence of DNA-PK inhibitor NU7441 plus Parp-1 inhibitor PJ34. CE formation was scored 1 h and 4 h post IR. Results represent the mean of 2 - 3 independent experiments ± SD.

Combined inhibition of DNA-PK and Parp-1 did not uncover an effect on CE formation in V79 (wt) cells as well as irs2 (HRR m) cells in addition to that observed with DNA-PK inhibition alone.

4.4.2.1 C-NHEJ contributes to CE formation in human 82-6 cells after exposure to high IR doses

In section **4.2.5**, we provided evidence that c-NHEJ contributes to PCC break repair in human 82-6 (wt) cells. Can we also detect an involvement of c-NHEJ to the formation of CEs in human 82-6 cells as well? Earlier reports have implicated c-NHEJ in the formation of CEs in human cells (Ghezraoui, et al. 2014). To address this question, we measured CE formation in 82-6 cells using the protocol described above. The results obtained are shown in **Figure 50**.

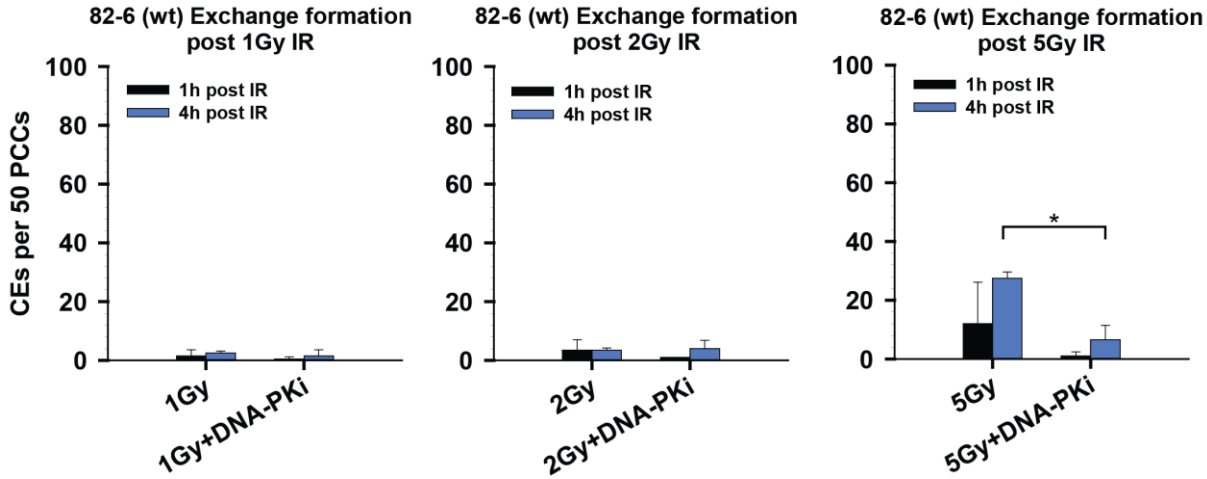

Figure 50: CE formation in human 82-6 (wt) cells after exposure to IR alone or in the presence of DNA-PK inhibitor. 82-6 cells were exposed to different IR doses alone or in the presence of DNA-PK inhibitor NU7441. CE formation was determined 1 h and 4 h post IR. Significance of differences was calculated using a two tailed student t-test (asterix designation $p<0.001$ ***, $p<0.01$ **, $p<0.05$ *). Data represent two independent experiments ± SD.

Similar, as for the results obtained with Chinese hamster cells, we could detect a clear contribution of c-NHEJ to CE formation after exposure of cells to 5 Gy IR in the presence of DNA-PK inhibitor. Formation of CEs was decreased to a quarter as compared to the IR alone control. Exposure of cells to 1 Gy or 2 Gy IR in the presence or absence of DNA-PKi did not result in differences with respect to CE formation.

The results outlined in this fourth part of the thesis have shown that first, the formation of CEs increases with increasing radiation dose. Secondly, defects in HRR or c-NHEJ renders cells more prone to CE formation. Thirdly, comparing CE formation to clonogenic survival we could show correlations between the two

endpoints. Fourthly, we could demonstrate a clear contribution of alt-EJ to CE formation in c-NHEJ deficient XR1 cells after exposure to 5 Gy IR.

Last but not least, our results suggest a clear contribution of c-NHEJ to the formation of CEs through inhibition of DNA-PK when cells are exposed to 5 Gy IR.

5. DISCUSSION

The repair of IR-induced DNA double strand breaks is of critical importance, for the cell, as un-repaired or misrepaired DSBs contribute to genomic instability, senescence and apoptosis, predisposing an organism to immunodeficiency, cancer or neurological disorders (O'Driscoll and Jeggo 2006; Thoms, et al. 2007). Yet, the underlying mechanisms determining the regulation of repair pathway choice are still not fully elucidated. The choice for a particular DSB repair pathway is not among equals and the selection for a particular repair pathway will ultimately determine the fate of the irradiated cell.

The primary aim of the present thesis was to contribute to the elucidation of a dose dependent regulation of DSB repair pathway choice, specifically in the G_2-phase of the cell cycle, where all described pathways are active. As endpoint, we chose chromatid breaks and their processing. While chromatid breaks are normally analyzed at metaphase, here we opted for the premature chromosome condensation approach that allows visualization and scoring of chromatid breaks not only for cells at metaphase, but also for cells throughout the G_2-phase of the cell cycle. The underlying assumption of all these experiments is that chromatid breaks reflect subsets of DSBs.

5.1 Validation of the premature chromosome condensation technique

Premature chromosome condensation has been intensively used to study the dynamics of IR induced chromatid breaks throughout the cell cycle. PCC, in contrast to classical cytogenetic, provides information about chromosomes in G_2-phase, while classical cytogenetics, report the final rejoining outcome. Moreover, PCC circumvents complications associated with the strong activation of G_2-checkpoint at high IR doses, and is not biased by cells, which for whatever reason are unable to reach metaphase.

One issue often raised when it comes to G_2 PCC break kinetics as analyzed using classical Giemsa staining concerns possible contamination with S-phase cells. Thus, the PCC technique does not allow discrimination between G_2 PCCs originating from cells that were in G_2 at irradiation, and G_2 PCCs coming from cells that were in S-phase at the time of IR but have since progressed to G_2 (see **Figure 14**). An

additional complication is that at times, late S-phase PCC may have appearance similar to G_2 PCCs that have sustained DNA damage.

We here developed a protocol which allows us to distinguish between PCCs resulting from cells in G_2 at the time of IR exposure and those deriving from S-phase that have progressed to G_2. The protocol involves labeling using an EdU pulse just before exposure to IR.

With this new approach, we were not only able to validate our PCC break kinetic experiments, but also to add cell cycle specificity to the PCC technique and open new avenues for addressing cell cycle specific questions in DNA damage response.

We demonstrated that there is not significant difference between the processing of IR induced PCC breaks, in EdU positive and negative PCCs when measured in a 6 h timeframe employed in the experiment described here (see **Figure 23**).

Comprehensive analysis has shown that the developed protocol allows us to study cell cycle changes upon exposure to IR. Thus, activation of cell cycle checkpoints upon IR exposure will be ultimately reflected in the fraction of EdU negative and positive PCCs found. G_2/M checkpoint activation, for example, will hold G_2 cells back from entering mitosis in an effort to prevent damaged DNA from being segregated (Deckbar, et al. 2007; Löbrich and Jeggo 2007). In line with this, we found a greater fraction of EdU negative PCCs remaining at the later time points in Chinese hamster cells exposed to IR (see **Figure 21**). Similar observations were also made by Bussink *et al.* who looked at the fraction of metaphases that came from G_2 and S-phase on the basis of BrdUrd staining. Also Bussink *et al*. found a progressive decrease in metaphases coming from the S-phase and a corresponding increase in metaphases coming from G_2-phase at later time points after 1 Gy IR (Bussink, et al. 1996).

Moreover, in line with findings by Soni (Soni 2010), we also observed abrogated checkpoint for HRR mutant cells, which was reflected by a faster increase in the fraction of EdU positive PCCs at the later time points post IR as compared to wildtype cells (see **Figure 23**, **B** and **C**).

We furthermore show that the amount of EdU incorporated in PCCs, can be used to discriminate between different sub stages of S-phase (see **Figure 17**and **Figure 18**). Similar observations were also made by Gotoh and colleagues, which used Cy3-2'-

deoxyuridine-5'-triphosphate to stain S-phase PCCs (Gotoh 2007). Also Li and colleagues could show a relationship between EdU incorporation and S-phase sub stages (Li, et al. 2014). Last but not least, also Bussink *et al.* confirmed, on the basis of classical cytogenetics, increased BrdUrd staining for early S-phase cells that reach metaphase (Bussink, et al. 1996).

Additionally, the observation of EdU distinct banding patterns (see **Figure 17**, **Figure 19**) on PCCs as well as on metaphase chromosomes hint towards precise timing of DNA replication for different chromosome regions. Indeed, literature searches revealed that EdU banding patterns coincide with so called replication time zones. Such banding patterns have even been employed for assessing the structure of chromosomes in relation to their banding patterns following DNA replication (Di Tomaso M.V. 2006; Goren and Cedar 2003; Hoshi O 2011).

With regard to PCC technique validation, we found that depending on the cell line, the fraction of G_2 cells that are condensed to G_2 PCCs is around 50 – 60% when comparing the PCC index to results obtained by two-parameter flow cytometry (**Supplementary Figure 4** and **Supplementary Figure 5**). The PCC index determined was around 3-7% when analyzing Giemsa stained slides (**Figure 24**). Studies carried out by others claim that the PCC index is around 20% (Gotoh 2009), which is different to the results obtained here. Those differences will need to be further addressed with more detailed approaches to uncover the real fraction of G_2 cells that is condensed to G_2 PCCs.

5.2 Contribution of DNA DSB repair pathways to the processing of IR induced PCC breaks

Our primary focus of the studies described here was to investigate a putative dose-dependent regulation of DSB repair pathway choice, by employing CB, as a model for DSB repair, overall.

As stated above, only a small subset of DSBs (10 – 20%) is converted to visible chromatid breaks (Martín, et al. 2014; Terzoudi, et al. 2008). Furthermore, abrogation of HRR or c-NHEJ has been associated with a higher susceptibility towards chromosomal breakage (Bryant, et al. 2008; Parshad, et al. 1984; Parshad and Sanford 2001; Taylor 1978). Determination of the percentage of DSBs that are

converted to PCC breaks using different Chinese hamster cell lines and one human cell line are in line with this observation (**Figure 31**, **Figure 32**, Table 3, Table 4).

The induction of PCC breaks followed a linear dose response relationship, which is similar to the induction of DSBs, and has been extensively described throughout the literature (Antonelli, et al. 2015; Barnard, et al. 2013; Gotoh 2009; Kawata, et al. 2004; Leatherbarrow, et al. 2006).

Employing chemical inhibition of DNA-PK and cell lines mutated in key components of c-NHEJ to uncover a contribution of c-NHEJ to CB repair, we indeed were able to show a dose dependent regulation of DSB repair pathway utilization. Thus, we showed through comprehensive analysis in different rodent and human cells, a critical role of c-NHEJ to PCC break processing after exposure of cells to relatively high IR (>2 Gy) doses (**Figure 27**, **Figure 29**, **Figure 32**, **Figure 33**) .

We moreover unraveled the critical importance of HRR at low IR doses, for PCC break processing which can compensate for abrogated c-NHEJ (see **Figure 27** and **Figure 32**). The importance of HRR at low IR doses was in particular obvious in HRR mutant cell lines, which failed to repair IR induced PCC breaks after low doses of IR (refer to **Figure 32**, **B** and **C**).These results are in agreement with previous experiments (Siemann 2013; Soni 2010; Soni, et al. 2014).

As stated before (Siemann 2013; Soni 2010), a contribution of Parp-1 dependent alt-EJ to PCC break rejoining could not be detected (refer to **Figure 36**, **Figure 37**, **Figure 38**).

Finally, our results show a clear dose dependent regulation of DSB repair pathways. **Figure 51** shows a graphic model summarizing our observations.

In this model CBs (as measured by PCC) are repaired predominantly by HRR at low IR doses (<2 Gy). Inhibition of c-NHEJ will have minor effects on CB repair, while inhibition or mutation of HRR will result in repair abrogation and increased formation of CEs. Yet, with increasing IR dose (> 2 Gy) DSB repair will be shunted to c-NHEJ and HRR will play no role in PCC break repair. Shunting of DSB repair pathways to c-NHEJ however, will also increase the formation of CEs. Chemical inhibition of c-NHEJ will lead to un-rejoined PCC breaks, while inhibition or mutation in HRR will not affect PCC break rejoining.

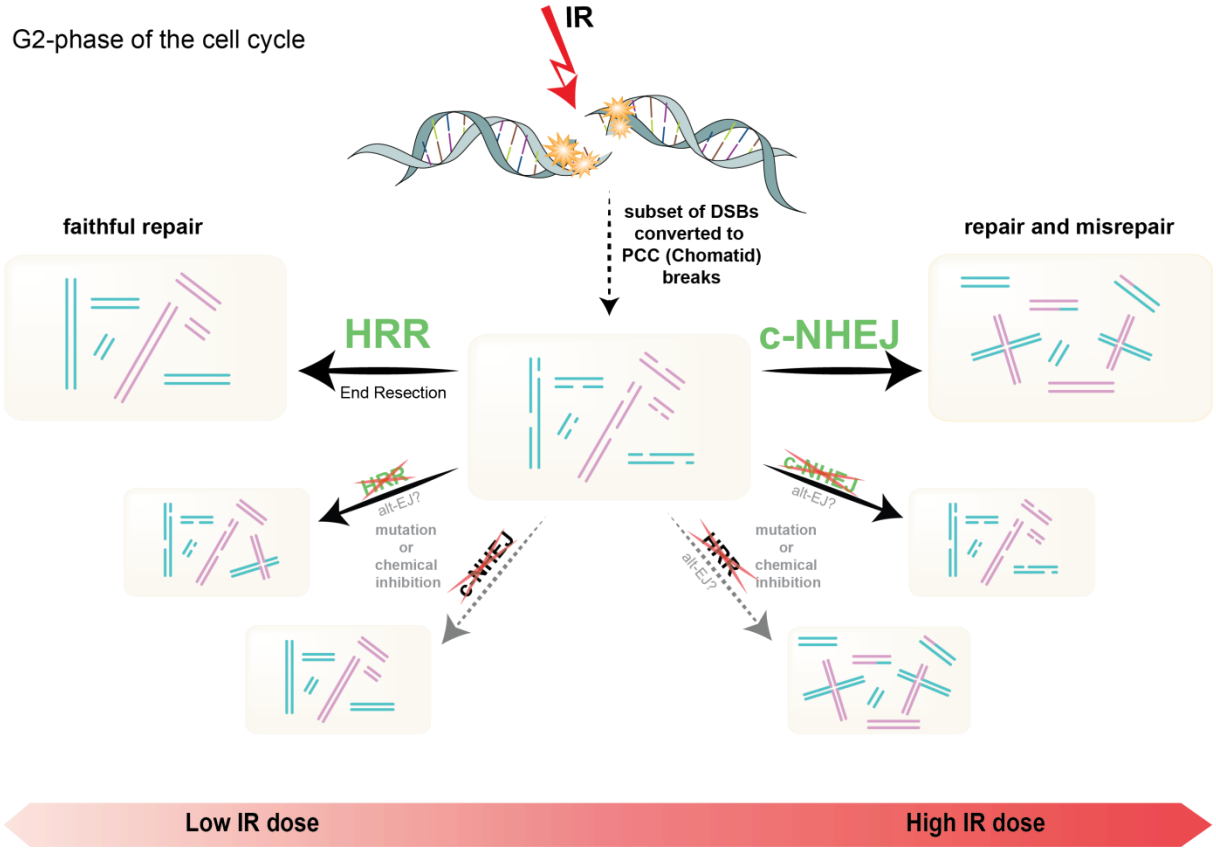

Figure 51: Graphical model for a dose dependent regulation of DSB repair pathways. For details refer to text.

The molecular determinants underlying such a dose dependent DSB repair pathway regulation remain elusive.

One determinant could be the increasing load of DSBs (and therefore CBs) with increasing IR dose. C-NHEJ is characterized by its speed in re-joining DSBs and probably cells want to make sure that breaks are not left un-rejoined. This would explain the shunting of DSBs to c-NHEJ with increasing IR dose.

Also, the biochemical nature of the DSB underlying the chromosome break may be a determining factor. Ionizing radiation in general causes a plethora of different kinds of damages, including base damages, sugar lesions, single strand breaks and of course DSBs. Thus, the composition and biochemical nature of a DSB at low and high IR doses may differ. In addition, the need to clean up the break to render them ligatable or the need for processing may contribute to DSB repair pathway choice.

The role of resection in the repair pathway choice needs to be addressed. In fact, several studies have indicated a critical role of DSB end resection in the decision of DSB repair pathways (Ceccaldi, et al. 2015; Kakarougkas and Jeggo 2014).

Considering that resection is critical for HRR to engage and that Ochs and colleagues (Ochs, et al. 2016) showed that an increasing load of DSBs triggers hyper-resection of DSB, investigating the role of resection in PCC break processing would be of outermost interest. One approach to elucidate the role of resection in PCC break processing could be to combine immunofluorescence with cytogenetics. Such an approach could include the visualization of molecules (foci experiments) important for DNA end resection, including amongst others RPA70, CtIP or Mre11.

5.3 Contributions of DNA DSB repair pathways to the formation of chromosomal exchanges as measured by premature chromosome condensation

Abrogation of key components of DSB repair pathways has been linked to CE formation, which in turn leads to tumorigenesis and genomic instability (Bunting and Nussenzweig 2013; Iarovaia 2014; Iliakis, et al. 2004; Kasparek and Humphrey 2011; Natarajan and Palitti 2008; Nussenzweig and Nussenzweig 2010; Soni, et al. 2014).

In agreement with this observation we found a 2 – 3 fold higher induction of CEs in HRR and c-NHEJ mutant cell lines as compared to CE induction in wildtype cells (**Figure 43**, **B**). Moreover, we could demonstrate that CE formation confers to an increased sensitivity to IR induced cell killing (**Figure 43**, **A**), which is in accordance to observations by Hlatky *et al*. and Sasai *et al*. (Hlatky, et al. 2002; Sasai, et al. 1994).

One repair pathway, repeatedly implicated in CE formation is alt-EJ. Particular role is attributed to Parp-1, since its inhibition decreases CE formation (Byrne, et al. 2014; Soni, et al. 2014; Wray, et al. 2013).

Results with G_2 PCCs, failed to show a clear contribution of alt-EJ to CE formation in Chinese hamster cell lines, regardless of the applied IR dose (**Figure 47** and **Figure 48**). These observations differ from previous findings from our lab. Parp-1 inhibition was shown to clearly decrease CE formation when measured by PCC technique or via classical cytogenetics at low IR doses (Siemann 2013; Soni 2010).

Explanations for the observed differences could be the use of aphidiciolin in previous PCC experiments (Siemann 2013). We also have to consider that we only investigated a time frame of 6 h post IR. Thus, processes involved in PCC processing may not be completed within the measured timeframe. Furthermore, we have to consider that results obtained with classical cytogenetics reflect the ultimate outcome of misrejoining events. Before cells enter mitosis, DSB may undergo further processing, or may become filtered through the G_2/M-checkpoint. Based on this speculation, a possible contribution of alt-EJ may be hidden when analyzing CE formation in G_2 via the PCC method.

Furthermore, we also have to keep in mind that we measured the contribution of alt-EJ only via Parp-1 inhibition. Yet, several studies have also suggested the existence of different alternative end joining pathways which are independent of Parp-1 (Decottignies 2013). For future experiments it would be very interesting to address the role of Ligase 1, Ligase 3 or polymerase θ in the formation of CEs, since all three molecules have been implicated in CE formation (Beagan and McVey 2015; Lu, et al. 2016; Puizina, et al. 2004; Simsek, et al. 2011; Yamaguchi-Iwai, et al. 1999).

However, a clear contribution of Parp-1 dependent alt-EJ was observed for XRCC4 mutated Chinese hamster cells after exposure to high IR doses (refer to **Figure 46**). Here Parp-1 inhibition reduced the number of CEs. In this respect it would be interesting in the future to check the contribution of alt-EJ also in cell lines which bear mutations in other key components of c-NHEJ like DNA-PKcs or Ku.

Although, we failed to show a clear contribution of alt-EJ to CE formation, we nonetheless were able to demonstrate a clear contribution of c-NHEJ to CE formation (refer to **Figure 47**, **Figure 48**, Figure **50**).

Generally, the role of c-NHEJ to CE formation has been discussed controversially in the literature. Both, the suppression of CEs, as well as the promotion of CEs by c-NHEJ has been suggested (Ferguson, et al. 2000; Ghezraoui, et al. 2014). Yet, we have to consider that c-NHEJ is by nature error prone, since it does not ensure joining of the correct DSB ends. Taken into consideration that c-NHEJ inhibition abrogated PCC break rejoining at high IR doses this observation is not beyond expectation.

Yet, we will have to address the question of who is in charge of the CEs, still seen after c-NHEJ inhibition and those CEs formed after low IR doses. As discussed above investigating the role of Lig1, Lig3 and polymerase θ could be one approach, but also the investigation of molecules involved in resection like Mre11 and CtIP could be of interest, since both have been implicated in CE formation (Roukos and Misteli 2014; Zhang and Jasin 2011).

6. SUMMARY

Our data show an IR dose dependent regulation of DSB repair pathways involved in the processing of IR induced chromatid breaks, as measured by PCC, in the G_2-phase of the cell cycle.

While at low doses (<2 Gy) mainly HRR is involved in the processing of IR induced PCC breaks, repair is shunted to c-NHEJ with increasing IR dose (> 2Gy). Administration of DNA-PK inhibitors, as well as the use of a c-NHEJ mutant cell line uncovered the importance of c-NHEJ at high IR doses, since cells showed clear PCC break repair abrogation. The critical importance of HRR at low IR doses, to the processing of IR induced PCC breaks, was demonstrated by using HRR mutant cell lines, which failed to repair PCC breaks after exposure to low IR doses.

We could show an IR dose dependent regulation of DSB repair pathways not only for rodent Chinese hamster cells but also for one human wildtype cell line.

Furthermore, we developed a protocol, which enables us to distinguish between G_2 PCCs coming from cells that were either in G_2 phase during IR or in S-phase on the basis of EdU incorporation. With this protocol, we were able to validate our results for PCC break kinetics. Moreover, the protocol opens new avenues for addressing cell cycle specific questions on a cytogenetic basis.

Our data also demonstrated that mutations in key molecules of DSB repair pathways, renders cells more prone to chromosomal breakage, as well as to CE formation, and that these endpoints correlate with radiosensitivity to killing.

While the contributions of DSB repair pathways to CE formation after low doses of IR needs to be further evaluated, we could nevertheless show a clear contribution of c-NHEJ to CE formation after higher (5 Gy) doses, since c-NHEJ inhibition let to decreased CE formation.

Future studies should focus on the mechanistic determinants of the observed regulation of DSB repair pathways. Also, the culprits of CE formation will need to be molecularly defined and characterized.

7. REFERENCES

Agarwal, Sheba, Agnieszka A. Tafel, and Roland Kanaar

2006 DNA double-strand break repair and chromosome translocations. DNA Repair 5(9-10):1075-1081.

Ahnesorg, Peter, Philippa Smith, and Stephen P. Jackson

2006 XLF Interacts with the XRCC4-DNA Ligase IV Complex to Promote DNA Nonhomologous End-Joining. Cell 124(2):301-313.

Antonelli, F., et al.

2015 Induction and Repair of DNA DSB as Revealed by H2AX Phosphorylation Foci in Human Fibroblasts Exposed to Low- and High-LET Radiation: Relationship with Early and Delayed Reproductive Cell Death. Radiation Research 183(4):417-431.

Aparicio, Tomas, Richard Baer, and Jean Gautier

2014 DNA double-strand break repair pathway choice and cancer. DNA Repair 19:169-175.

Audebert, M., B. Salles, and P. Calsou

2004 Involvement of Poly(ADP-ribose) Polymerase-1 and XRCC1/DNA Ligase III in an Alternative Route for DNA Double-strand Breaks Rejoining. Journal of Biological Chemistry 279:55117-55126.

Aylon, Yael, Batia Liefshitz, and Martin Kupiec

2004 The CDK regulates repair of double-strand breaks by homologous recombination during the cell cycle. EMBO Journal 23(24):4868-4875.

Barnard, Stephen, Simon Bouffler, and Kai Rothkamm

2013 The shape of the radiation dose response for DNA double-strand break induction and repair. Genome Integrity 4(1):1.

Beagan, Kelly, and Mitch McVey

2015 Linking DNA polymerase theta structure and function in health and disease. Cellular and Molecular Life Sciences 73(3):603-615.

Bryant, P.E., H. Mozdarani, and C. Marr

2008 G2-phase chromatid break kinetics in irradiated DNA repair mutant hamster cell lines using calyculin-induced PCC and colcemid-block. Mutation Research 657(1):8-12.

Bunting, Samuel F., and Andre Nussenzweig

2013 End-joining, translocations and cancer. Nature Reviews. Cancer 13(7):443-454.

Burma, Sandeep, Benjamin P. C. Chen, and David J. Chen

2006 Role of non-homologous end joining (NHEJ) in maintaining genomic integrity. DNA Repair 5(9-10):1042-1048.

Bussink, J, PJ Tofilon, and WA Brock

1996 Repair of chromosome and DNA breaks versus cell survival in Chinese hamster cells. International Journal of Radiation Biology 70(1):23-32.

Byrne, Michael, et al.

2014 Mechanisms of oncogenic chromosomal translocations. Annals of the New York Academy of Sciences 1310(1):89-97.

Ceccaldi, Raphael, Beatrice Rondinelli, and Alan D. D'Andrea

2015 Repair Pathway Choices and Consequences at the Double-Strand Break. Trends in Cell Biology 26(1):52-64.

Chan, Sze Ham, Amy Marie Yu, and Mitch McVey

2010 Dual Roles for DNA Polymerase Theta in Alternative End-Joining Repair of Double-Strand Breaks in Drosophila. PLoS Genetics 6(7):e1001005.

Chiruvella, Kishore K., Zhuobin Liang, and Thomas E. Wilson

2013 Repair of Double-Strand Breaks by End Joining. Cold Spring Harbor Perspectives in Biology 5(5):a012757.

Cho, Nam Woo, and Roger A. Greenberg

2015 DNA repair: Familiar ends with alternative endings. Nature 518(7538):174-176.

Clouaire, T., and G. Legube

2015 DNA double strand break repair pathway choice: a chromatin based decision? Nucleus 6(2):107-113.

Cornforth, M.N.

2001 Analyzing radiation-induced complex chromosome rearrangements by combinatorial painting. Radiation Research 155:643-659.

Davis, Anthony J., and David J. Chen

2013 DNA double strand break repair via non-homologous end-joining. Translational Cancer Research 2(3):130-143.

Deckbar, Dorothee, et al.

2007 Chromosome breakage after G2 checkpoint release. Journal of Cell Biology 176(6):749-755.

Decottignies, Anabelle

2013 Alternative end-joining mechanisms: a historical perspective. Frontiers in Genetics 4:Article 48.

Demond, M.

2016 The influence of chromatin structure on DNA double strand break repair pathway choice. PhD Thesis.

Deriano, Ludovic, and David B. Roth

2013 Modernizing the Nonhomologous End-Joining Repertoire: Alternative and Classical NHEJ Share the Stage. Annual Review of Genetics 47:451-73.

Di Tomaso M.V., Martinez-Lopez W., Folle G.A., Palitti F.

2006 Modulations of chromosome damage localization by DNA replication timing. International Journal of Biology 82(12):877-886.

DiBiase, S. J., et al.

2000 DNA-dependent protein kinase stimulates an independently active, nonhomologous, end-joining apparatus. Cancer Research 60:1245-1253.

Dueva, Rositsa, and George Iliakis

2013 Alternative pathways of non-homologous end joining (NHEJ) in genomic instability and cancer. Translational Cancer Research 2(3):163-177.

Duque, A, and P Rakic

2011 Different effects of bromodeoxyuridine and [3H]thymidine incorporation into DNA on cell proliferation, position, and fate. Journal of Neuroscience 31(42):15207-15217.

Durante, M., et al.

2013 From DNA damage to chromosome aberrations: Joining the break. Mutation Research/Genetic Toxicology and Environmental Mutagenesis 756(1-2):5-13.

Fan, Xiaoxiang

2009 Interplay between ATM and ATR for the regulation of cellular responses to DNA damage. PhD Thesis.

Ferguson, D. O., and F. W. Alt

2001 DNA double strand break repair and chromosomal translocation: Lessons from animal models. Oncogene 20:5572-5579.

Ferguson, D. O., et al.

2000 The nonhomologous end-joining pathway of DNA repair is required for genomic stability and the suppression of translocations. Proceedings of the National Academy of Sciences of the United States of America 97(12):6630-6633.

Frit, Philippe, et al.

2014 Alternative end-joining pathway(s): Bricolage at DNA breaks. DNA Repair 17:81-97.

Ghezraoui, Hind, et al.

2014 Chromosomal Translocations in Human Cells Are Generated by Canonical Nonhomologous End-Joining. Molecular Cell 55(6):829-842.

Goodhead, D.T.

1994 Initial events in the cellular effects of ionizing radiations: clustered damage in DNA. International Journal of Radiation Biology 65(1):7-17.

Goren, A., and H. Cedar

2003 Replicating by the clock. Nat Rev Mol Cell Biol 4(1):25-32.

Gotoh, E.

2007 Visualizing the dynamics of chromosome structure formation coupled with DNA replication. Chromosoma 116(5):453-62.

—

2009 Drug-induced premature chromosome condensation (PCC) protocol: cytogenetic approached in mitotic chromosome and interphase chromatin. Methods in Molecular Biology 523:88-92.

Hall, Eric J., and Amato J. Giaccia

2006 Radiobiology for the Radiologist. Philadelphia, Baltimore, New York, London, Buenos Aires, Hong Kong, Sydney, Tokyo: Lippincott Williams & Wilkins.

Heyer, Wolf-Dietrich, Kirk T. Ehmsen, and Jie Liu

2010 Regulation of Homologous Recombination in Eukaryotes. Annual Review of Genetics 44:113-139.

Hlatky, L., et al.

2002 Radiation-induced chromosome aberrations: insights gained from biophysical modeling. BioEssays 24:714-723.

Hoshi O, Ushiki T.

2011 Replication Banding Patterns in Human Chromosomes Detected Using 5-ethynyl-2'-deoxyuridine Incorporation. Acta Histochemica et Cytochemica 44(5):233-237.

Howard, Sean M., Diana A. Yanez, and Jeremy M. Stark

2015 DNA Damage Response Factors from Diverse Pathways, Including DNA Crosslink Repair, Mediate Alternative End Joining. PLoS Genetics 11(1):e1004943.

Iarovaia , Rubtsov ., Ioudinkova, Tsfasman , Razin, Vassetzky

2014 Dynamics of double strand breaks and chromosomal translocations. Molecular Cancer 13:249.

Iliakis, G.

2009 Backup pathways of NHEJ in cells of higher eukaryotes: Cell cycle dependence. Radiotherapy and Oncology 92:310-315.

Iliakis, G., et al.

2004 Mechanisms of DNA double strand break repair and chromosome aberration formation. Cytogenetic and Genome Research 104:14-20.

Iliakis, G., et al.

2003 DNA damage checkpoint control in cells exposed to ionizing radiation. Oncogene 22:5834-5847.

Iliakis, G., et al.

2007 Backup Pathways of Nonhomologous End Joining May Have a Dominant Role in the Formation of Chromosome Aberrations. *In* Chromosomal Alterations. G. Obe, Vijayalaxmi, ed. Pp. 67-85. Berlin, Heidelberg, New York: Springer Verlag.

Iliakis, George, Tamara Murmann, and Aashish Soni

2015a Alternative end-joining repair pathways are the ultimate backup for abrogated classical non-homologous end-joining and homologous recombination repair: Implications for the formation of chromosome

translocations. Mutation Research-Genetic Toxicology and Environmental Mutagenesis 793:166-175.

—

2015b Alternative end-joining repair pathways are the ultimate backup for abrogated classical non-homologous end-joining and homologous recombination repair: Implications for the formation of chromosome translocations. Mutation Research/Genetic Toxicology and Environmental Mutagenesis 793:166-175.

Jeppesen, Peter

2000 Immunofluorescence in cytogenetic analysis: method and applications. Genetics and Molecular Biology 23(4):1107 - 1114.

Johnson, R.T., and P.N. Rao

1970 Mammalian cell fusion: Induction of premature chromosome condensation in interphase nuclei. Nature 226:717-722.

Kakarougkas, A, and P A Jeggo

2014 DNA DSB repair pathway choice: an orchestrated handover mechanism. British Journal of Radiology 87(1035):20130685.

Kasparek, Torben R., and Timothy C. Humphrey

2011 DNA double-strand break repair pathways, chromosomal rearrangements and cancer. Seminars in Cell & Developmental Biology 22(8):886-897.

Kawata, T., et al.

2004 G2 chromatid damage and repair kinetics in normal human fibroblast cells exposed to low- or high-LET radiation. Cytogenetic and Genome Research 104(1-4):211-215.

Kent, Tatiana, et al.

2015 Mechanism of microhomology-mediated end-joining promoted by human DNA polymerase θ. Nature Structural & Molecular Biology 22(3):230-237.

Khanna, Kum Kum, and S. P. Jackson

2001 DNA double-strand breaks: signaling, repair and the cancer connection. Nature Genetics 27:247-254.

Kinner, A., et al.

2008 γ-H2AX in recognition and signaling of DNA double-strand breaks in the context of chromatin. Nucleic Acids Research 36(17):5678-5694.

Krejci, Lumir, et al.

2012 Homologous recombination and its regulation. Nucleic Acids Research 40(13):5795-5818.

Leatherbarrow, E.L., et al.

2006 Induction and quantification of γ-H2AX foci following low and high LET-irradiation. International Journal of Radiation Biology 82(2):111-118.

Lengauer, C., K. W. Kinzler, and B. Vogelstein

1998 Genetic instabilities in human cancers. Nature 396:643-649.
Li, B., et al.

2014 Different rates of DNA replication at early versus late S-phase sections: multiscale modeling of stochastic events related to DNA content/EdU (5-ethynyl-2'deoxyuridine) incorporation distributions. Cytometry A 85(9):785-97.
Lieber, M.R., et al.

2004 The mechanism of vertebrate nonhomologous DNA end joining and its role in V(D)J recombination. DNA Repair 3:817-826.
Lieber, Michael R.

2010a The Mechanism of Double-Strand DNA Break Repair by the Nonhomologous DNA End-Joining Pathway. Annual Review of Biochemistry 79:1.1-1.31.
—

2010b NHEJ and its backup pathways in chromosomal translocations. Nature Structural & Molecular Biology 17(4):393-395.
Löbrich, Markus, and Penny A. Jeggo

2007 The impact of a negligent G2/M checkpoint on genomic instability and cancer induction. Nature Reviews. Cancer 7(11):861-869.
Lomax, ME, Folkes LK, O'Neill P.

2013 Biological consequences of radiation-induced DNA damage: relevance to radiotherapy. Clin Oncol (R Coll Radiol) 25(10):578-85.
Lu, Guangqing, et al.

2016 Ligase I and ligase III mediate the DNA double-strand break ligation in alternative end-joining. Proceedings of the National Academy of Sciences of the United States of America 113(5):1256-1260.
Mahaney, Brandi L., Katheryn Meek, and Susan P. Lees-Miller

2009 Repair of ionizing radiation-induced DNA double-strand breaks by non-homologous end-joining. Biochemical Journal 417:639-650.
Mansour, Wael Y., Tim Rhein, and Jochen Dahm-Daphi

2010 The alternative end-joining pathway for repair of DNA double-strand breaks requires PARP1 but is not dependent upon microhomologies. Nucleic Acids Research 38(18):6065-6077.
Martín, Marta, et al.

2014 γH2AX foci on apparently intact mitotic chromosomes: Not signatures of misrejoining events but signals of unresolved DNA damage. Cell Cycle 13(19):3026-3036.
Mateos-Gomez, Pedro A., et al.

2015 Mammalian polymerase [thgr] promotes alternative NHEJ and suppresses recombination. Nature 518(7538):254-257.
Matos, Joao, and Stephen C. West

2014 Holliday junction resolution: Regulation in space and time. DNA Repair 19:176-181.

Mazin, Alexander V., et al.

2010 Rad54, the motor of homologous recombination. DNA Repair 9(3):286-302.

Miura, Tomisato, and William F. Blakely

2011 Optimization of calyculin A-induced premature chromosome condensation assay for chromosome aberration studies. Cytometry Part A 79A(12):1016-1022.

Mladenov, Emil, and George Iliakis

2011 Induction and Repair of DNA Double Strand Breaks: The Increasing Spectrum of Non-homologous End Joining Pathways. Mutation Research 711:61-72.

Mladenov, Emil, et al.

2016 DNA double-strand-break repair in higher eukaryotes and its role in genomic instability and cancer: Cell cycle and proliferation-dependent regulation. Seminars in Cancer Biology 37-38:51-64.

Murakami, Hajime, and Scott Keeney

2008 Regulating the formation of DNA double-strand breaks in meiosis. Genes & Development 22(3):286-292.

Natarajan, A.T.

2002 Chromosome aberrations: past, present and future. Mutation Research 504:3-16.

Natarajan, Adayapalam T., and Fabrizio Palitti

2008 DNA repair and chromosomal alterations. Mutation Research/Genetic Toxicology and Environmental Mutagenesis 657(1):3-7.

Nussenzweig, A., and M.C. Nussenzweig

2007 A Backup DNA Repair Pathway Moves to the Forefront. Cell 131:223-225.

Nussenzweig, André, and Michel C. Nussenzweig

2010 Origin of Chromosomal Translocations in Lymphoid Cancer. Cell 141(1):27-38.

O'Driscoll, M., and P.A. Jeggo

2006 The role of double-strand break repair - insights from human genetics. Nature Reviews. Genetics 7:45-54.

O'Neill, P., and P. Wardman

2009 Radiation chemistry comes before radiation biology. International Journal of Radiation Biology 85(1):9-25.

Ochi, Takashi, et al.

2015 PAXX, a paralog of XRCC4 and XLF, interacts with Ku to promote DNA double-strand break repair. Science 347(6218):185-188.

Ochs, F., et al.

2016 53BP1 fosters fidelity of homology-directed DNA repair. Nat Struct Mol Biol 23(8):714-21.

Parshad, R., et al.

1984 Chromosomal radiosensitivity of human tumor cells during the G2 cell cycle period. Cancer Research 44:5577-5582.

Parshad, Ram, and Katherine K. Sanford

2001 Radiation-induced chromatid breaks and deficient DNA repair in cancer predisposition. Critical Reviews in Oncology/Hematology 37(2):87-96.

Paul, Katja, et al.

2013 DNA ligases I and III cooperate in alternative non-homologous end-joining in vertebrates. PLoS ONE 8(3):e59505.

Paull, Tanya T., and Rajashree A. Deshpande

2014 The Mre11/Rad50/Nbs1 complex: Recent insights into catalytic activities and ATP-driven conformational changes. Experimental Cell Research 329(1):139-147.

Pilch, D.R., et al.

2003 Characteristics of γ-H2AX foci at DNA double-strand breaks sites. Biochemistry and Cell Biology 81:123-129.

Podhorecka, Monika, Andrzej Skladanowski, and Przemyslaw Bozko

2010 H2AX Phosphorylation: Its Role in DNA Damage Response and Cancer Therapy. Journal of Nucleic Acids 2011:ID 920161.

Puizina, J., et al.

2004 Mre11 Deficiency in Arabidopsis Is Associated with Chromosomal Instability in Somatic Cells and Spo11-Dependent Genome Fragmentation during Meiosis. Plant Cell 16:1968-1978.

Revell, S.H.

1974 The breakage-and-reunion theory and the exchange theory for chromosomal aberrations induced by ionizing radiation: a short history. Advances in Radiation Biology 4:367-416.

Richardson, C., and M. Jasin

2000 Frequent chromosomal translocations induced by DNA double-strand breaks. Nature 405:697-700.

Roukos, Vassilis, Bharat Burman, and Tom Misteli

2013 The cellular etiology of chromosome translocations. Current Opinion in Cell Biology 25(3):357-364.

Roukos, Vassilis, and Tom Misteli

2014 The biogenesis of chromosome translocations. Nature Cell Biology 16(4):293-300.

San Filippo, J., P. Sung, and H. Klein

2008 Mechanism of Eukaryotic Homologous Recombination. Annual Review of Biochemistry 77:229-257.
Sarbajna, Shriparna, and Stephen C. West

2014 Holliday junction processing enzymes as guardians of genome stability. Trends in Biochemical Sciences 39(9):409-419.
Saribasak, Huseyin, et al.

2011 XRCC1 suppresses somatic hypermutation and promotes alternative nonhomologous end joining in Igh genes. Journal of Experimental Medicine 208(11):2209-2216.
Sasai, K., et al.

1994 Prediction of human cell radiosensitivity: comparison of clonogenic assay with chromosome aberrations scored using premature chromosome condensation with fluorescence in situ hybridization. International Journal of Radiation Oncology Biology Physics 30(5):1127-32.
Savage, J.R.K.

1975 Classification and relationships of induced chromosomal structural changes. Journal of Medical Genetics 12:103-122.
Sax, K.

1940 An analysis of X-ray induced chromosomal aberrations in tradescantia. Genetics 25:41-68.
Schatz, David G., and Patrick C. Swanson

2011 V(D)J Recombination: Mechanisms of Initiation. Annual Review of Genetics 45:167-202.
Schipler, Agnes, and George Iliakis

2013 DNA double-strand-break complexity levels and their possible contributions to the probability for error-prone processing and repair pathway choice. Nucleic Acids Research 41(16):7589-7605.
Schipler, Agnes, et al.

2016 Chromosome thripsis by DNA double strand break clusters causes enhanced cell lethality, chromosomal translocations and 53BP1-recruitment. Nucleic Acids Research in press:NAR-01037-D-2016 R1 - 9KW487.
Shaltiel, Indra A., et al.

2015 The same, only different – DNA damage checkpoints and their reversal throughout the cell cycle. Journal of Cell Science 128(4):607-620.
Shibata, A., and P. A. Jeggo

2014 DNA Double-strand Break Repair in a Cellular Context. Clinical Oncology 26(5):243-249.
Shovman, Olga, et al.

2008 An improved assay for radiation-induced chromatid breaks using a colcemid block and calyculin-induced PCC combination. Mutagenesis 23(4):267-270.
Siemann, M.

2013 Contributions of NHEJ and HRR in the processing of DNA double strand breaks and chromosome breaks throughout the cell cycle. PhD Thesis.
Simsek, Deniz, et al.

2011 DNA Ligase III Promotes Alternative Nonhomologous End-Joining during Chromosomal Translocation Formation. PLoS Genetics 7(6):e1002080.
Simsek, Deniz, and Maria Jasin

2010 Alternative end-joining is suppressed by the canonical NHEJ component Xrcc4-ligase IV during chromosomal translocation formation. Nature Structural & Molecular Biology 17(4):410-416.
Soni, A.

2010 The Role of Homologous Recombination Repair in the processing of G2-chromosomal breaks and maintenance of G2-checkpoint. PhD Thesis.
Soni, Aashish, et al.

2014 Requirement for Parp-1 and DNA ligases 1 or 3 but not of Xrcc1 in chromosomal translocation formation by backup end joining. Nucleic Acids Research 42(10):6380-6392.
Stavnezer, Janet, Jeroen E. J. Guikema, and Carol E. Schrader

2008 Mechanism and Regulation of Class Switch Recombination. Annual Review of Immunology 26(1):261-292.
Sulli, Gabriele, Raffaella Di Micco, and Fabrizio d'Adda di Fagagna

2012 Crosstalk between chromatin state and DNA damage response in cellular senescence and cancer. Nature Reviews. Cancer 12(10):709-720.
Suwaki, Natsuko, Kerstin Klare, and Madalena Tarsounas

2011 RAD51 paralogs: Roles in DNA damage signalling, recombinational repair and tumorigenesis. Seminars in Cell & Developmental Biology 22(8):898-905.
Symington, Lorraine S, and Jean Gautier

2011 Double-Strand Break End Resection and Repair Pathway Choice. Annual Review of Genetics 45:247-271.
Takata, M., et al.

1998 Homologous recombination and non-homologous end-joining pathways of DNA double-strand break. EMBO Journal 17:5497-5508.
Taylor, A.M.R.

1978 Unrepaired DNA strand breaks in irradiated ataxia telangiectasia lymphocytes suggested from cytogenetic observations. Mutation Research 50:407-418.
Terzoudi, G.I., et al.

2008 Premature chromosome condensation reveals DNA-PK independent pathways of chromosome break repair. International Journal of Oncology 31(1):145-152.
Thoms, K.-M., C. Kuschal, and S. Emmert

2007 Lessons learned from DNA repair defective syndromes. Experimental Dermatology 16:532-544.

Trujillo, K.M., et al.

1998 Nuclease activities in a complex of human recombination and DNA repair factors Rad50, Mre11, and p95. Journal of Biological Chemistry 273:21447-21450.

Vignard, Julien, Gladys Mirey, and Bernard Salles

2013 Ionizing-radiation induced DNA double-strand breaks: A direct and indirect lighting up. Radiotherapy and Oncology 108(3):362-369.

Wang, Huichen, et al.

2005 DNA Ligase III as a Candidate Component of Backup Pathways of Nonhomologous End Joining. Cancer Research 65(10):4020-4030.

Wray, Justin, et al.

2013 PARP1 is required for chromosomal translocations. Blood 121(21):4359-4365.

Wu, Wenqi, et al.

2008 Enhanced Use of Backup Pathways of NHEJ in G_2 in Chinese Hamster Mutant Cells with Defects in the Classical Pathway of NHEJ. Radiation Research 170:512-520.

Wurm, Florian M., and David Hacker

2011 First CHO genome. Nat Biotech 29(8):718-720.

Yamaguchi-Iwai, Y., et al.

1999 Mre11 is essential for the maintenance of chromosomal DNA in vertebrate cells. EMBO Journal 18(23):6619-6629.

Zhang, Yu, and Maria Jasin

2011 An essential role for CtIP in chromosomal translocation formation through an alternative end-joining pathway. Nature Structural & Molecular Biology 18(1):80-84.

Zhou, B.B., and S. J. Elledge

2000 The DNA damage response: putting checkpoints in perspective. Nature 408:433-439.

Zimmermann, Michal, et al.

2013 53BP1 Regulates DSB Repair Using Rif1 to Control 5′ End Resection. Science 339(6120):700-704.

8. SUPPLEMENTARY DATA

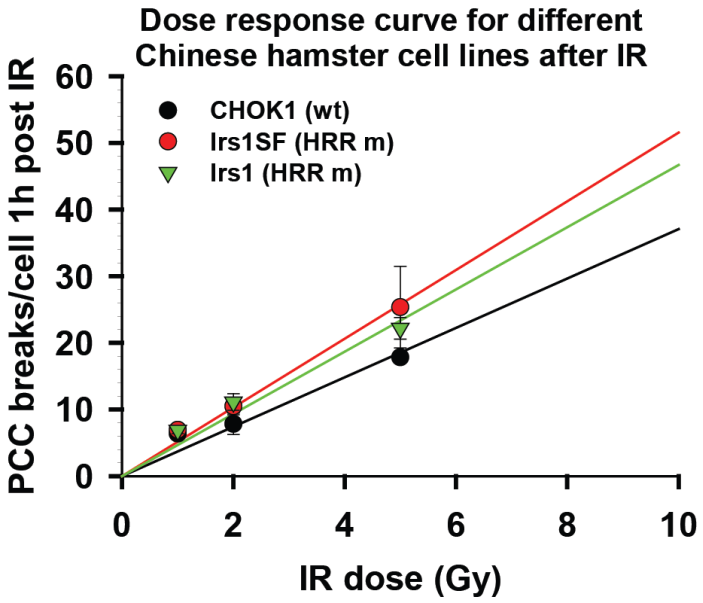

Supplementary Figure 1: Dose Response curve for IR-induced PCC break induction in different Chinese hamster cell lines.

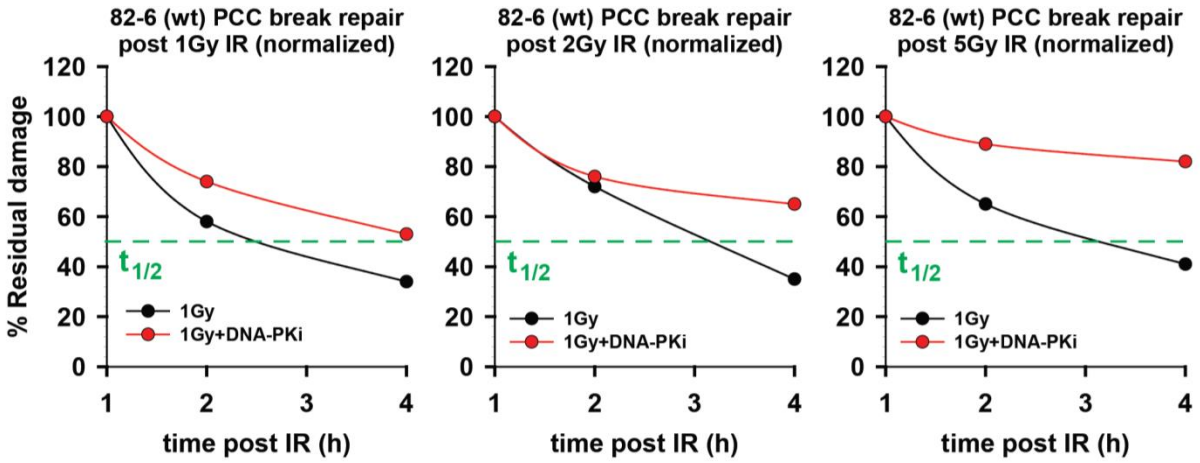

Supplementary Figure 2: PCC break repair in 82-6 cells. Breaks have been normalized to the 1h time point. The green line serves as an orientation for the time at which 50% of the breaks are resolved.

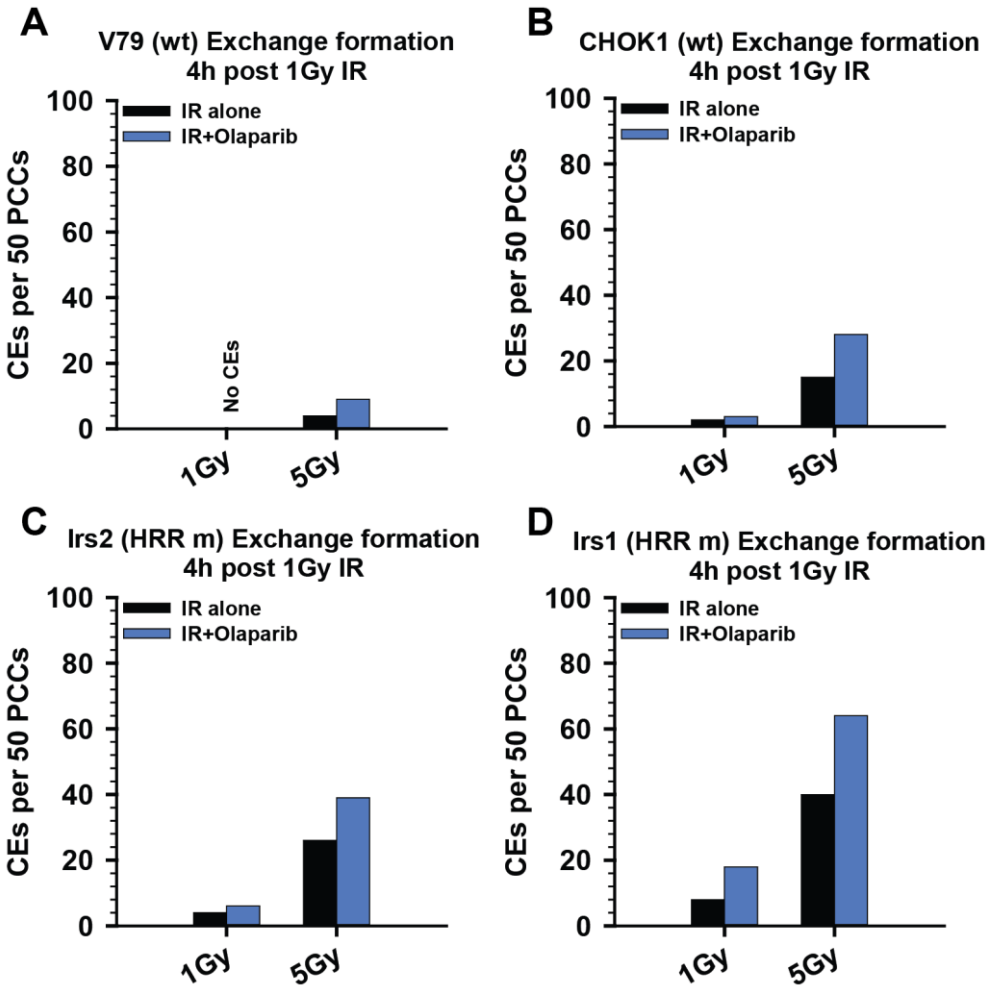

Supplementary Figure 3: CE formation upon inhibition of Parp-1 with Olaparib after exposure of different Chinese Hamster cell lines to IR. A) V79 and B) CHOK1 wildtype cells as well as two HRR mutant cell lines C) Irs2 and D) Irs1 were exposed to 1Gy or 5Gy IR alone or in the presence of Parp-1 inhibitor Olaparib. CE formation was scored 4h later. Data represent one experiment.

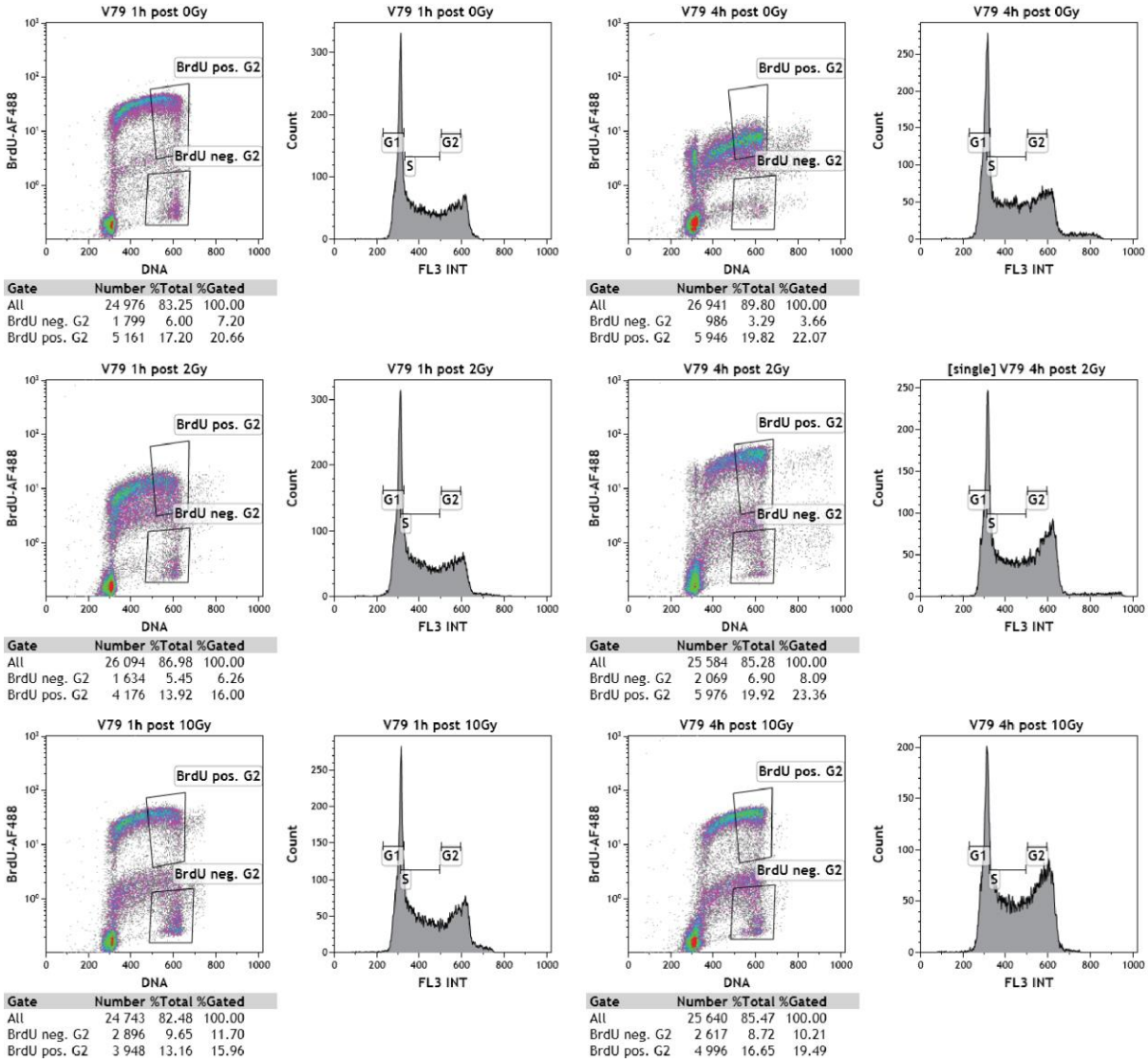

Supplementary Figure 4: Determination of BrdU positive and negative G_2 cells for V79 (wt) after exposure to different IR doses.

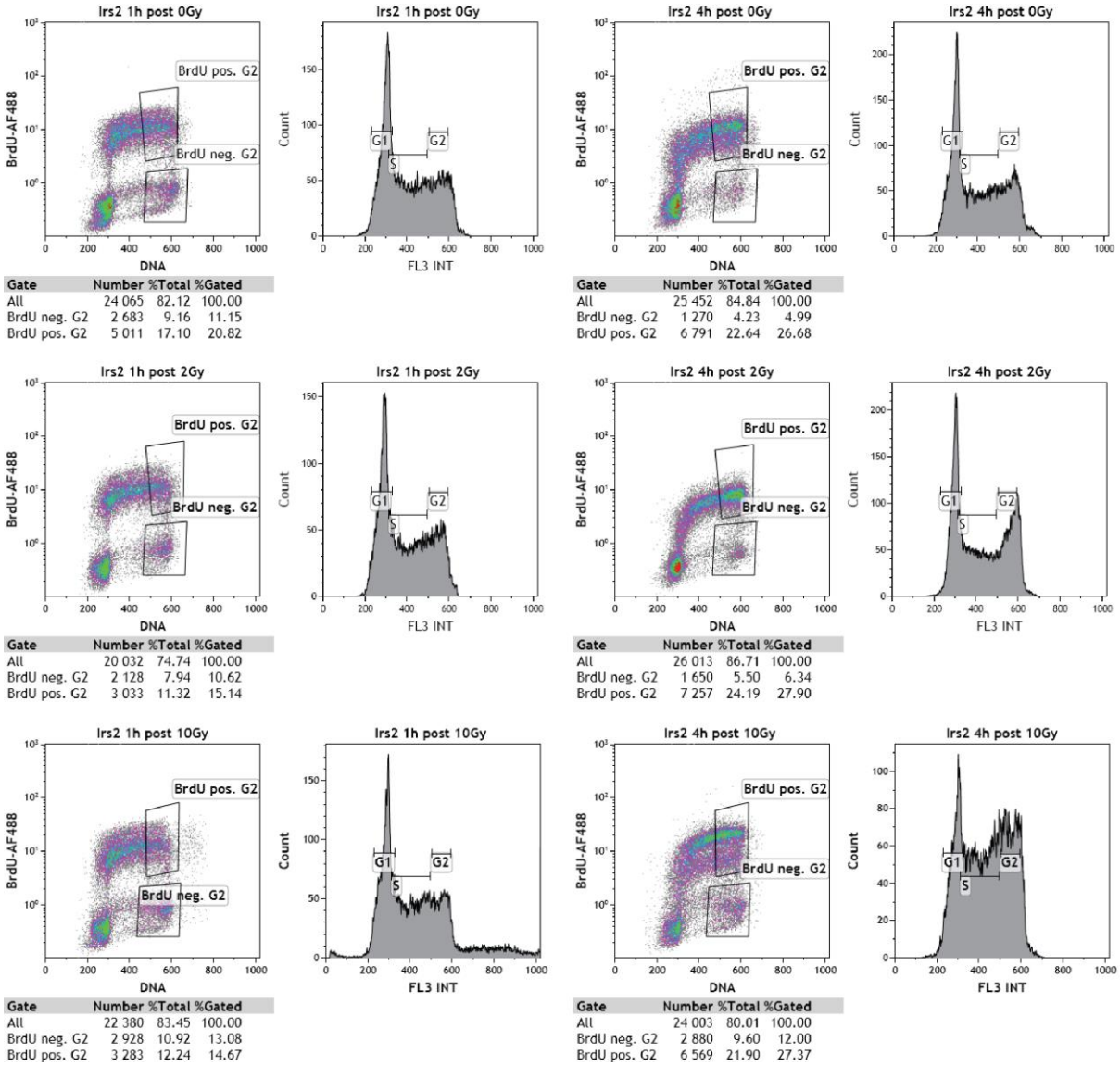

Supplementary Figure 5: Determination of BrdU positive and negative G_2 cells for Irs2 (HRR) cells after exposure to different IR doses.

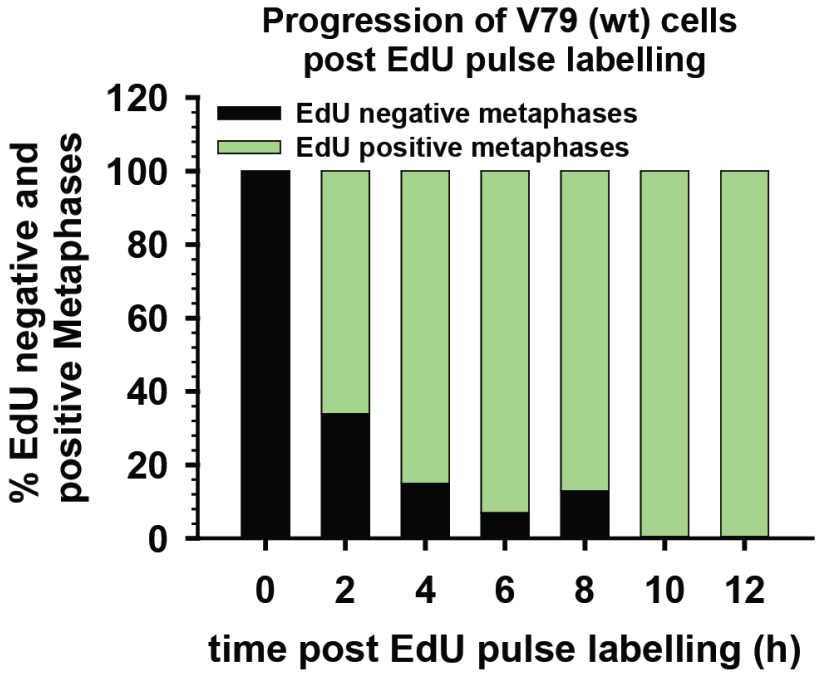

Supplementary Figure 6: Determination of the fraction of EdU negative and EdU positive metaphases for V79 (wt) cells after EdU pulse labelling.

Supplementary Table 1: % Residual damage determined for different Chinese hamster cell lines after exposure to IR alone or in the presence of Parp-1 inhibitor PJ34. The residual damage was determined by normalizing the number of breaks obtained 4h post IR (Residual) to the initial number of PCC breaks (Initial damage).

Cell line	IR dose	% Residual damage IR alone	% Residual damage IR+Parp-1i (PJ34)
V79 (wt)	1	44	36
	2	14	18
	5	33	31
Irs2 (Rad51B m)	1	72	76
	2	49	54
	5	59	52
Irs1 (XRCC2 m)	1	57	53
	2	30	41
	5	39	43
Irs1SF (XRCC3 m)	1	83	79
	2	54	48
	5	39	44
XR1 (XRCC4 m)	1	51	40
	2	46	55
	5	98	96

ACKNOWLEDGMENTS

Doing PhD is somehow like going on a long journey. This journey is interesting and exciting but one must face many obstacles and difficult moments. Yet these hurdles and experiencing hard times give us valuable lessons, which strengthen our personality and broaden our mental horizon.

I had a lot of support during this “PhD” journey and it is my pleasure to acknowledge those people who helped me and made this journey a great experience.

First of all, I would like to express my sincere thanks to Prof. Dr. Iliakis, who gave me the opportunity to perform my PhD Thesis in his Institute. I appreciate his kind supervisions throughout the time, fruitful scientific discussions as well as having always an open door to step by when problems raised. He has been not only a great supervisor but also a great example, as a person with great commitment to science.

I would also like to express my greatest thanks to Dr. Aashish Soni for his supervision and help during my PhD time and especially for his patience with me. He helped me to focus and had always an open ear for various kinds of issues.

Further thanks go to Vladimir Nikolov for his big help on scientific questions and suggestions and also for personal talks, which are also needed to stay focused during the PhD journey. With this respect, I also would like to thank Lisa Marie Krieger for support in the lab, especially when times got little challenging.

Generally, I would like to thank all members of the Institute of Medical Radiation Biology that I got to know during the time of my PhD Thesis.

I also would like to acknowledge the DFG for funding my project and being part of the GRK1431, which gave me the opportunity to further acquire knowledge and strengthen personal skills.

Thanks also goes to the Medical Faculty of the University of Duisburg-Essen for providing me a stipend to finish my PhD Thesis.

I believe that Journeys are never possible without the support of the family. Therefore, I would like to thank my family. In particular, my husband Bikash Konda for being always there for me and providing support in any kind of situation with his

love, altruism and patience. Without him many steps would not have been that easier.

Last but not least, I would like to thank my mother, my sister and my brother for their support throughout my whole studies and always believing in my capabilities.

Der Lebenslauf ist in der Online-Version aus Gründen des Datenschutzes nicht enthalten.

Der Lebenslauf ist in der Online-Version aus Gründen des Datenschutzes nicht enthalten.

Der Lebenslauf ist in der Online-Version aus Gründen des Datenschutzes nicht enthalten.

DECLARATION

Erklärung:

Hiermit erkläre ich, gem. § 6 Abs. (2) g) der Promotionsordnung der Fakultät für Biologie zur Erlangung der Dr. *rer. nat.*, dass ich das Arbeitsgebiet, dem das Thema „The contribution of DNA DSB repair pathways to the repair of chromosome breaks throughout the cell cycle“ zuzuordnen ist, in Forschung und Lehre vertrete und den Antrag von Frau Tamara Murmann-Konda befürworte und die Betreuung auch im Falle eines Weggangs, wenn nicht wichtige Gründe dem entgegenstehen, weiterführen werde.

Essen, den_____ _____

Unterschrift eines Mitglieds der Universität Duisburg-Essen

Erklärung:

Hiermit erkläre ich, gem. § 7 Abs. (2) d) + f) der Promotionsordnung der Fakultät für Biologie zur Erlangung des Dr. rer. nat., dass ich die vorliegende Dissertation selbständig verfasst und mich keiner anderen als der angegebenen Hilfsmittel bedient, bei der Abfassung der Dissertation nur die angegeben Hilfsmittel benutzt und alle wörtlich oder inhaltlich übernommenen Stellen als solche gekennzeichnet habe.

Essen, den_____ _____

Unterschrift der Doktorandin

Erklärung:

Hiermit erkläre ich, gem. § 7 Abs. (2) e) + g) der Promotionsordnung der Fakultät für Biologie zur Erlangung des Dr. rer. nat., dass ich keine anderen Promotionen bzw. Promotionsversuche in der Vergangenheit durchgeführt habe und dass diese Arbeit von keiner anderen Fakultät/Fachbereich abgelehnt worden ist.

Essen, den_____ _____

Unterschrift der Doktorandin